

Evaluation of selective cyclooxygenase-2 (COX-2) inhibitors as radiosensitizing agents for cancer therapy

by

Alison Marshall

A thesis submitted in partial fulfillment of the requirements for the degree of

Master of Science

in

Experimental Oncology

Department of Oncology  
University of Alberta

© Alison Marshall, 2014

## ABSTRACT

Tumour resistance to chemo- and radiotherapy often prevents successful cancer therapy. This has promoted the search for novel agents that target specific molecular pathways linked to tumour resistance to cancer therapy. Among these novel agents are inhibitors of the inducible isoform of the cyclooxygenase (COX) enzyme, COX-2, which is involved in the regulation of angiogenesis, migration and invasion of cells, and the inhibition of apoptosis. The aim of the project is to study novel selective COX-2 inhibitors to enhance the efficacy of radiotherapy and chemotherapy. COX-2 expression levels in various cell lines were determined via western blot. HCA-7 cells, a human colorectal cell line, were found to have a high baseline expression of COX-2, while HCT-116 cells, also a human colorectal cell line, were not found to express COX-2. The metabolic and proliferative activity of HCA-7 and HCT-116 cells were characterized through cell uptake studies involving 2-deoxy-2-[<sup>18</sup>F]fluoro-D-glucose ([<sup>18</sup>F]FDG), and 3'-deoxy-3'-[<sup>18</sup>F]fluorothymidine ([<sup>18</sup>F]FLT). The cells were treated with varying concentrations of selective COX-2 inhibitors in combination with radiotherapy. Inhibitors included celecoxib, the current “gold standard” for selective COX-2 inhibitors as radiosensitizers, and a novel pyrimidine-based selective COX-2 inhibitor, pyricoxib. Toxicity of the compounds was examined through the methylthiazol tetrazolium (MTT) assay. Occurrence of apoptotic events were measured by labelling cells with annexin V-FITC and propidium iodide (PI) followed by flow cytometry. Cells were treated with GIEMSA stain and β-galactosidase stain to examine cell morphology and level of senescence. HCA-7 and HCT-116 cells were found to have high metabolic and proliferative activity based on their [<sup>18</sup>F]FDG and [<sup>18</sup>F]FLT cell uptake profile,

respectively. Pyricoxib was found to be less toxic to cells than celecoxib. Cells were resistant to radiation-induced cell death at doses up to 20 Gy. Cells treated with selective COX-2 inhibitors did not exhibit decreased cell metabolic activity indicative of increased cell death after irradiation compared to non-irradiated cells based on the MTT assay. Neither compound appeared to produce a significant radiosensitization response based on apoptotic events, but in fact appeared to produce a radioprotective effect. When examined by GIEMSA stain in HCA-7 cells, both drugs produced more large cells with less tumour-like populations when combined with irradiation compared to the control and to HCT-116 cells. Finally, chemoradiation with coxibs did not result in an increased number of senescent cells compared to either therapy alone. Only pyricoxib in the COX-2 positive cells produced an enhanced level of senescence, but it was not greater than an additive effect.

## **PREFACE**

The cellular uptake and blocking studies described in Chapter 3.2 of this thesis have been published as O. Tietz, M. Wang, A. Marshall, S.K. Sharma, J. Way, M. Wuest, and F. Wuest, “F-18-Labelled radiotracers for molecular imaging of cyclooxygenase-2 (COX-2) expression in cancer,” 2014, *Journal of Labelled Compounds and Radiopharmaceuticals*, vol. 56, S3-S3. I was responsible for performing the cellular uptake and blocking studies and contributed to manuscript edits. O. Tietz was the primary data collector and wrote the manuscript. M. Wang, S.K. Sharma, J. Way, and M. Wuest assisted with data collection and contributed to manuscript edits. F. Wuest was the supervisory author and was involved with concept formation and manuscript composition.

## **DEDICATION**

I dedicate this thesis to my brother, Craig ‘Jesus’ Marshall, for feeding me chocolate and letting me sleep until 1 pm.

## **ACKNOWLEDGEMENT**

I would first and foremost like to thank my supervisor Dr. Frank Wuest for his continuous support and guidance throughout the project. I would like to thank my committee members Dr. David Murray and Dr. Razmik Mirzayans. Thank you to the Flow Cytometry Lab in the Department of Experimental Oncology at the Cross Cancer Institute for help with the flow cytometry part of this project. Thank you to Bonnie Andrais as well, for help with setting up the MTT assay and imaging parts of this project. Thank you to the Wuest lab for affording such a friendly, team-oriented environment to work in. Finally, thank you to my family and friends for their constant love and support throughout my years at university thus far.

Copyright material belonging to a third-party and referenced herein may have been reproduced with permission, separately licensed, or the author has exercised their right to fair dealing under the Canadian Copyright Act. Further reproduction of the material outside the context of this thesis may require permission from the copyright owner.

## TABLE OF CONTENTS

|   |    |
|---|----|
| 1. Introduction                                   | 1  |
| 1.1. Cyclooxygenase: the molecule                 | 2  |
| 1.2. Prostaglandin E <sub>2</sub>                 | 8  |
| 1.3. COX-2 and cancer                             | 11 |
| 1.4. NSAIDs and COXIBs                            | 16 |
| 1.5. Radiation therapy and its biological effects | 17 |
| 1.6. Tumour radiosensitivity                      | 19 |
| 1.7. COX-2 inhibitors as radiosensitizers         | 20 |
| 1.8. PET imaging of cancer                        | 23 |
| 1.9. Hypothesis and objectives                    | 28 |
| 2. Materials and Methods                          |    |
| 2.1. General                                      | 29 |
| 2.2. Statistics                                   | 30 |
| 2.3. Compounds                                    | 31 |
| 2.4. Western Blot                                 | 32 |
| 2.5. Cellular Uptake Studies                      | 33 |
| 2.6. Bicinchoninic Acid (BCA) Assay               | 34 |
| 2.7. Methyl Thiazol Tetrazolium (MTT) Assay       | 35 |
| 2.8. Flow cytometry                               | 36 |
| 2.9. Microscopy                                   | 38 |
| 3. Results  |    |
| 3.1. Western Blot                                 | 40 |

|      |  |    |
|------|--|----|
| 3.2. | Cellular Uptake Studies  | 41 |
| 3.3. | Methyl Thiazol Tetrazolium (MTT) Assay                                     | 48 |
| 3.4. | Flow cytometry   | 52 |
| 3.5. | Microscopy   | 55 |
| 4.   | Discussion   |    |
| 4.1. | Paradigm shift of radiosensitization studies – impact of biological model? | 63 |
| 4.2. | Coxib off-target effects   | 65 |
| 4.3. | SIPS and p53   | 69 |
| 5.   | Summary and Conclusions  | 73 |
| 6.   | Future Directions  | 74 |

## LIST OF TABLES

|         |  |    |
|---------|--|----|
| Table 1 | COX-2 expression in malignant carcinomas | 12 |
|---------|--|----|

## LIST OF FIGURES OR ILLUSTRATIONS

|           |  |    |
|-----------|--|----|
| Figure 1  | Cyclooxygenase molecule structure                                  | 3  |
| Figure 2  | Prostanoid synthesis through the activity of COX                   | 7  |
| Figure 3  | The role of prostaglandin E <sub>2</sub> in cancer                 | 9  |
| Figure 4  | Structure of aspirin and ibuprofen; NSAIDs                         | 14 |
| Figure 5  | Structures of celecoxib, valdecoxib, rofecoxib, and SC-236; coxibs | 15 |
| Figure 6  | COX-2 downstream effects in relation to cardiovascular events      | 16 |
| Figure 7  | Biological effects of direct and indirect radiation on cells       | 17 |
| Figure 8  | Depiction of how a PET scan works                                  | 23 |
| Figure 9  | Mechanism of FDG uptake and trapping in cells for PET imaging      | 25 |
| Figure 10 | Mechanism of FLT uptake and trapping in cells for PET imaging      | 26 |
| Figure 11 | Structures and IC <sub>50</sub> values of celecoxib and pyricoxib  | 31 |
| Figure 12 | Western Blot   | 40 |
| Figure 13 | Uptake of [ <sup>18</sup> F]FDG in HCA-7 cells                     | 42 |
| Figure 14 | Uptake of [ <sup>18</sup> F]FDG in HCT-116 cells                   | 42 |
| Figure 15 | Uptake of [ <sup>18</sup> F]FLT in HCA-7 cells                     | 44 |
| Figure 16 | Uptake of [ <sup>18</sup> F]FLT in HCT-116 cells                   | 44 |
| Figure 17 | Uptake of [ <sup>18</sup> F]pyricoxib in HCA-7 cells               | 45 |
| Figure 18 | Uptake of [ <sup>18</sup> F]pyricoxib in HCA-7 and HCT-116 cells   | 46 |
| Figure 19 | Blocking study of [ <sup>18</sup> F]pyricoxib in HCA-7 cells       | 47 |
| Figure 20 | Cytotoxicity of drugs in HCA-7 cells                               | 49 |
| Figure 21 | Cytotoxicity of drugs in HCT-116 cells                             | 49 |
| Figure 22 | MTT radiosensitization study in HCA-7 cells                        | 51 |
| Figure 23 | MTT radiosensitization study in HCT-116 cells                      | 51 |
| Figure 24 | Apoptosis in HCA-7 cells   | 53 |
| Figure 25 | Apoptosis in HCT-116 cells   | 54 |
| Figure 26 | GIEMSA staining of HCA-7 cells                                     | 56 |
| Figure 27 | GIEMSA staining of HCT-116 cells                                   | 57 |
| Figure 28 | β-galactosidase staining of HCA-7 cells                            | 59 |
| Figure 29 | % senescent HCA-7 cells  | 60 |
| Figure 30 | β-galactosidase staining of HCT-116 cells                          | 61 |
| Figure 31 | % senescent HCT-116 cells  | 62 |

## **LIST OF SYMBOLS, NOMENCLATURE, OR ABBREVIATIONS**

AP-1 – activator protein 1

APC – anaphase promoting complex

AP-C – Adenoma Prevention with celecoxib

APPROVe – Adenomatous Polyp Prevention on Vioxx

ARE – AU response element

BCA – bichinchoninic acid

cAMP – cyclic adenosine monophosphate

C/EBP – Ccaat-enhancer-binding protein

COX – cyclooxygenase

Coxib – selective COX-2 inhibitor

CREB – cAMP response element-binding protein

CT – computed tomography

CXCL – chemokine ligand

DMEM – Dulbecco's modified eagle medium

DMSO – dimethylsulfoxide

DNA – deoxyribonucleic acid

EDTA – ethylenediaminetetraacetic acid

EGF – epidermal growth factor

ER – endoplasmic reticulum

ERK – extracellular signal-related kinase

FAP – familial adenomatous polyposis

FBS – fetal bovine serum

FDG - fluorodeoxyglucose

FGF – fibroblast growth factor

FITC – fluorescein isothiocyanate

FLT - fluorodeoxythymidine

FSA – murine fibrosarcoma cell line

GLUT – glucose transporter

GSK – glycogen synthase kinase

HCA-7 – human colorectal adenocarcinoma cell line

HCT-116 – human colorectal carcinoma cell line

HEPES – 4-(2-hydroxyethyl)-1-piperazineethanesulfonic acid

HN5 – human head and neck cancer cell line

IFN - interferon

IL - interleukin

iNOS – inducible nitric oxide synthase

JNK – c-Jun N-terminal kinase

LPS – lipopolysaccharide

MAPK – mitogen-activated protein kinase

MEK – mitogen-activated protein kinase kinase

MMP – matrix metalloproteinase

MRI – magnetic resonance imaging

mRNA – messenger ribonucleic acid

NF – nuclear factor

NFAT – nuclear factor of activated T-cells

NFSA – murine fibrosarcoma cell line

NO – nitric oxide

NSAID – non steroidal anti-inflammatory drug

NSCLC – non-small-cell lung carcinoma

NT – nucleoside transporter

PBS – phosphate buffered saline solution

PBST – phosphate buffered saline/tween solution

PCNA - proliferating cell nuclear antigen

PET – positron emission tomography

PG – prostaglandin

PI – propidium iodide

PI3K – phosphoinositide 3-kinase

PKA – protein kinase A

PL - phospholipase

PPAR – peroxisome proliferator-activated receptor

PPRE – peroxisome proliferator response element

pRB – retinoblastoma protein

PreSAP – Prevention Spontaneous Adenomatous Polyps

PVDF – polyvinylidene fluoride

RIPA – radioimmunoprecipitation assay

RNA – ribonucleic acid

RT – room temperature

RXR – retinoid X receptor

SDS-PAGE – sodium dodecyl sulfate polyacrylamide gel electrophoresis

SIPS – stress induced premature senescence

TCF – transcription factor

tCREB – T-lymphocyte cAMP response element-binding protein

TGF – transforming growth factor

TK1 – thymidine kinase 1

TNF – tumour necrosis factor

TRE – tissue plasminogen activator response element

TX - thromboxane

UTR – untranslated region

VEGF – vascular endothelial growth factor

## **1. INTRODUCTION**

Each year, solid tumors are responsible for millions of deaths worldwide, and this number is increasing. While recent advances have improved the prognosis for these patients, it is still imperative to discover novel and more effective methods of treatment. There is a need for new targets for anticancer treatment, resulting in the development of novel compounds that target specific molecular pathways linked to tumor resistance to radiotherapy and cytotoxic agents. Among these novel agents, inhibitors of cyclooxygenase (COX), the key enzyme involved in the conversion of arachidonic acid into prostaglandins (PGs), represent a particularly promising class of compounds for chemoprevention and cancer therapy. COX-2 is over-expressed in a wide variety of carcinomas, often found in more aggressive malignancies that lead to poor survival. COX-2 inhibition has also been correlated with tumor radiosensitization in multiple cases involving both different cell types and selective inhibitors.

### 1.1 *CYCLOOXYGENASE: THE MOLECULE*

There are three known isoforms of the COX enzyme. COX-1 is constitutively expressed in most tissues, while COX-2 is induced at sites of inflammation, and in cellular growth and differentiation (127). The second form of COX is induced by cytokines (TNF- $\alpha$ , IL-1), growth factors (EGF, VEGF, platelet-derived growth factor, FGF, TGF- $\beta$ ), mitogenic substances (LPS), and oncogenes (src, ras) (115; 114; 86; 159; 58). Although COX-2 is inducible, it has been found to be constitutively expressed at very low levels in certain areas of the body including the kidneys, brain, tracheal epithelia, and reproductive tissues (127). COX-3 is a splicing variant of COX-1, and while its exact function remains to be determined, it may be involved with pain and fever management (20).

COX-1 and COX-2 are similar in size and structure. At the N-terminus of COX-2, a hydrophobic signal peptide domain, which is shorter than that of COX-1 by 17 amino acids, guides the protein into the endoplasmic reticulum (ER) lumen. An EGF-like unit in charge of forming the COX-2 homodimers is found within the dimerization domain. Both COX-1 and COX-2 consist of two identical subunits each with two active sites; a cyclooxygenase and a heme-containing peroxidase site. However, the COX-2 catalytic site, while vastly similar to that of COX-1, consists of a more exposed substrate cavity that allows bulkier substrates and selective COX-2 inhibitors to bind. The L-shaped, hydrophobic cavity extends from the membrane-binding domain to the center of the enzyme in both cases, where substrate and inhibitor entry is controlled by a protein gate complex. The upper surface of COX-1 and COX-2 contains the peroxidase activity, separated from the long, hydrophobic cyclooxygenase active site channel domain by the

heme group. At the C-terminus of COX-2 is an instability membrane domain that aids in the control of the degradation of the protein. Also at the C-terminus is a short sequence of amino acids that comprises the ER retention signal. COX can be found on the luminal side of the ER as well as the nuclear membrane, where it is anchored by four short amphipathic  $\alpha$ -helices found in the membrane-binding domain.

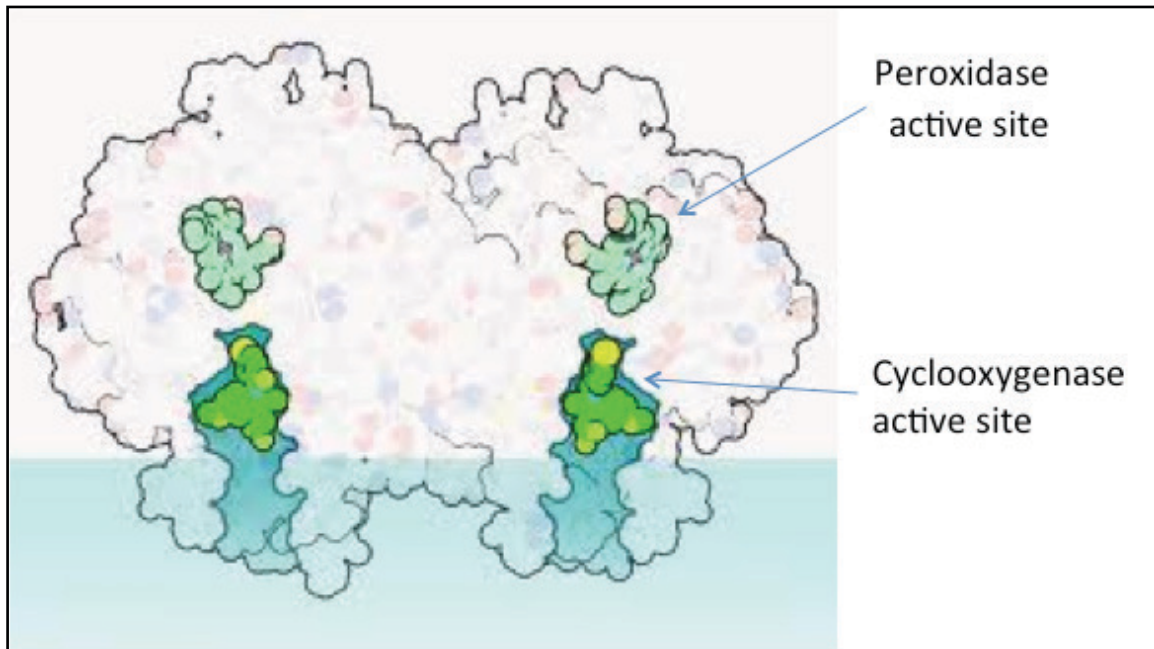


Figure 1: Cyclooxygenase molecule structure. May 2001 molecule of the month by David Goodsell.

Both isoforms of COX undergo post-translational modification including N-glycosylation at multiple asparagine residues as the main alteration, and S-nitrosylation by nitric oxide and nitric oxide synthase (102). Asp53, Asp130, Asp396, and Asp580, four of the potential N-glycosylation sites, are found within the COX-2 catalytic domain. N-glycosylation at Asp53, Asp130, and Asp396 controls the production of a 72 kDa folded COX-2 in an active conformation, while N-glycosylation at Asp580 varies and generates a 74 kDa form of the protein (102). While the exact function of Asp580 has yet

to be discovered, the catalytic activity of COX-2 increases when Asp580 N-glycosylation is removed (119). COX-2 S-nitrosylation at cysteine 256 has been found to be brought about by an interaction between inducible nitric oxide synthase (iNOS) and COX-2, resulting in an enhancement of the catalytic activity of COX-2 (70).

The genes that encode COX-1 and COX-2 are found on different chromosomes. The gene for COX-1 is 22 kb long with 11 exons and no TATA box (75). The final product generated is 2.7 kb in length. The COX-2 gene is 8.3 kb in length containing 10 exons, and the product formed is 4.3-4.5 kb long (77). Furthermore, a TRE (TPA-response element; 12-O-tetradecanoylphorbol-13-acetate) is present in the first exon of the COX-2 gene. 17 copies of the Shaw-Kamen sequences, responsible for message stability, 3 polyadenylation signals, and multiple AREs (AU-rich elements), which cause the short half-life of COX-2 mRNA due to prompt degradation, are found within the 3' untranslated region (23). Alternative splicing and single nucleotide polymorphism create further COX-2 gene variants, with evidence suggesting these variants may be involved in pathophysiological processes (9).

The COX-2 gene is manipulated by a multitude of signals, including oncogenes (*Ha-ras*, *v-src*, *her-2/neu*, *wnt1*) and cytokines (TGF- $\beta$ 1, TGF- $\alpha$ , TNF- $\alpha$ , IFN- $\gamma$ , interleukins) that act on transcriptional activation sites and a CCATT/enhancer binding protein (C/EBP) site found within the 5' untranslated region to regulate expression of this immediate early response gene (75). tCREB, *Myb*, cAMP, NF-IL-6, NF- $\kappa$ B, NFAT, PEA3, and AP-1 are some of the factors that are able to act on *cis*-acting elements within the promoter (75). COX-2 can be upregulated by growth factors and other stimuli that trigger the ERK and JNK MAPK cellular-signaling pathways through the use of the

cAMP response element on COX-2 (130; 157). TNF is able to induce COX-2 production through the NF-IL-6 and NF- $\kappa$ B sites, while AP-1 acts through the use of the histone deacetylase activity in the CREB-binding protein/p300 co-activator complex (22; 131). Wild-type p53, on the other hand, inhibits the transcription of COX-2 through competitive inhibition with TATA-binding protein for binding to the TATA-box (129). COX-2 transcription is also inhibited by steroids and anti-inflammatory cytokines, including IL-4, IL-10, and IL-13 (99).

Studies investigating the relationship between COX-2 and CRC (CRC) give the impression that the enzyme is of particular importance in promoting this type of malignancy. For instance, when the *APC* gene is mutated in a CRC zebrafish model and human cell lines, COX-2 expression was either directly or indirectly induced (44). One study showed COX-2 was able to be upregulated by increasing expression of C/EBP- $\beta$  and its subsequent binding to the COX-2 promoter, while another study showed the elevated COX-2 levels induced by the *APC* mutation were reduced when treated with retinoic acid, which decreases C/EBP- $\beta$  production (44).

The *c-Myb* transcription factor, part of the *Myb* factors which are broadly expressed and important in cell growth, is able to bind to its binding site within the COX-2 promoter and initiate COX-2 transcription (129). COX-2 and *c-Myb* are found in high amounts at mRNA and protein levels in CRC cells lines, tissue arrays, and adenomas which suggest *c-Myb* may induce COX-2 in early stages of CRC (112). Various other cancer types, including lung and breast cancer, myeloid leukemia, melanoma, neuroblastoma, and osteogenic sarcoma, have also been found to overexpress *c-Myb* (24).

COX-2 is also regulated by post-transcriptional and post-translational mechanisms induced during disease-related processes, for example carcinogenesis and inflammation, by controlling transcript stability and protein synthesis and degradation rates. This is achieved through binding at the Shaw-Kamen motifs in its 3'-UTR by regulatory proteins, such as IL-1 $\beta$  and HuR, which help control message stability and translational efficiency once bound. For instance, through the interaction of IL-1 $\beta$  – induced RNA-binding proteins with sequences found in the COX-2 3'UTR, the half-life of COX-2 mRNA is increased (27). Furthermore, COX-2 message stability in CRC is associated with the binding of HuR, an RNA-binding protein, to the Shaw-Kamen sequences (40).

COX acts by two linked reactions. In the first reaction, phospholipase A<sub>2</sub> liberates arachidonic acid from the plasma membrane, which is then transformed into PGG<sub>2</sub>, an unstable intermediate, through the cyclooxygenase activity of COX. COX then converts PGG<sub>2</sub> into PGH<sub>2</sub> through the use of the peroxidase activity. Next, PGH<sub>2</sub> is metabolized into biologically active prostanoids by a variety of synthases specific to each prostanoid (77). Prostanoids include prostaglandins (PGD<sub>2</sub>, PGE<sub>2</sub>, PGI<sub>2</sub>, PGF<sub>2 $\alpha$</sub> ) and thromboxanes (TXA<sub>2</sub>, TXB<sub>2</sub>) which perform an array of biological functions, including gastrointestinal mucosa protection (PGI<sub>2</sub>), vasodilation (PGD<sub>2</sub>, PGE<sub>2</sub>, PGI<sub>2</sub>, TXA<sub>2</sub>), platelet aggregation (PGE<sub>2</sub>, PGI<sub>2</sub>, TXA<sub>2</sub>), regulation of cell growth and differentiation, renal function, immunomodulation, as well as mediating pain, fever (PGE<sub>2</sub>), and inflammation. These short-lived prostanoids are released from the cells instantly, and exhibit both autocrine and paracrine activity through binding to high-affinity G-protein-coupled membrane receptors on the cell surface.

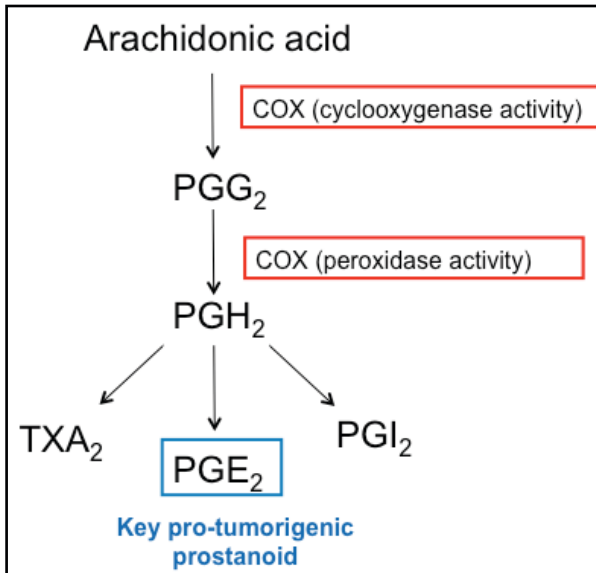


Figure 2: Prostanoid synthesis through the activity of COX. Adapted from (54).

The receptors for prostanoids consist of different types and subtypes that bind specific ligands, but are able to cross-bind other prostanoids. The receptor types are DP receptors (DP<sub>1</sub>, DP<sub>2</sub>) for PGD<sub>2</sub>, EP receptors (EP<sub>1</sub>, EP<sub>2</sub>, EP<sub>3</sub>, EP<sub>4</sub>) that bind PGE<sub>2</sub>, FP receptors for PGF<sub>2α</sub>, IP receptors for PGI<sub>2</sub>, and TP receptors for TxA<sub>2</sub> (126; 132). EP<sub>2</sub> and EP<sub>4</sub> have been found to mainly intercede downstream in proinflammatory and promalignant signals elicited by PGE<sub>2</sub> by activating adenylate cyclase (126; 132). This triggers an enhanced concentration of intracellular cAMP that stimulates GSK3 and kinases, including PKA or PI3K (12). GSK3 activates β-catenin, a protein in a pathway that regulates cell proliferation (12). EP<sub>1</sub> is known to use phospholipase C/inositol triphosphate for signalling, resulting in the mobilization of calcium within cells (14). EP<sub>3</sub>, on the other hand, increases IP<sub>3</sub> and calcium, and causes a decrease in intracellular cAMP through the inhibition of adenylatecyclase (126; 132). Furthermore, some PGs are also able to bind to receptors in the cell nucleus called peroxisome proliferator-activated receptors (PPARs) (14). For instance, PGI<sub>2</sub> can bind to PPARδ and PPARγ is able to bind PGJ<sub>2</sub> (14).

## 1.2 PROSTAGLANDIN $E_2$

The major prostaglandin involved in mediating the COX-2 pro-survival response is  $PGE_2$ . Once synthesized,  $PGE_2$  is carried out of the cell by PG transporter, and subsequently binds to an EP receptor, triggering a multitude of signalling pathways involved in inhibiting cell death. For instance, the binding of  $PGE_2$  to its receptor promotes the transactivation of EGFR, which leads to the stimulation of ERK and PI-3K/Akt pro-survival and migratory pathways and the movement of Shc-Grb2-Sos complex to activate the Ras protein. Once activated, Ras is able to promote the ERK and PI-3K pathways in addition to the MAPK pathway, leading to adhesion and migration of malignant cells, as well as angiogenesis (103; 122; 15). Transactivation of EGFR is caused by the formation of a signalling complex of  $EP_4$  receptors with  $\beta$ -arrestin-1 and c-Src when stimulated by  $PGE_2$ , the latter of which are involved in regulating metastasis (103). ERK and MAPK pathway signalling stimulates gene expression that gives rise to Bcl-2 proteins, responsible for deterring apoptosis (11). Triggering the PI-3K, on the other hand, results in the prevention of apoptosis through inactivation of BAD, a pro-apoptotic protein that exerts its effects through the inhibition of Bcl-2 in the mitochondria (148). Activation of the PI-3K/Akt pathway also enhances invasion and migration during metastasis (148). In addition,  $PGE_2$  signaling is able to cross-activate the downstream components of the EGFR signaling pathway, such as  $TGF\alpha$ .

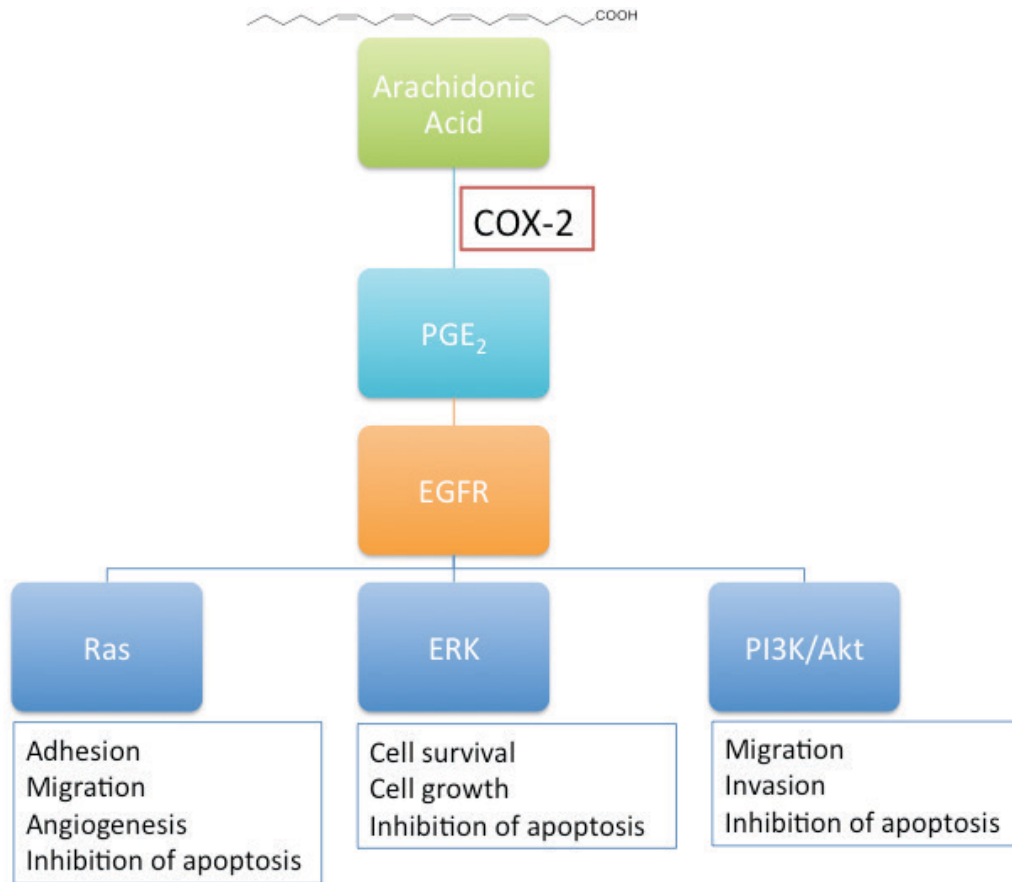


Figure 3: The role of prostaglandin E<sub>2</sub> in cancer. Adapted from (92).

Another role of PGE<sub>2</sub> in eliciting the COX-2 pro-survival response is its enhancement of Wnt signalling in the progression of malignancies. At the end of the Wnt pathway is the  $\beta$ -catenin/TCF transcriptional complex that triggers the transcription of numerous genes targeted by Wnt, such as *cyclin D1*, *c-myc*, *c-jun*, *VEGF*, and *PPAR $\delta$*  (50). Lack of signalling by the Wnt pathway results in the phosphorylation of  $\beta$ -catenin by GSK-3 $\beta$ , which causes it to stay bound to the cytoplasmic destruction complex which includes Axin/conductin, GSK-3 $\beta$ , and APC, and creates a signal for its ubiquitin-dependent degradation by proteasomes (50). When Wnt is present,  $\beta$ -catenin degradation is inhibited, and is instead localized to the nucleus where it promotes expression of genes implicated in early neoplasia (10). One study found that PGE<sub>2</sub> promotes the expression of

Wnt target genes, including *cyclin D1* and *VEGF* through increased phosphorylation of GSK-3 $\beta$ , which prevents  $\beta$ -catenin degradation and allows transcription regulated by  $\beta$ -catenin/TCF to occur (121).

Stimulation of proangiogenic factors including VEGF and bFGF is another way PGE<sub>2</sub> exerts its effects on cells. In endothelial cells, VEGF and bFGF are both able to upregulate COX-2 and PL-A<sub>2</sub> expression, which generates PGE<sub>2</sub>, giving rise to a positive feedback loop (128). Furthermore, it has been discovered that PGE<sub>2</sub> is able to regulate angiogenesis through chemokine receptor signalling. The prostaglandin is capable of promoting expression of CXCR4, a chemokine receptor involved in the assembly of microvessels in vivo and induced by VEGF and bFGF (118). PGE<sub>2</sub> also exerts its proangiogenic effects through upregulation of the chemokine CXCL1 from in vivo malignancies as well as through the stimulation of in vitro microvascular endothelial cell migration and tube formation (149).

PPARs, part of the nuclear receptor family, take part in apoptosis, carcinogenesis, and immune function, amongst other functions. PPARs are able to regulate transcription through many different means, with ligand binding to the protein starting the main mechanism. This binding causes the receptor to undergo a change in conformation that leads to dissociation of co-repressors, heterodimerization with RXR- $\alpha$ , and recruitment of co-activators, resulting in activation of target genes with a PPRE direct response element (46). In a study of CRC, PGE<sub>2</sub> was found to be able to activate PPRE by transactivation of PPAR $\delta$  through a pathway that utilizes PI-3K/Akt, thereby increasing tumor growth (150).

### 1.3 COX-2 AND CANCER

Besides using PGE<sub>2</sub> in the ways mentioned in the previous section, COX-2 is able to elicit its pro-survival effect on cancer cells through the use of various other mechanisms. One of these other mechanisms is the increase of cell proliferation and inhibition of apoptosis in cancer cells. In intestinal epithelial cells, COX-2 is upregulated when the MEK pathway, a pathway that regulates apoptosis through modulation of Bcl protein expression and activity, is activated (73). The Bcl proteins acted on by COX-2 to cause the resistance to apoptosis include increased anti-apoptotic Bcl proteins such as Bcl-X<sub>2</sub> and Bcl-2, phosphorylated Bad, and decreased pro-apoptotic Bcl proteins including Bak and Bax (73; 142).

COX-2 is also able to promote angiogenesis in tumours. The enzyme has been found to be expressed in both neoangiogenic and pre-existing vasculature within and bordering tumours in numerous types of cancer, including colon, breast, and lung (72). While the complete mechanism by which COX-2 promotes angiogenesis is not known, it may be due to increased expression of VEGF. One study of Lewis lung tumours found a significant reduction in VEGF levels in COX-2 knockout mice compared to the wild-type, as well as a decrease in vascular density and VEGF mRNA (154). Another study was able to find a correlation between COX-2 and VEGF expression and the microvessel density in colorectal tumours (25).

Cell migration and invasion are other hallmarks of cancer that are linked with COX-2, in particular through the EGFR pathway. For example, the transactivation of EGFR gives rise to the promotion of COX-2 in an AP-1-mediated approach (31). In addition, one study found COX-2 to be responsible for activating matrix MMP-2 and

increasing membrane MMP RNA levels in CRC cells, resulting in increased invasiveness (141). Furthermore, binding sites for NFATs, transcription factors that further breast and colon cancer cell invasiveness, are found within the COX-2 promoter region, next to the AP-1 binding sites (161). It was found that NFAT activation leads to increased expression of COX-2 and PGE<sub>2</sub>, as well as tumor cell invasion (161).

Through the peroxidase activity of COX-2, the enzyme is capable of generating DNA mutagens. When PGH<sub>2</sub> is isomerized, a mutagen known to cause DNA frame shift mutations and base-pair substitutions, malondialdehyde, is formed (89). Additionally, COX-2 involvement with substrates such as aromatic and heterocyclic amines, and polycyclic hydrocarbon derivatives can lead to production of carcinogens (153).

The involvement of COX-2 in these many pathways makes the enzyme an enticing target for cancer therapy, including the enhancement of radiotherapy.

| Cancer type       | Percent expressing COX-2                        |
|-------------------|---|
| Head and neck     | 100%  |
| Melanoma          | 83%   |
| <b>Colorectal</b> | <b>&gt;80%, including pre-malignant lesions</b> |
| Lung              | 60-64%  |
| Pancreas          | 47%   |
| Breast            | 43%   |
| Bladder           | 34%   |

Table 1: COX-2 expression in malignant carcinomas (92).

According to the Canadian Cancer Society, CRC is one of the top 4 newly diagnosed cancers (around 13,500 new cases of CRC are diagnosed every year in Canada; the province of Alberta is expected to register about 1,000 new cases of CRCs per year). COX-2 is overexpressed in a variety of human cancers, including head and neck, lung, melanoma, and colorectal (92). Cox-2 overexpression is generally associated with poor clinical prognosis, which includes reduced survival and more aggressive tumours (92). In addition, COX-2 is overexpressed in more than 80% of CRC cases, including pre-malignant lesions (43). COX-2 expression in various malignant and pre-malignant cancers as well as COX-2 involvement in several pro-carcinogenic signalling cascades provides the basis for medical intervention using COX-2 inhibitors.

#### 1.4 NSAIDS AND COXIBS

Non-steroidal anti-inflammatory drugs (NSAIDs) such as aspirin and ibuprofen are able to inhibit both isoforms of the COX enzyme. When taken regularly, NSAIDs have been found to reduce colorectal polyp size and occurrence, and decrease the chance of contracting cancers including colon, bladder, and lung (55; 17). Treatment with NSAIDs has also been shown to stop the progression of familial adenomatous polyposis (FAP) by inducing regression and decreasing the quantity of intestinal polyps (147). However, NSAIDs are known to cause undesirable side effects including gastrointestinal problems, such as ulcers, and haemorrhagic stroke when taken for continued periods of time.

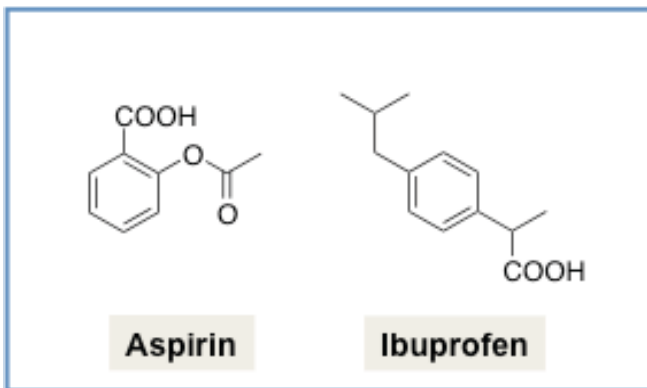


Figure 4: Structure of aspirin and ibuprofen; NSAIDs.

In order to alleviate the adverse side effects associated with NSAIDs, selective COX-2 inhibitors (coxibs) such as celecoxib, SC-236, valdecoxib, and rofecoxib were developed. Coxibs primarily exert their anti-cancer effects through the inhibition of COX-2 as well as through COX-2 independent ways, the mechanisms of which are not yet known.

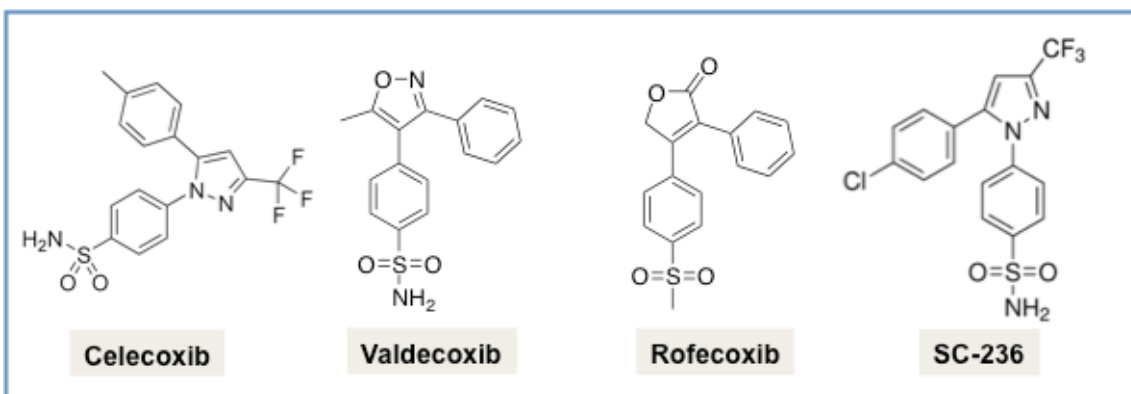


Figure 5: Structures of celecoxib, valdecoxib, rofecoxib, and SC-236; coxibs.

Three clinical trials examined the effectiveness of coxibs in patients with CRC; Adenoma Prevention with celecoxib (AP-C), Prevention Spontaneous Adenomatous Polyps (PreSAP), and Adenomatous Polyp Prevention on Vioxx (APPROVe), all of which found coxibs to be very successful (7; 3; 90). Another study found celecoxib to greatly reduce neovascularisation, metastasis, and tumor growth (6). Unfortunately, the APPROVe and AP-C trials found coxibs to cause increases in cardiovascular events such as heart attack and stroke (53). Decreased PGI<sub>2</sub> production as a result of the COX-2 inhibition is the main mechanism behind the cardiovascular side effects; however additional mechanisms are also implicated (1).

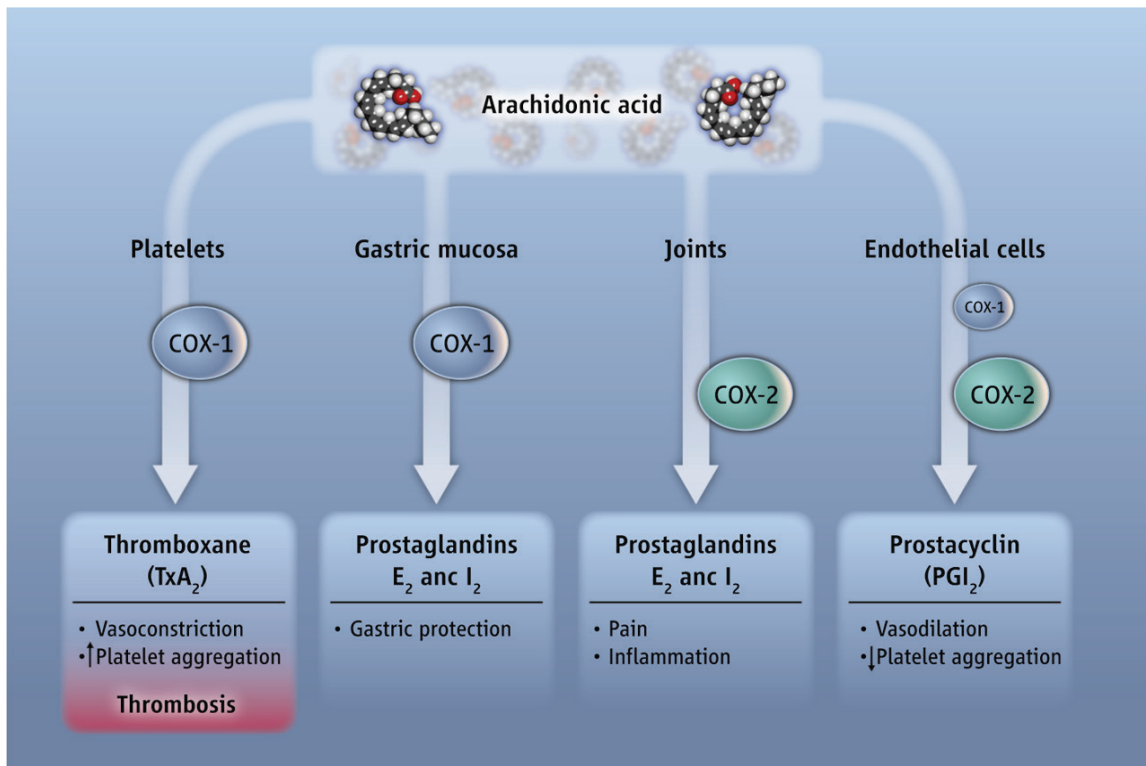


Figure 6: COX-2 downstream effects in relation to cardiovascular events (16).

Recently, it has been discovered that the increased cardiovascular risk associated with coxibs isn't an individual drug side effect but is a direct pharmacologic consequence of the inhibition of COX-2 (Figure 6). When the COX-2 gene was deleted in vascular endothelial and smooth muscle cells, the synthesis and release of nitric oxide (NO), a strong vasodilator, was decreased (16). This resulted in reduced vascular relaxation, as well as a heightened predisposition to hypertension and thrombosis (16). Therefore, the mechanism of increased cardiovascular risk from COX-2 inhibition is from specifically blocking COX-2 in blood vessels and not other tissues in the body (16). Furthermore, the cardiovascular risk is not limited to coxibs, but is in fact linked to all drugs that block COX-2 in blood vessels, including all NSAIDs (16).

### 1.5 RADIATION THERAPY AND ITS BIOLOGICAL EFFECTS

Radiation therapy is a common cancer treatment used to kill cells through either directly or indirectly ionizing DNA to cause DNA damage. Direct ionization involved radiation interacting with the atoms of DNA or another component of a cell that is critical for its survival or ability to reproduce (Figure 7). Indirect ionization of DNA, on the other hand, is brought about by the production of free radicals that cause DNA damage. In some cases, the cell exposed to radiation may be damaged but still retain the ability to reproduce; however, the daughter cells may lack a critical component and be unable to survive. Alternatively, the cell affected by radiation may simply become mutated, and pass along this mutation upon reproducing. However, if the effect on the DNA or ability to reproduce is significant enough, the cell will die. This provides the basis for radiation therapy.

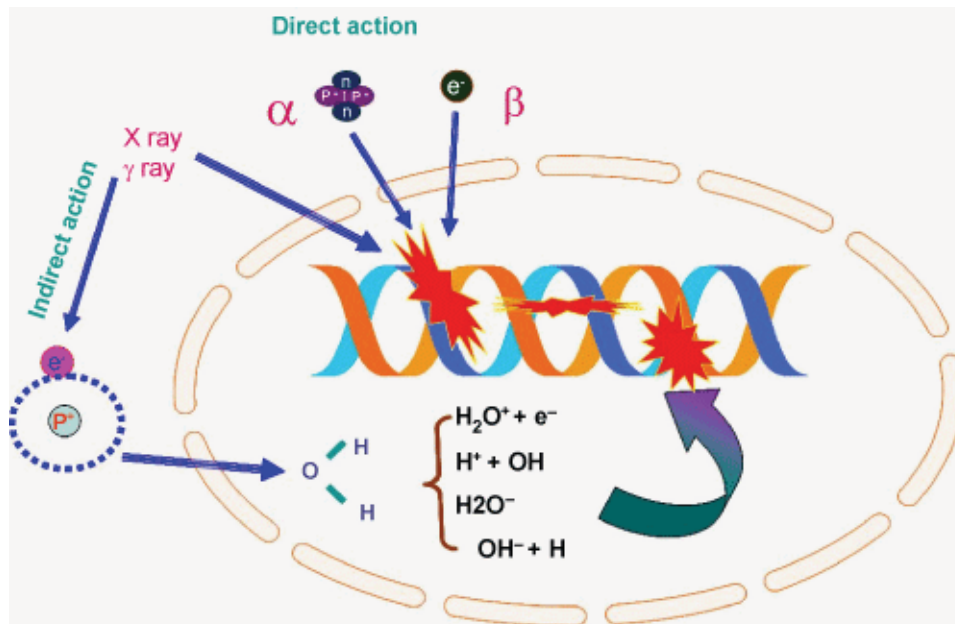


Figure 7: Biological effects of direct and indirect radiation on cells (143).

Radiation therapy can be externally applied (external-beam radiation therapy), or from a source placed inside the body (brachytherapy, systemic radiation therapy) (81). The dose of radiation given to a patient is in part dependent on the part of the body being treated; for instance, reproductive tissues and the colon are more sensitive to radiation than bones (81). A typical radiation therapy plan involves external-beam radiation therapy in which a patient receives daily small doses every day for several weeks (81). This is done to minimize damage to normal tissues as well as increase the possibility that the cancer cells are being exposed to radiation at DNA-damage-sensitive points in the cell cycle, which will lead to optimal treatment response (81).

## 1.6 TUMOUR RADIOSENSITIVITY

Radiosensitivity measures the survival and functionality of tumor cells after receiving doses of radiation comparable to treatment levels. Radiosensitivity of cells can be affected by various factors, including the reaction of chemical drug compounds with an assortment of cell components to bring about an enhanced response to radiation treatment. One of the means by which drugs are able to produce an improved radioresponse is through increased DNA damage such as strand breaks, or interference with DNA repair (145; 5; 41). p53 is an important protein involved in regulating DNA repair and cell cycle checkpoints, and as such is critical in determining the response mediated by radiation-damaged cells (57). While WT p53 normally resides in cells in low levels to limit the effect it has, cells that are exposed to radiation have been found to alter p53, resulting in its activation and accumulation, (57). While this activation of p53 was initially thought to result in either cell survival or apoptosis, it has become evident that senescence is the most common result in cells expressing WT p53 that undergo radiation therapy (57).

Chemicals are also able to alter the tumor niche, as well as target specific cells like hypoxic cells to elicit an increased response to radiotherapy (106). Furthermore, drugs can target growth factors and proteins that carry out cell signalling such as COX-2 (155; 8).

### 1.7 COX-2 INHIBITORS AS RADIOSENSITIZERS

Coxibs have been proposed to make cancer cells more sensitive to chemotherapy and radiotherapy (8; 32). Most radiosensitization studies have used celecoxib, such as a study by Raju *et al.* that found the drug to inhibit DNA repair mechanisms (110). In this study, celecoxib was shown to downregulate the expression of NF- $\kappa$ B and inhibit the kinase activity of DNA-PK, resulting in radiosensitization of the HN5 cell line due to impaired DNA strand break repair (110). Another study found celecoxib to slow NFSA tumour growth in an enhanced manner when combined with radiation (32). Further, celecoxib was discovered to result in an enhancement factor of 1.43 in A431 tumour xenografts when combined with radiation (94).

Importantly, success with celecoxib as a tool for radiosensitization has also been found in a phase I clinical trial in patients with NSCLC. When celecoxib was given concurrently with radiotherapy, local progression-free survival was 66% at 1 year and slightly higher than 42% at 2 years (82). Moreover, a phase II clinical trial was conducted in which 35 patients with rectal cancer were treated with a combination of radiation, 5-FU, and celecoxib (35). This study found that the combination was safe and resulted in better pathological outcomes in patients compared to those that did not receive celecoxib (35). Interestingly, *in vitro* and *in vivo* experiments that were performed beforehand observed that while no radiosensitizing effect was observed *in vitro* in either the COX-2 negative (HCT-116) or positive (HCA-7) cell lines, the tumours produced by the COX-2 negative cell line displayed a substantial delay in growth for combination therapy compared to radiation alone (35). This result was thought to highlight the impact the tumour microenvironment can have (35).

Rofecoxib is another coxib used to examine radiosensitization. In a study examining epithelial cell viability, rofecoxib was discovered to inhibit cell growth and movement, functions that were further hindered upon combination of treatment with irradiation (37).

Quite a bit of success has been found with the use of coxib SC-236 as a radiosensitizing agent. One study using the human glioma cell line U251 observed that the combination of SC-236 with radiation decreased cell survival *in vitro* through enhanced apoptotic death and cell detachment compared to treatment with either radiation or SC-236 alone (107). It was further found that U251 tumor xenografts exhibited a substantial decrease in tumour growth *in vivo* when treated with the combination of radiation and SC-236; a decrease that was found to be more than the additive effects of radiation and the compound (107). Similarly, *in vivo* studies performed with FSA and NFSA tumours found SC-236 to enhance tumour growth delay and shrinkage when combined with radiation therapy (73; 93). Another study found SC-236 to induce radiosensitivity through arresting cells in the G2/M cell cycle phase (111). However, almost all other data does not support this mechanism (124).

Multiple studies have found coxibs to induce radiosensitivity through COX-2 independent mechanisms, including impaired DNA repair through the inhibition of EGFR nuclear transport (39). Conversely, more recent studies comparing chemotherapy alone or in combination with coxibs have not shown the benefits discovered in the initial studies (2). This is also true for radiosensitization studies on human glioma and prostate cancer cells, which found radiosensitization to occur after administration of COX-2 inhibitors regardless of COX-2 level in the cells (100; 76). Rather than being dependent on the level

of expression of COX-2, the application of the various COX-2 inhibitors prior to exposure to irradiation was the determining factor in cell death (76).

Further investigation into the effectiveness of coxib combination therapy is needed, with focus on individual cancer types as well as the level of COX-2 expression in the tumour. Additionally, examination of the mechanisms behind radiosensitization and chemoprevention related to coxibs, particularly the COX-2 dependent versus independent mechanisms, would be highly beneficial.

## 1.8 PET IMAGING OF CANCER

A PET (positron emission tomography) scan is a nuclear imaging technique that uses radiation to produce 3-dimensional, color images of the functional processes within the human body. The machine detects pairs of gamma rays that are emitted indirectly by a tracer (positron-emitting radionuclide; for example, carbon-11 or fluorine-18) that is placed in the body on a biologically active molecule (Figure 8). The images are reconstructed by computer analysis, and reveals how parts of the patients body function by the way they break down the radiotracer. A PET image displays different levels of positrons according to brightness and color. In relation to cancer, PET scans can be used for diagnosis, as well as to monitor therapy and progression of the disease.

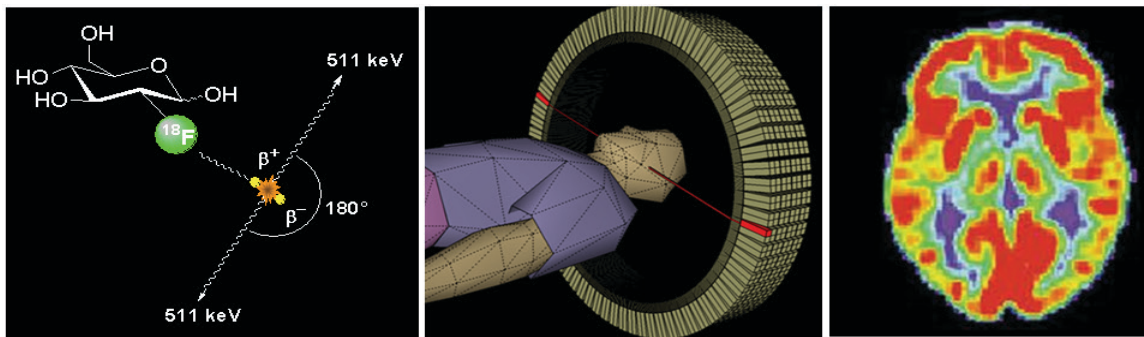


Figure 8: Depiction of how a PET scan works. Courtesy of Jens Langner from the University of Michigan website.

PET scans are excellent agents for the imaging of cancer because they are noninvasive and have been found to be more specific and sensitive than CT or MRI scans. Two radiotracers employed often in the clinic, [ $^{18}\text{F}$ ]FDG (2-deoxy-2- $^{18}\text{F}$ fluoro-D-glucose) and [ $^{18}\text{F}$ ]FLT (3'-deoxy-3'- $^{18}\text{F}$ fluorothymidine), both use the isotope fluorine-18, which has a half-life of roughly 110 minutes. FDG is a glucose analogue and is transported into cells via the same carrier, glucose transporters (GLUT) (Figure 9)

(125). However, FDG is taken into cells at a much higher rate than glucose, and mainly uses transporters GLUT-1 and GLUT-3 (125). After entering the cells, FDG is phosphorylated by hexokinase II, and due to the missing hydroxyl group at position 2', is unable to be acted on by glucose-6-phosphate isomerase II (G6-PI II) (125). This results in the inability of FDG to proceed any further down the glucose metabolic pathway, and instead it is only able to leave the cell slowly through the action of glucose-6-phosphatase (125). This is essentially how FDG is trapped in the cell, and is the basis for the data FDG-PET scans analyze

The data from FDG-trapping in patients is able to provide information on up-regulation of glucose metabolism in cancer, depicting where tumours are located in a patient as well as the size of tumours (45; 125). However, due to high background-levels of FDG uptake in certain areas of the body, such as the brain, its use is limited to a certain extent (125). In addition, cells also take up FDG rapidly in inflammatory environments, which can lead to ineffective diagnoses or monitoring of therapy, in particular with regards to surgery follow-up (36).

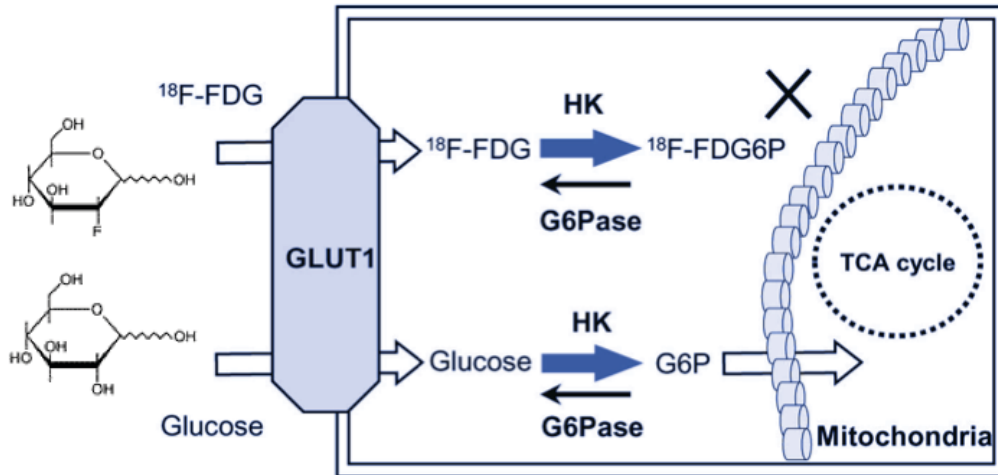


Figure 9: Mechanism of FDG uptake and trapping in cells for PET imaging (63).

$[^{18}\text{F}]\text{FLT}$  is an analogue of pyrimidine that gives insight into the activity of thymidine-kinase-1 during mitosis, specifically the S-phase (113). FLT gains entry into cells through the action of  $\text{Na}^+$ -dependent active nucleoside transporters (NTs) and, to a lesser extent, through passive diffusion (Figure 10) (113). Once FLT is inside the cell, it is phosphorylated by thymidine kinase 1 (TK1) (113). Like FDG, it cannot proceed further down the pathway due to the missing hydroxyl group but remains trapped in the cell due to the phosphate group (113). FLT uptake is cell cycle-dependent and is thought to depict the amount of actively proliferating cells, as TK1 levels increase slightly before and during S-phase (113). FLT uptake may present a more accurate treatment response in comparison to FDG as inflammatory cells have only a minor tendency to proliferate upon entry into a tumour, resulting in the inflammatory response having less of an effect on FLT uptake (47). However, while it may be a promising tool for examining therapeutic response, several studies have found it to show lower uptake than FDG in various tumours, lending doubt to its use as a reliable diagnostic tool (26; 38).

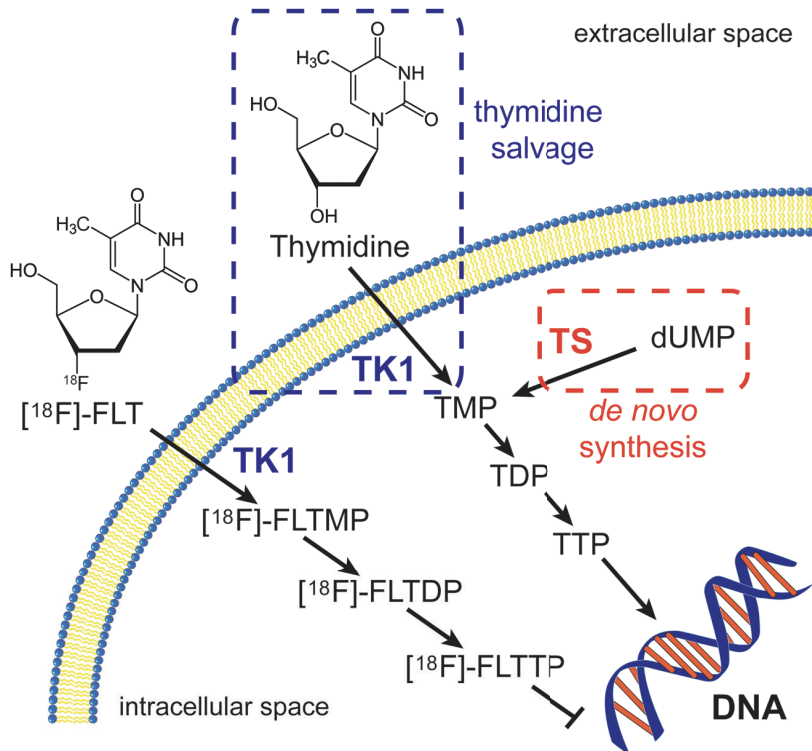


Figure 10: Mechanism of FLT uptake and trapping in cells for PET imaging (91).

Based on the successes and failures of the above-mentioned radiotracers, our lab aimed to develop a radiotracer based on the detection of COX-2-increased cell metabolism. This would not only be a tool that could be used to gain a greater understanding of the role of COX-2 in cancer, but could also be used for other diseases including arthritis. Currently, only *ex vivo* methods are possible for examining COX-2 expression, and these methods are invasive and arduous (139). Some  $^{18}\text{F}$ - and  $^{11}\text{C}$ -labeled COX-2 inhibitors have been developed, but the compounds have had many barriers preventing their success (48; 134;139; 144). One such barrier is high lipophilicity of the tracers, which resulted in inconsistent results, possibly due to nonspecific binding (48; 134; 139; 144). Stability of the compounds *in vivo* is also an issue (48; 134; 139; 144).

The new selective COX-2 tracer developed in our lab has the potential to be used not only as an imaging agent, but also as a possible therapeutic agent for cancer therapy. This project deals with using the non-radiolabeled form of the compound as a selective COX-2 inhibitor, and examining its potential for use as a radiosensitizing agent for cancer therapy.

## 1.9 *HYPOTHESIS AND OBJECTIVES*

The objective of this project was to evaluate a novel selective COX-2 inhibitor as a potential radiosensitizing agent for cancer therapy. It was hypothesized that through improved potency and selectivity, the novel selective COX-2 inhibitor would enhance the efficacy of radiation therapy. The aim of the project was to 1) establish and characterize a working biological model for assessing the role of COX-2 in CRC and its therapeutic implications; and 2) to determine the effects on an enhanced efficacy of radiotherapy through increased apoptotic events induced by the novel COX-2 inhibitor.

## **2. MATERIALS AND METHODS**

### *2.1 General*

All experiments were performed with cell lines HCA-7 (human colon adenocarcinoma; colony 29, ECACC 2091238) and HCT-116 (human CRC; ATCC CCL-247). HCA-7 cells express both mutant and WT p53 and it is believed the mutant form is dominant, while HCT-116 cells express only p53 WT. Cells were routinely cultivated in Dulbecco's Modified Eagle Medium: Nutrient Mixture F-12 (DMEM/F-12, in house) medium, supplemented with 10 % (v/v) heat-inactivated fetal bovine serum (FBS, Gibco 12483), penicillin-streptomycin (1 %; Gibco 15140), 2-[4-(2-hydroxyethyl) piperazin-1-yl] ethanesulfonic acid (HEPES, 10mM; Gibco 15630), and L-glutamine (2 mM; Gibco 25030) at 37 °C and 5 % CO<sub>2</sub> in a humidified incubator.

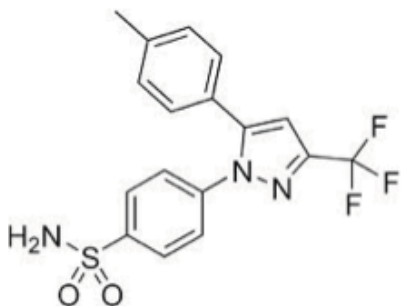
## 2.2 *Statistics*

All data was compiled as mean  $\pm$  SEM. The data from the cellular uptake and blocking studies was examined by the unpaired Student's t-test using GraphPad PRISM software. The data from the MTT radiosensitization experiments, flow cytometry, and  $\beta$ -galactosidase staining was examined by two-way ANOVA using GraphPad PRISM software.

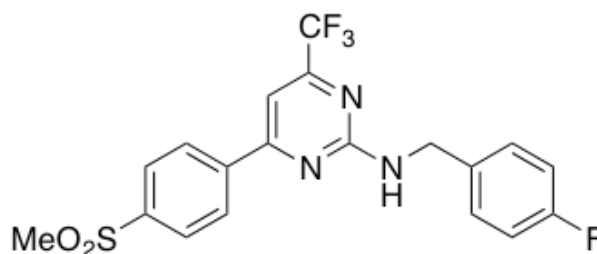
### 2.3 Compounds

N-(4-Fluorobenzyl)-4-[4-(methylsulfonyl)phenyl]-6-(trifluoromethyl)pyrimidin-2-amine (Pyricoxib) was synthesized in house according to the procedure published by Tietz *et al.* (140).

Celecoxib was obtained from LC Laboratories (Catalogue #C-1502).



**Celecoxib**  
IC<sub>50</sub> (COX-2): 40 nM



**Pyricoxib**  
IC<sub>50</sub> (COX-2): 7 nM

Figure 11: Structures and IC<sub>50</sub> values of celecoxib and pyricoxib.

## 2.4 Western Blot

For the *in vitro* Western Blot against COX-2, 50 µg of protein for each sample was heated at 95 °C for 10 minutes and then loaded and run at 120V for 1 hour on IDGel (IR121s). Transfer from the SDS-PAGE to PVDF (Polyvinylidene fluoride) membrane was done at 4 °C overnight at 35V. The membrane was then washed in PBS once for 5 minutes before blocking in 5 % skim milk + 0.1 % Tween-20 + PBS for 1 hour at room temperature (RT). The membrane was then washed once with PBST (PBS+0.1 % Tween-20) for 5 minutes, followed by incubation with the COX-2 primary antibody (1:500; Santa Cruz sc-70879 mouse monoclonal) and β-actin primary antibody (1:1000; Sigma A5060 rabbit monoclonal) for 1 hour at RT. Two more washes with PBST for 5 minutes each were done, followed by incubation of the membrane with the COX-2 secondary antibody (1:1500; Santa Cruz sc-2005 goat anti mouse) and β-actin secondary antibody (1:10000; Sigma A0545 goat anti rabbit) for 1 hour at RT. The membrane was washed with PBST 3 times for 5 minutes each, followed by one wash with PBS for 5 minutes. The membrane was then incubated with a 1:1 mixture of substrates from Pierce ECL Western Blotting Substrate (Thermo Scientific 32209) for 1 minute before gently rinsing with water and then developed.

## 2.5 Cellular Uptake Studies

For the uptake studies, cells were seeded in 12-well plates at a density of 400,000 cells/mL and grown to 90-95 % confluence. The cell tracer uptake experiments using compounds 2-deoxy-2- $^{18}\text{F}$ fluoro-D-glucose ( $^{18}\text{F}$ FDG), 3'-deoxy-3'- $^{18}\text{F}$ fluorothymidine ( $^{18}\text{F}$ FLT), and  $^{18}\text{F}$ Pyricoxib (300 KBq/mL; specific activity: >40 GBq/ $\mu\text{mol}$ ) were performed in triplicate.  $^{18}\text{F}$ FDG and  $^{18}\text{F}$ FLT uptake studies were done in Krebs buffer and Krebs buffer + 5 mM Glucose at 37 °C for 5, 10, 15, 30, 60, 90, and 120 min.  $^{18}\text{F}$ Pyricoxib uptake studies were done in Krebs buffer at 4 and 37 °C for 5, 10, 15, 30, 60, 90 and 120 min. All uptake studies began with a 1 hour preincubation with KREBS buffer. For blocking studies for  $^{18}\text{F}$ Pyricoxib, the cells were preincubated with 10  $\mu\text{M}$  and 100  $\mu\text{M}$  of either non-radiolabeled pyricoxib, celecoxib, rofecoxib, or SC58125 for 30 min before the radiotracer was added. All blocking data was obtained 60 min after addition of the radiotracer. The tracer uptake was stopped with 1 mL ice-cold PBS, the cells were washed two times with PBS and lysed in 0.4 mL Radioimmunoprecipitation assay (RIPA) buffer. The radioactivity in the cell extracts was measured with a PerkinElmer WIZARD2 Automatic gamma counter. Uptake data for all experiments are expressed as percent of injected dose per 1 mg protein (%ID/mg protein).

## 2.6 *Bicinchoninic Acid (BCA) Assay*

Protein was quantified from the cellular uptake studies by adding 300  $\mu\text{L}$  CellLytic M Cell Lysis Reagent (Sigma C2978) per well (2 wells per compound or treatment tested) and then leaving the plate on the shaker for 10 minutes. The contents of each well were then put in separate Eppendorf tubes and centrifuged (4  $^{\circ}\text{C}$  at 10,000 rpm for 8 minutes). The samples were left in -20  $^{\circ}\text{C}$  until use.

The BCA assay was performed by loading 25  $\mu\text{L}$  of each standard (800, 600, 400, 300, 200, 100, 50  $\mu\text{g}/\text{mL}$ , blank) and sample into individual wells of a 96 well plate. A mix of 1:50 of B:A BCA reagents was made, and 200  $\mu\text{L}$  of the mixture was added to each well. The plate was then incubated for 25 minutes in a 37  $^{\circ}\text{C}$  and 5%  $\text{CO}_2$  incubator before reading the plate at 562 nm.

## 2.7 *Methyl Thiazol Tetrazolium (MTT) Assay*

To begin the MTT assay, cells were seeded in 96-well plates in 200  $\mu\text{L}$  of culture medium. After adding cells to wells, the plate was put on a shaker for 10-15 minutes to ensure cells were evenly distributed within the wells, not clumped along the edges. The plates were then incubated in  $37^{\circ}\text{C}$  for 48 hours. Next, the drugs of interest were added to each well (8 wells per drug) and placed on a shaker for 5 minutes to mix the drugs well, followed by incubation for 24 hours. For the toxicity assay, concentrations of 1000, 300, 100, 30, 10, 3, and 1  $\mu\text{M}$  of both celecoxib and pyricoxib were used. For the radiation sensitivity assay, concentrations of 30 and 75  $\mu\text{M}$  of both celecoxib and pyricoxib were used. For the radiation sensitivity assay, drugs were removed from wells and 200  $\mu\text{L}$  of fresh culture medium per well was added immediately before irradiation to 5, 10, 15, or 20 Gy. 72 hours after irradiation, media was aspirated from wells and washed 2 times with PBS to remove loosely attached and dead cells. 100  $\mu\text{L}$ /well of media and 10  $\mu\text{L}$  of MTT reagent were added directly to the medium of each well and mixed gently for 1 minute on a shaker, followed by incubation for 4 hours at  $37^{\circ}\text{C}$ . 100  $\mu\text{L}$  of Solubilization Buffer was then added to each well, and the plates were foil wrapped and placed on the shaker for 30 minutes. The absorbance in each well was then measured at 570 nm and 690 nm (for background absorbance) using a microplate reader.

## 2.8 *Flow cytometry*

To begin the flow cytometry assay for analysis of apoptotic cells, cells were seeded in 6-well plates in 2 mL of culture medium. After adding cells to wells, the plate was put on a shaker for 10-15 minutes to ensure even distribution of cells within the wells. The plates were then incubated in 37°C for 48 hours. Next, the drugs of interest (concentrations of 30 and 75  $\mu$ M of both celecoxib and pyrcoxib) were added to each well (2 wells per drug) and placed on a shaker for 5 minutes to mix the drugs well, followed by incubation for 24 hours. The drugs were then removed from wells and 2 mL of fresh culture medium per well was added before irradiation to 5, 10, 15, or 20 Gy. 72 hours after irradiation, 0.25% Trypsin-EDTA was warmed to 37°C in a water bath. Old media was collected and put in a centrifugation tube to ensure that detached/floater cells were included. 0.3 mL 0.25% Trypsin-EDTA was added to detach the cells, and the plates were then placed in a 37°C incubator for 2 minutes. 3 mL  $\text{Ca}^{2+}$ - and  $\text{Mg}^{2+}$ - free PBS (10X the amount of trypsin added) was added to the trypsin and cells.

The cells were transferred to sterile centrifuge tubes (the same ones containing old medium with detached/floater cells), and spun down (1300 rpm for 4 minutes), followed by removal of the supernatant. Cells were resuspended in 2 mL of PBS, spun down again, and PBS was removed. Cells were then suspended in 1-5 mL 1X Binding Buffer, and cell counts were performed. Cells were then spun down once more, and the Binding Buffer was removed. Cells were resuspended in 1X Binding Buffer at  $10^6$  cells/mL. 100  $\mu$ L of cell solution was transferred to a 5 mL flow tube for each treatment, followed by the addition of 3  $\mu$ L FITC-Annexin V and 3  $\mu$ L PI (propidium iodide) to each flow tube. Cells were vortexed and incubated for 15 minutes at RT in the dark. 400  $\mu$ L of 1X

Binding Buffer was then added to each tube and the cells were analyzed by flow cytometry within 1 hour.

## 2.9 *Microscopy*

For the staining experiments, cells were seeded in 6-well plates in 2 mL of culture medium. After adding cells to wells, the plate was put on a shaker for 10-15 minutes to ensure even distribution of cells within the wells. The plates were then incubated in 37 °C for 48 hours. Next, the drugs of interest (concentrations of 30 and 75 µM of both celecoxib and pyricoxib) were added to each well (2 wells per drug) and placed on a shaker for 5 minutes to mix the drugs well, followed by incubation for 24 hours. The drugs were then removed from wells and 2 mL of fresh culture medium per well was added before irradiation to 5 or 10 Gy.

For the GIEMSA staining experiment, 72 hours after irradiation the media was removed from the wells and the wells were washed once with PBS and once with a 1:1 mixture of PBS:methanol, followed by the addition of 1 mL methanol per well to fix the cells. Cells were then stored in the -20 °C freezer until use. The methanol was removed from each well and the plates were left to dry for 10 minutes before adding the stain (1:20 dilution of the stain with deionized water). The stain was left on the cells for 5 minutes and then removed, the cells were rinsed briefly with deionized water to remove excess stain, and left for 10 minutes to dry once more. Images were then taken at 10X magnification using Motic software.

For the β-galactosidase experiment, the Sigma Senescence Cells Histochemical Staining Kit (Catalog # CS0030) was used. 72 hours after irradiation, cells were washed with 1 mL of PBS per well followed by fixation with 1.5 mL per well of 1x Fixation Buffer for 6 minutes. Cells were then rinsed twice with 1 mL of PBS per well, and 1 mL per well of the Staining Mixture was then added. The cells were incubated at 37 °C

without CO<sub>2</sub> for 12 hours. The Staining Mixture was then removed and 1 mL of PBS per well was added. Images were taken at 10X magnification using Andor software.

### 3. RESULTS

#### 3.1 *Western Blot*

In order to properly characterize the cell lines used, a Western Blot was performed in order to evaluate the COX-2 expression levels in both the COX-2 positive (HCA-7) and COX-2 negative (HCT-116) cell lines. As shown in Figure 12, HCA-7 cells showed high expression levels of COX-2, while HCT-116 cells exhibited no expression of the enzyme.

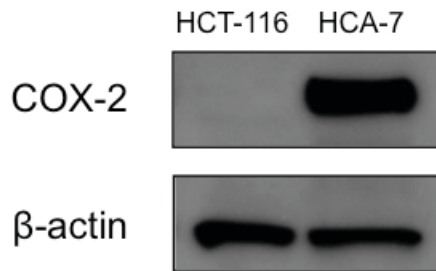


Figure 12: Evaluation of COX-2 levels in CRC cell lines. After SDS-PAGE, Western Blotting was used for detection of COX-2 in HCT-116 and HCA-7 cell lines.  $\beta$ -actin was used as loading controls.

This process was repeated several times, at various passage numbers, in order to determine whether COX-2 expression levels were constant. Both cell lines were found to maintain consistent COX-2 expression or lack thereof after numerous passages.

### 3.2 *Cellular Uptake Studies*

Cellular uptake studies were performed with [ $^{18}\text{F}$ ]FDG, [ $^{18}\text{F}$ ]FLT, and [ $^{18}\text{F}$ ]pyricoxib in order to determine the metabolic, proliferative, and COX-2 activity of each cell line, respectively.

As shown in Figures 13 and 14, the two cell lines had similar metabolic activity based on [ $^{18}\text{F}$ ]FDG uptake. Furthermore, [ $^{18}\text{F}$ ]FDG uptake was shown to be blocked, reducing the uptake of the tracer to nearly zero, when cells were treated with 5 mM glucose along with the tracer. This complete blocking effect demonstrated that the correct uptake mechanism in both cell lines was intact.

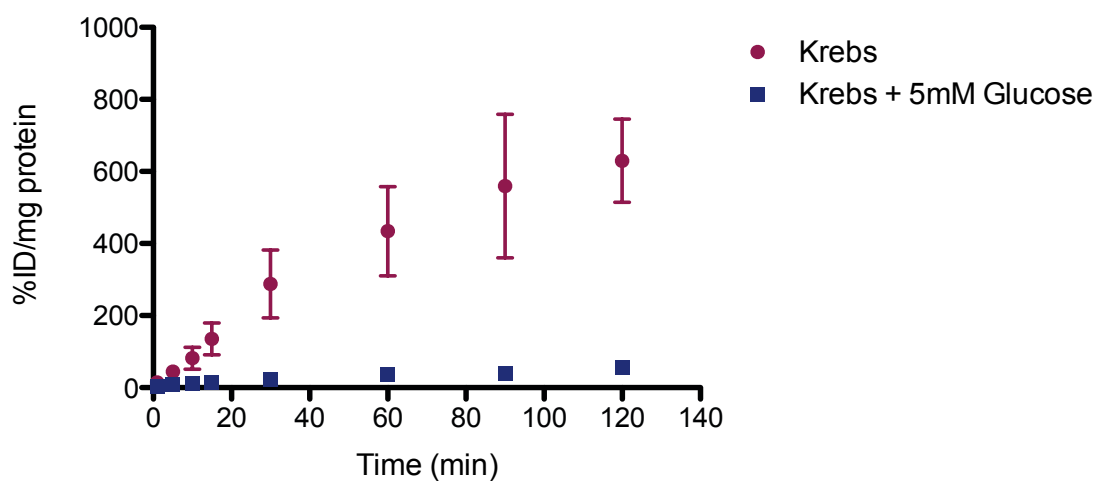


**Figure 13:** Uptake of [<sup>18</sup>F]FDG in HCA-7 cells at 37 °C in Krebs buffer or Krebs + 5 mM Glucose (n=3). Data as mean ± SEM.

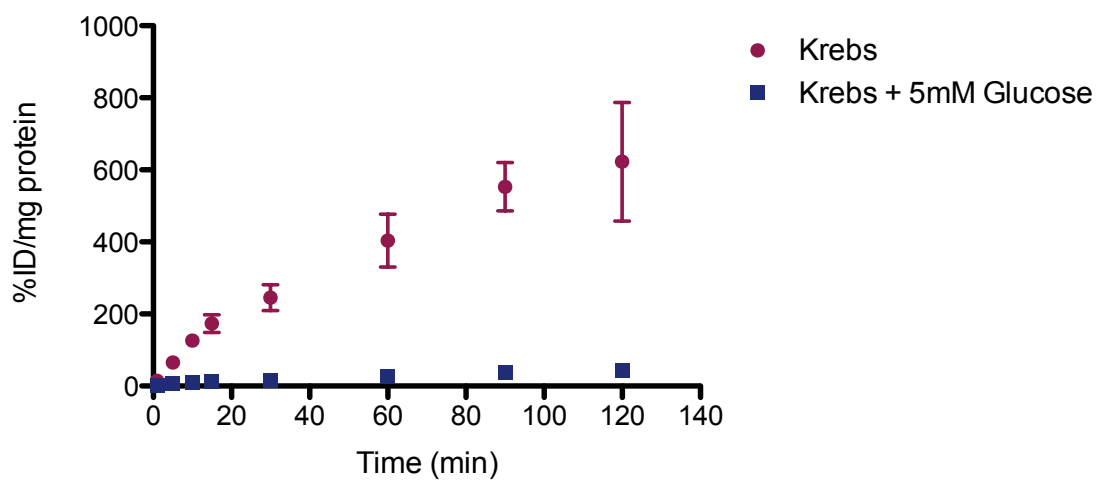


**Figure 14:** Uptake of [<sup>18</sup>F]FDG in HCT-116 cells at 37 °C in Krebs buffer or Krebs + 5 mM Glucose (n=3). Data as mean ± SEM.

The cell lines were then found to demonstrate similar [ $^{18}\text{F}$ ]FLT uptake profiles, as shown in Figures 15 and 16. Uptake increased over time, leveling out with slight fluctuations at 60 minutes elapsed time. As expected, uptake was not hindered by the addition of 5 mM glucose, validating the mechanism through which the tracer was taken up.

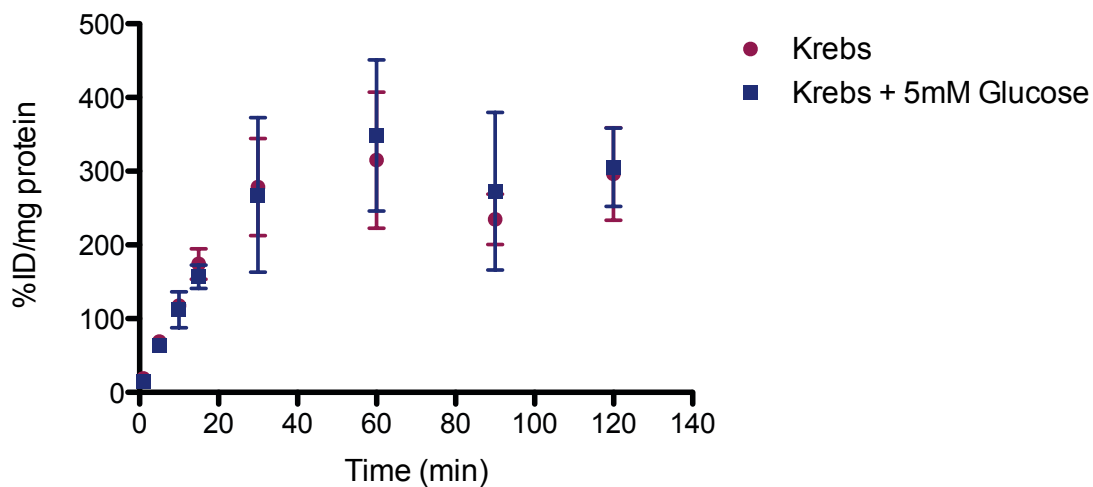


Figure 15: Uptake of [<sup>18</sup>F]FLT in HCA-7 cells at 37 °C in Krebs buffer or Krebs + 5 mM Glucose (n=3). Data as mean ± SEM.

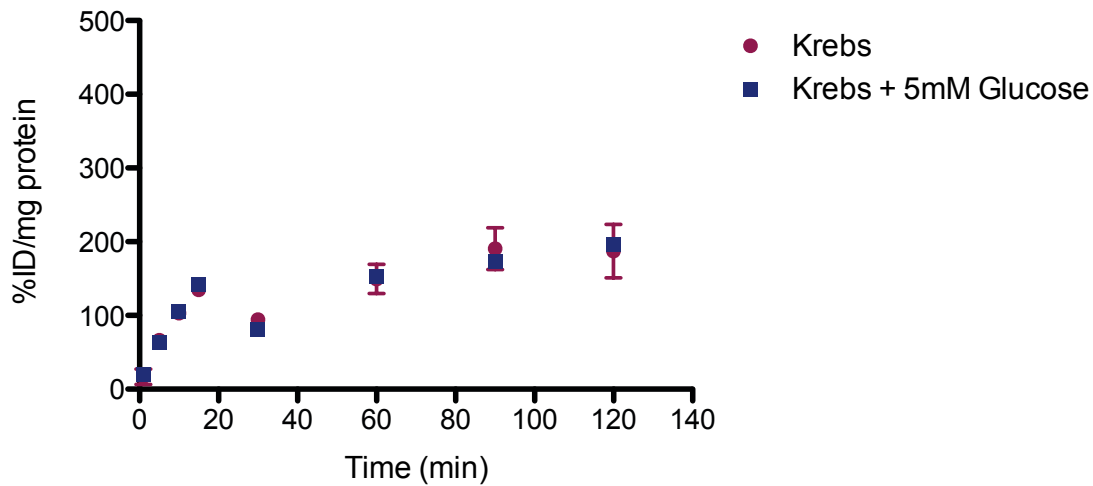


Figure 16: Uptake of [<sup>18</sup>F]FLT in HCT-116 cells at 37 °C in Krebs buffer or Krebs + 5 mM Glucose (n=2). Data as mean ± SEM.

As shown in Figure 17, [<sup>18</sup>F]pyricoxib was taken up into COX-2 positive cells, reached maximum levels at 30 minutes, and remained in the cells at a constant level until the end of the assay. Furthermore, this action was not hindered in an ATP-dependent manner, but is in fact an ATP-independent uptake mechanism, based on the similar uptake of the tracer at 4 °C.

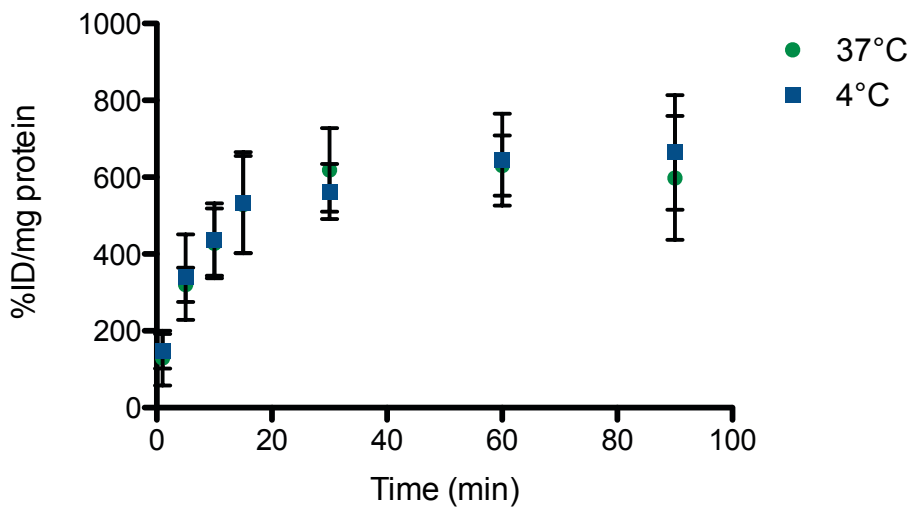


Figure 17: Uptake of [<sup>18</sup>F]pyricoxib in HCA-7 cells at 37 °C and 4 °C (n=3). Data as mean ± SEM.

Additionally, the COX-2 positive cells showed a significantly higher level of uptake of [ $^{18}\text{F}$ ]pyricoxib compared to COX-2 negative cells (Figure 18). This allowed us to conclude that the uptake of [ $^{18}\text{F}$ ]pyricoxib was at least partially due to the tracer interacting with COX-2. We surmise that the compound is kinetically trapped in the active site, due to the path through the ER membrane and long channel the compound must travel through to bind to the active site. This kinetic trapping is thought to result in the constant high uptake level seen at the later time points of the uptake study.

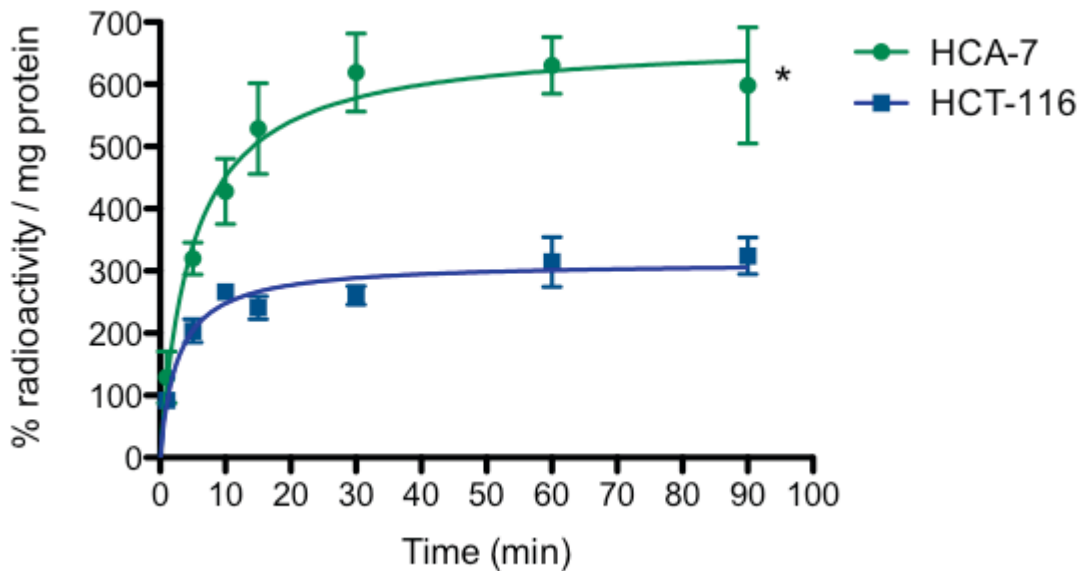
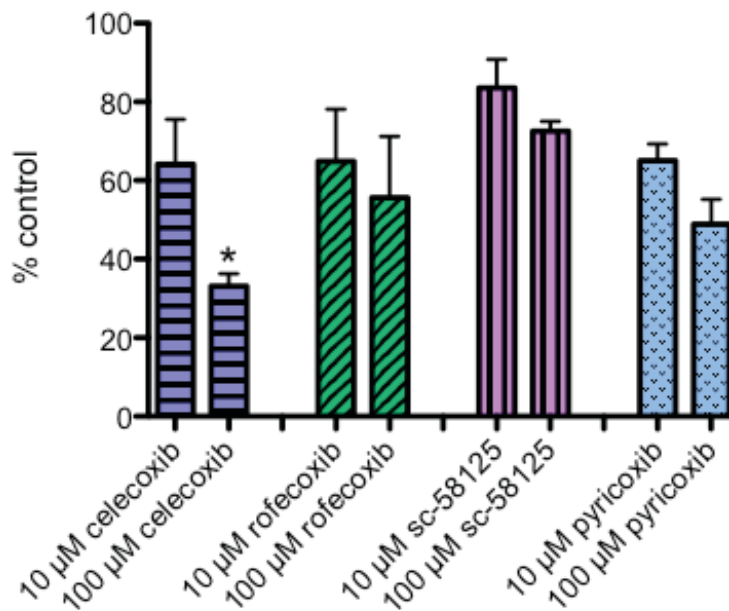


Figure 18: Uptake of [ $^{18}\text{F}$ ]pyricoxib in HCA-7 and HCT-116 cells at 37 °C (n=3). Data as mean  $\pm$  SEM.

After performing a series of blocking studies, we found that there seemed to be a concentration-dependent blocking effect on the tracer (Figure 19). Uptake of the tracer could be significantly reduced by up to 70% by preincubation of the cells with 100  $\mu\text{M}$  celecoxib compared to the 10  $\mu\text{M}$  dose of the drug. All other compounds produced a similar trend; however, not one that was statistically significant.



**Figure 19:** Uptake of [ $^{18}\text{F}$ ]pyricoxib in HCA-7 cells pre-incubated with 10 and 100  $\mu\text{M}$  COX-2 inhibitors: celecoxib, SC58125, rofecoxib, pyricoxib (n=3). Data as mean  $\pm$  SEM.

Furthermore, although high doses of each compound were used to block the tracer, uptake could not be reduced to zero. This suggests that while the uptake of [ $^{18}\text{F}$ ]pyricoxib is at least in part due to COX-2, some of the uptake is likely due to non-specific and off-target binding.

### 3.3 *Methyl Thiazol Tetrazolium (MTT) Assay*

The first set of MTT assays was done in order to determine the cytotoxicity profiles of each compound, celecoxib and pyricoxib, on both cell lines (Figures 20 and 21). The compounds were found to have similar cytotoxicity profiles; both followed a similar curve, and the drop in the curve occurred at similar concentrations. However, after a certain concentration, celecoxib produced zero proliferative and metabolically active cells in both cell lines while the curve produced by pyricoxib leveled out at approximately 50% proliferative and metabolically active cells in COX-2 positive cells and did not reduce to zero in COX-2 negative cells. It was observed that at doses exceeding 100  $\mu$ M, the compounds formed a precipitate. This difference in outcome at the highest concentration of compound tested could be due to precipitation of the compound.

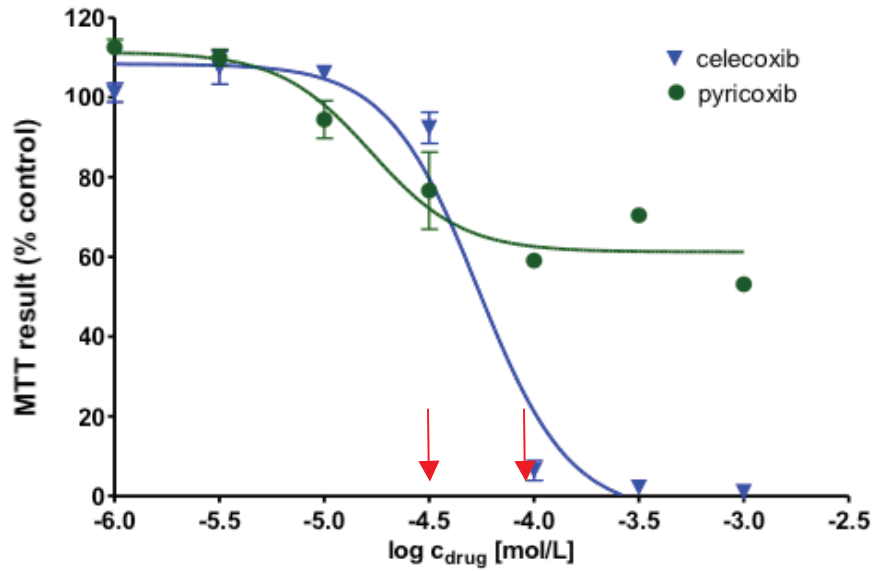


Figure 20: HCA-7 absorbance as percent control 72 h after treatment with 24 h celecoxib or pyricoxib (1, 3, 10, 30, 100, 300, 1000  $\mu$ M each) (n=3). Data as mean  $\pm$  SEM.

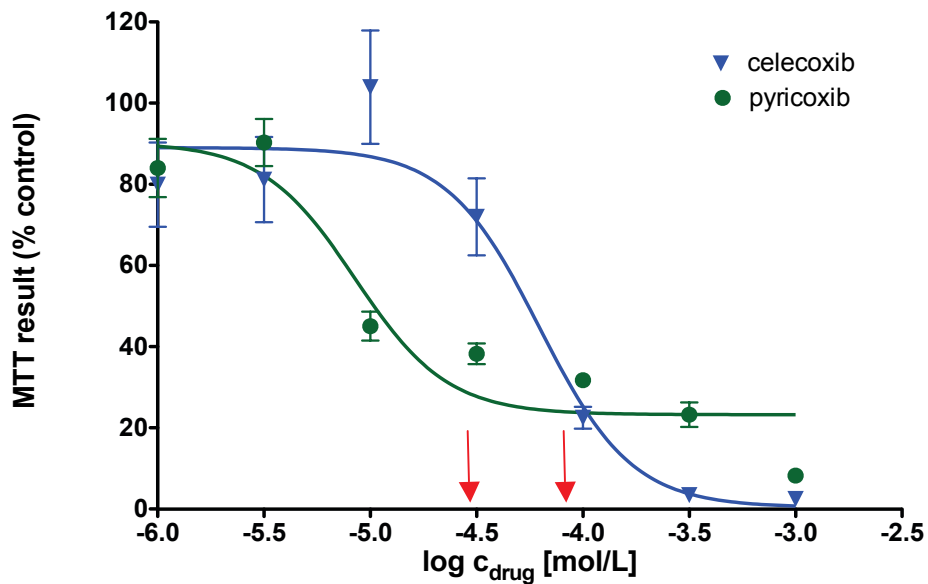


Figure 21: HCT-116 absorbance as percent control 72 h after treatment with 24 h celecoxib or pyricoxib (1, 3, 10, 30, 100, 300, 1000  $\mu$ M each) (n=3). Data as mean  $\pm$  SEM.

The curves were also used in order to determine the optimal two concentrations of the drugs to carry forward in subsequent assays. The ideal concentrations would not be so cytotoxic as to outright kill the cells or leave none able to proliferate and metabolize, nor so low that no response would be evident, but would be at a high enough concentration to elicit a response that could be enhanced. Based on this reasoning and their placement on the curves in Figures 20 and 21, the concentrations of 30 and 75  $\mu\text{M}$  (indicated by red arrows) were chosen for both drugs.

The second set of MTT assays was performed in order to produce preliminary radiosensitization results of the two concentrations of each compound at various radiation doses. The data set for each drug dose was compared back to the control treatments at each radiation dose in order to produce the curves for Figures 22 and 23. If a significant difference between the control and treated cells had been produced, the curves in Figures 22 and 23 would have negative slopes, indicative of an enhanced response in the treated cells, which could possibly be due to radiosensitization. However, there was no significant difference between the control and treated cells, in either cell line, with regards to relative cell proliferation and metabolism as indicated by the MTT assay. This led us to conclude that based on the MTT assay, at the conditions examined, a radiosensitizing effect was not evident.

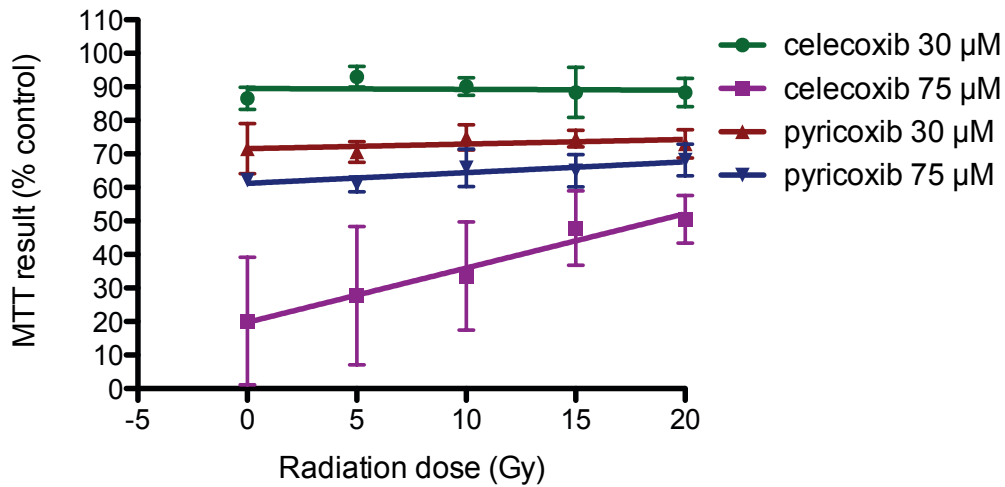


Figure 22: HCA-7 absorbance as percent control 72 h after treatment with 30 and 75 μM celecoxib and pyricoxib for 24 h, followed by irradiation to 0, 5, 10, 15, and 20 Gy (n=3). Data as mean ± SEM.

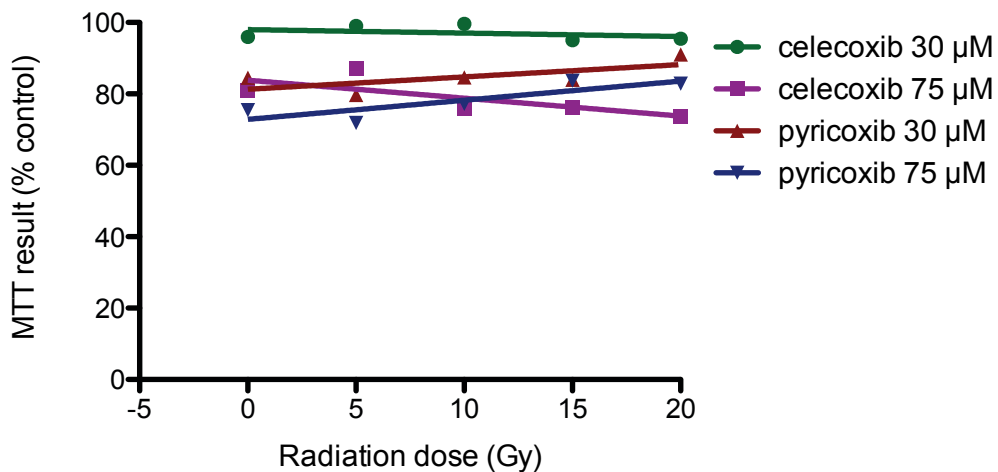


Figure 23: HCT-116 absorbance as percent control 72 h after treatment with 30 and 75 μM celecoxib and pyricoxib for 24 h, followed by irradiation to 0, 5, 10, 15, and 20 Gy (n=3). Data as mean ± SEM.

### 3.4 *Flow cytometry*

Flow cytometry with annexin V-FITC and PI was then carried out in order to determine whether treatment with the drugs in combination with radiation produced an enhanced cell-killing effect through increased apoptotic events. Both cell lines were resistant to radiation-induced apoptosis. The COX-2 positive cell line, HCA-7, was found to have 50% of cells undergo apoptosis at extremely high radiation doses of up to 20 Gy. HCT-116 cells, the COX-2 negative cell line, were just as resistant to radiation, with only approximately 25% of cells undergoing apoptosis when irradiated with 20 Gy.

It was observed that in the HCA-7 cells, treatment with pyrcoxib produced more apoptotic cells than the DMSO control without irradiation. However, this effect was not amplified once the cells were irradiated; rather, it appears that application of the drug at increasing radiation doses produced a radioprotective effect (Figure 24). Neither concentration of celecoxib, on the other hand, resulted in enhanced levels of apoptosis compared to the control without radiation. Similar to pyrcoxib, when the COX-2 positive cells were treated with celecoxib at increasing radiation doses, a radioprotective effect was observed.

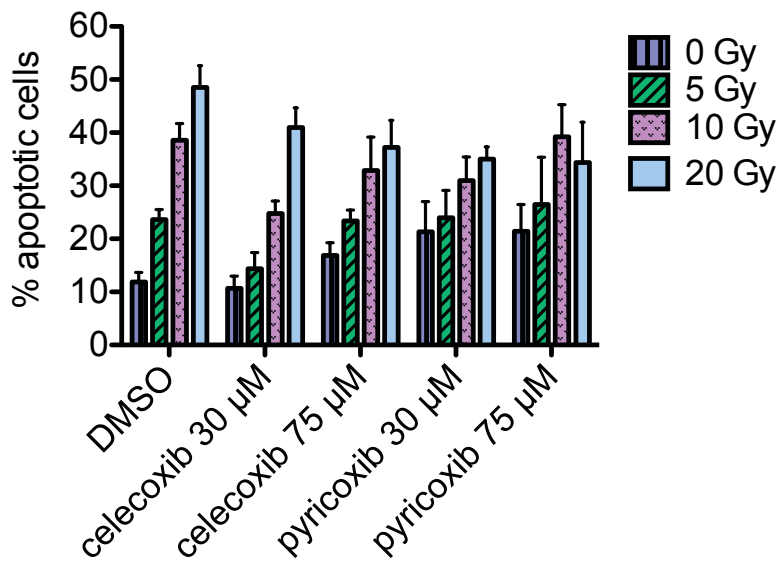


Figure 24: HCA-7 percent apoptotic cells 72 h after treatment with 30 and 75 μM celecoxib and pyrrocoxib for 24 h alone, or followed by irradiation to 5, 10, or 20 Gy (n=3). Data as mean ± SEM.

Conversely, in the COX-2 negative cell line, while neither compound appeared to produce a significant radiosensitization response based on apoptotic events, the radioprotective effect of the drugs seen in the HCA-7 cells was not evident (Figure 25). In addition, pyricoxib was not found to result in more apoptotic cells than the control cells in the absence of radiation. This suggests that pyricoxib by itself is able to stimulate cell death at least in part through the induction of apoptosis in a COX-2 dependent manner.

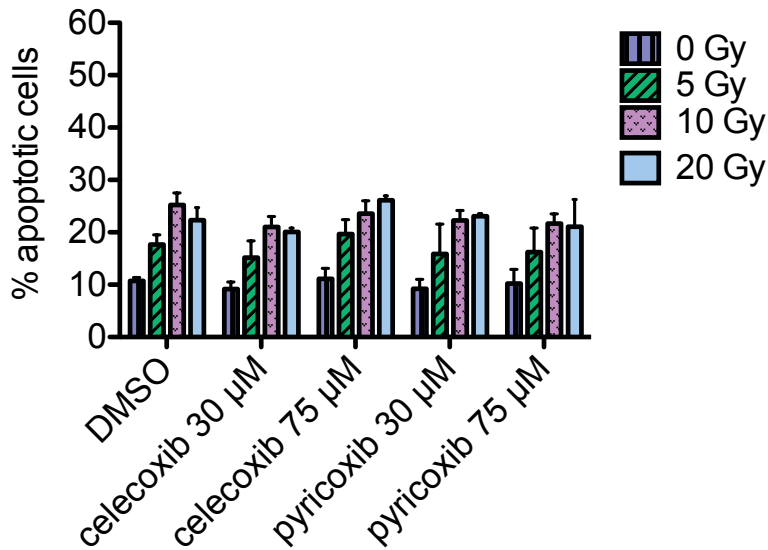


Figure 25: HCT-116 percent apoptotic cells 72 h after treatment with 30 and 75 μM celecoxib and pyricoxib for 24 h alone, or followed by irradiation to 5, 10, or 20 Gy (n=3). Data as mean ± SEM.

### 3.5 *Microscopy*

In order to provide some insight into the seemingly radioprotective effect and lack of radiosensitizing response of the compounds, a series of imaging experiments were performed; GIEMSA staining in order to visualize cell morphology differences between treatments, and  $\beta$ -galactosidase staining to provide information on whether the unexpected response was due to cells escaping apoptosis through senescence.

#### **GIEMSA staining**

In the HCA-7 cell line, as the radiation dose was increased, regardless of treatment conditions, the cells became enlarged and produced smaller tumour-like populations (Figure 26). However, both drugs were found to produce more large cells with less tumour-like populations when combined with irradiation compared to the control. This effect was most notable at the higher of the two doses for each drug (see Appendices for all images taken).

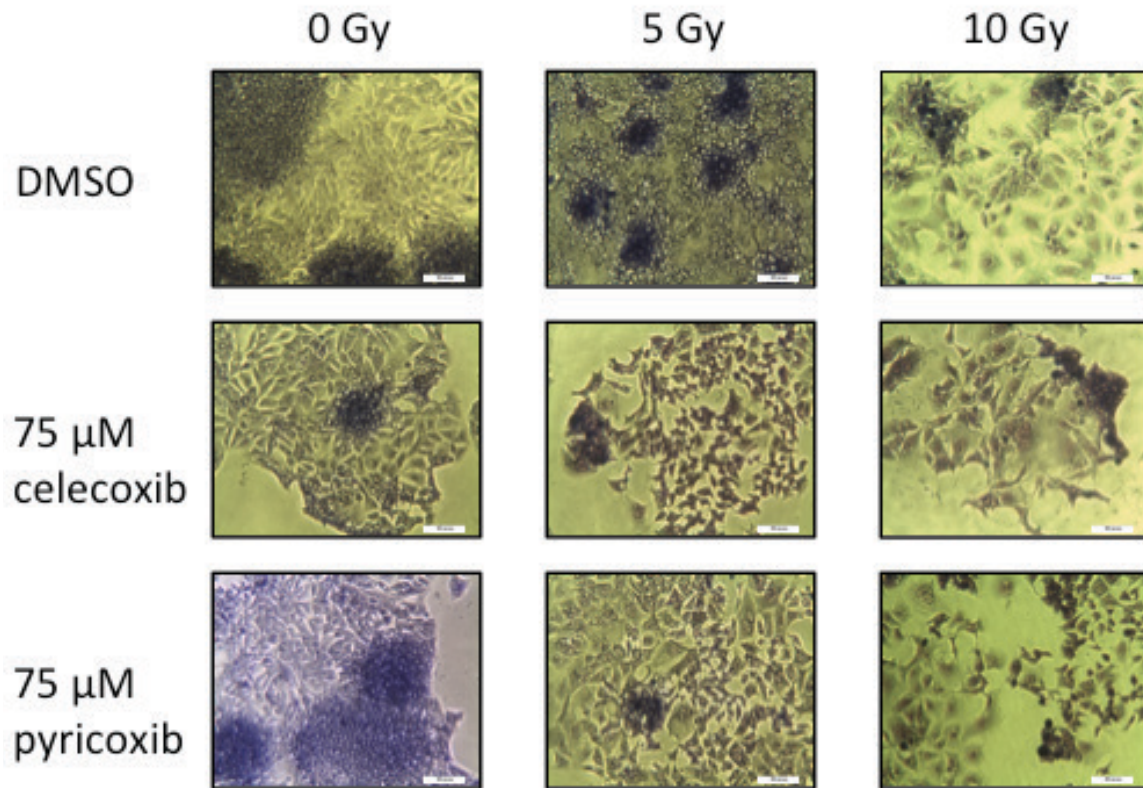


Figure 26: GIEMSA staining of HCA-7 cells 72 h after treatment with 75 μM celecoxib and pyricoxib for 24 h alone, or followed by irradiation to 5 or 10 Gy. Images taken at 10X magnification.

Similar to the COX-2 positive cell line, the HCT-116 cell line produced more large cells with increasing doses of radiation, regardless of the treatment conditions (Figure 27). However, unlike the HCA-7 cells, the effect was not enhanced when irradiation was combined with application of the compounds.

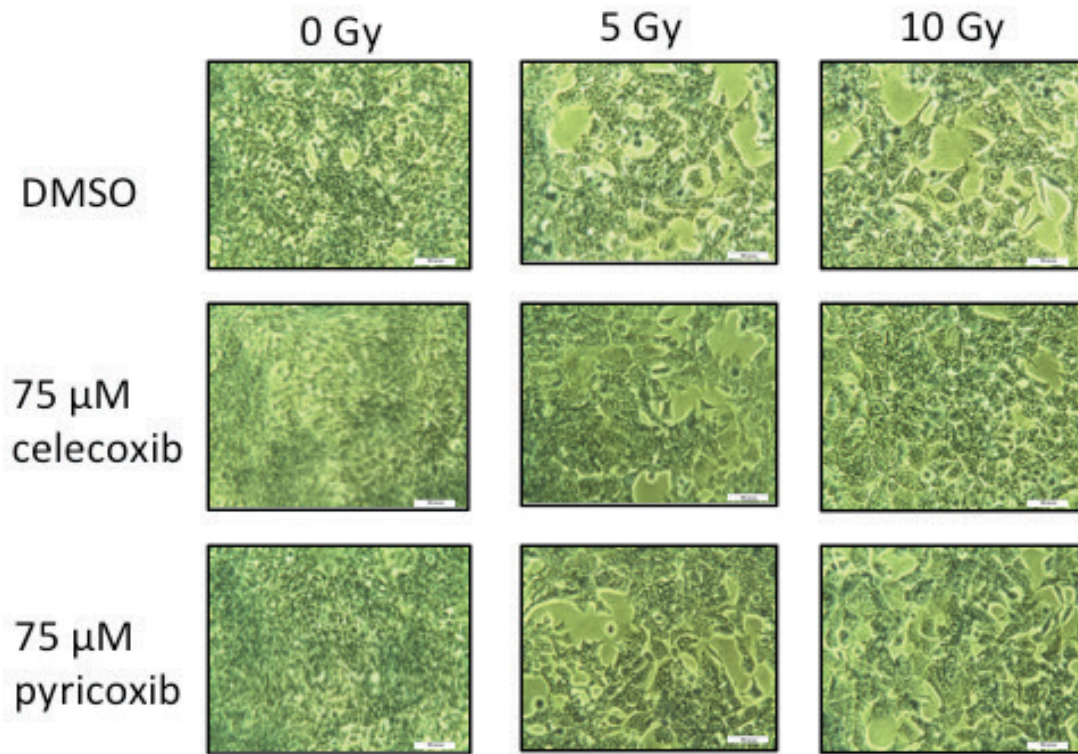


Figure 27: GIEMSA staining of HCT-116 cells 72 h after treatment with 75  $\mu$ M celecoxib and pyricoxib for 24 h alone, or followed by irradiation to 5 or 10 Gy. Images taken at 10X magnification.

These results suggest that both celecoxib and pyricoxib, through the inhibition of COX-2, are able to alter the morphology of cells. As large cells are often indicative of cells undergoing senescence, we next sought to provide preliminary information on whether senescence was in fact the process that was occurring.

### **$\beta$ -galactosidase staining**

Both cell lines were found to produce an increasing number of senescent cells at increasing radiation doses, regardless of treatment conditions (Figures 28-31). The HCT-116 cells produced relatively low levels of senescence in the absence of radiation compared to the HCA-7 cells; the HCT-116 cells ranged from 3-6% senescent while the HCA-7 cells ranged from 15-40% senescent (Figures 27-30). However, the cell lines produced similar percentages of senescent cells at the highest radiation dose of 10 Gy; the COX-2 positive cells ranged from approximately 48-63%, while the COX-2 negative cells ranged from 39-60% (Figures 28-31).

In the COX-2 positive cells, pyrcoxib 30  $\mu$ M consistently produced the most senescent cells; however, this increase in senescence was not greater than what would be expected from an additive effect. In the absence of radiation with regards to the HCA-7 cells, treatment with celecoxib at both concentrations resulted in more cells that stained positively for  $\beta$ -galactosidase than in the control and pyrcoxib. Interestingly, when celecoxib was combined with radiation, the resulting levels of senescent HCA-7 cells were more comparable to those in the other treatments, even dropping below the levels found in the pyrcoxib-treated cells.

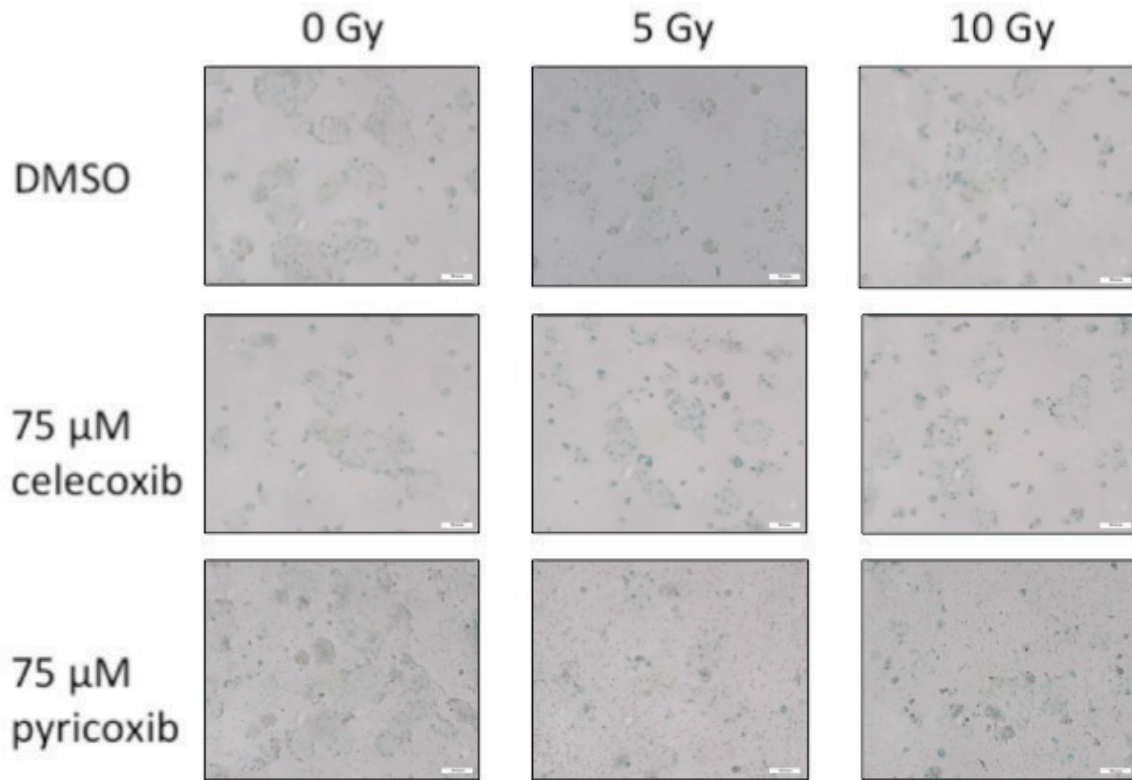


Figure 28:  $\beta$ -galactosidase staining of HCA-7 cells 72 h after treatment with 75  $\mu$ M celecoxib and pyricoxib for 24 h alone, or followed by irradiation to 5 or 10 Gy. Images taken at 10X magnification.

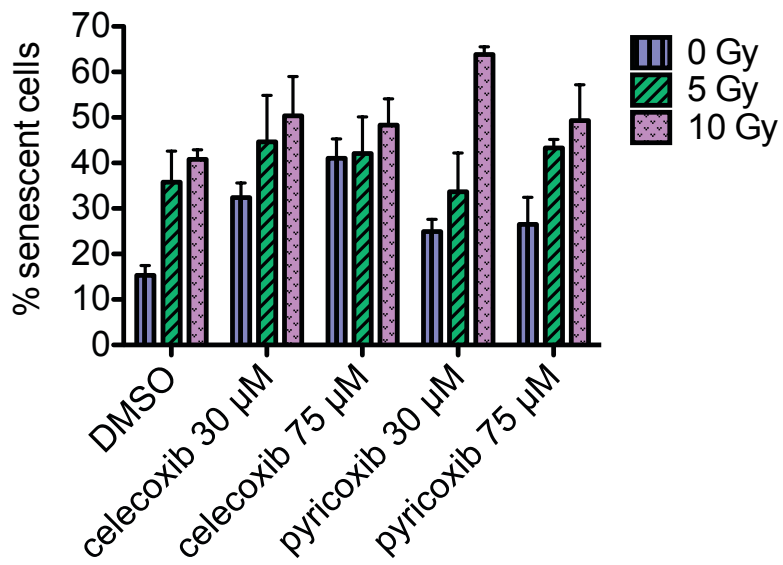


Figure 29: Percent senescent cells as determined by  $\beta$ -galactosidase staining of HCA-7 cells 72 h after treatment with 30 and 75  $\mu$ M celecoxib and pyricoxib for 24 h alone, or followed by irradiation to 5 or 10 Gy. Data as mean  $\pm$  SEM.

The amount of senescence in the COX-2 negative cells did not vary among treatment groups at each radiation dose. Rather, the most significant effect on senescence was observed to be due to increasing the radiation dose. This increase in senescence based on radiation dose was much more evident in the COX-2 negative cell line than in the COX-2 positive cell line, which demonstrated the similar trend of increasing senescence at increasing radiation doses but did so in a much less dramatic fashion.

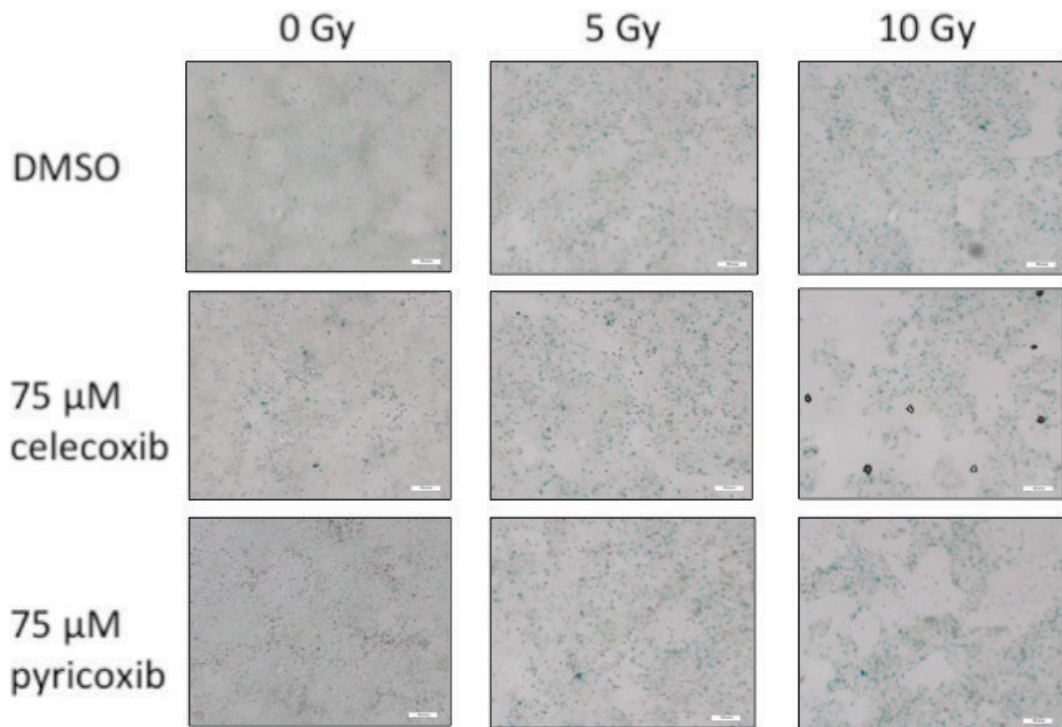


Figure 30:  $\beta$ -galactosidase staining of HCT-116 cells 72 h after treatment with 75  $\mu$ M celecoxib and pyricoxib for 24 h alone, or followed by irradiation to 5 or 10 Gy. Images taken at 10X magnification.

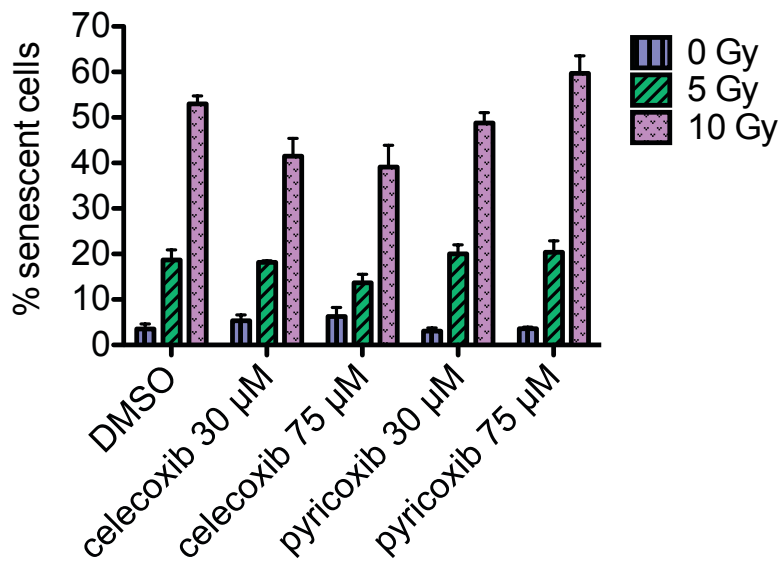


Figure 31: Percent senescent cells as determined by  $\beta$ -galactosidase staining of HCT-116 cells 72 h after treatment with 30 and 75  $\mu$ M celecoxib and pyricoxib for 24 h alone, or followed by irradiation to 5 or 10 Gy. Data as mean  $\pm$  SEM.

Based on these results, we concluded that applying increasing doses of radiation to cells, regardless of the COX-2 status, results in increasing levels of senescence. Further, as celecoxib produced higher levels of senescent cells compared to the non-irradiated control in the HCA-7 cell line but not the HCT-116 cell line, we concluded celecoxib may be able to induce senescence through the inhibition of COX-2. Additionally, at the maximum radiation dose examined, while pyricoxib was not able to enhance levels of senescence any more than might be expected from an additive effect in the HCA-7 cells, the levels were not increased at all compared to the control in the HCT-116 cells. This led us to conclude that like celecoxib, through the inhibition of COX-2, it could be possible for pyricoxib to induce cell senescence.

## 4. DISCUSSION

### 4.1 PARADIGM SHIFT OF RADIOSENSITIZATION STUDIES - IMPACT OF BIOLOGICAL MODEL?

There is a problem with one of the most commonly used biological models for CRC. There is an abundance of literature that suggests COX-2 plays a role in CRC, and that the selective inhibition of COX-2 produces a radiosensitizing effect (61; 120; 33; 151; 165). However, many of these studies used HT-29 cells, which express COX-2 in varying levels (61; 120; 33; 151; 165). Our study initially used HT-29 cells, and found the expression of COX-2 to be inconsistent. We found the varying levels of COX-2 to produce inconsistent experimental results, and therefore discontinued use with the cell line. Furthermore, the form of COX-2 expressed by HT-29 cells has been found to be catalytically inactive (59). These studies, while successful in inducing radiosensitivity *in vitro* were generally not as successful *in vivo*, which may be due to the difference in levels of active COX-2 *in vitro* versus *in vivo*.

In addition to the HT-29 cell line, our study initially performed experiments with the Ward Colon Tumour (WCT) cell line, a COX-2 positive rat colorectal cell line, and HCT-15, a COX-2 negative human colorectal cell line. We found these cell lines to also be inappropriate models as after being in culture for a short period of time, the WCT cells stopped expressing COX-2 and the HCT-15 cells began to express COX-2. This unreliable expression or lack-of with regards to COX-2 led us to stop experiments with these cell lines, and finally led us to the cell lines discussed in this thesis, HCA-7 and HCT-116.

More recently, unlike the initial studies, radiosensitization in *in vitro* and *in vivo* CRC studies has not been achieved through the inhibition of COX-2 (34; 35). These newer studies, however, used different CRC cell lines, including the COX-2 positive cell line used in this project; HCA-7. This leads to the question of how large a role the biological model plays in the success of studies examining radiosensitivity of cancer cells, and highlights the importance of finding and characterizing an appropriate model for study. Based on this, it was important for this study to characterize the cell lines to ensure their suitability for the project. In addition, any findings from this study should be applicable only to CRC, as the same study done in another cancer type and model may produce different results, as demonstrated in the literature.

#### 4.2 COXIB OFF-TARGET EFFECTS

To add to the problems with the current biological model associated with the evaluation of COX-2 in CRC, there is a problem with the selectivity of the compounds currently being used in these evaluations. While NSAIDs and coxibs are able to successfully target COX-2, each independent drug also seems to have individual off-target effects apart from COX-2. These off-target effects can be grouped into 3 main categories; cell cycle progression, angiogenesis and metastasis, and apoptosis.

Celecoxib has been found to affect the cell cycle through activating p53; increasing expression of p21<sup>waf1</sup> and p27<sup>kip1</sup>; inducing G<sub>1</sub>-phase arrest followed by reduced expression of cyclins A, B, and D; the inhibition of PKB and PDK-1; through the loss of CDK activity; and by increasing ceramide levels and inhibiting ODC (66; 52; 67; 88; 96; 4; 79; 84; 101). These effects are off-target as the concentration of celecoxib needed in order to inhibit COX-2 activity is significantly lower than that required to inhibit the cell cycle (51). Furthermore, these activities were unable to be reversed by the addition of PGE<sub>2</sub>, and more selective COX-2 inhibitors such as rofecoxib did not produce the same effects (56).

Celecoxib has also been found to prevent the activation of Egr-1, a transcription factor involved in the transcriptional regulation of FGF and other cytokines and receptors implicated in angiogenesis and tumour growth (138; 69). Celecoxib has also been found to inhibit matrix metalloprotease 9 and decrease the release of matrix metalloproteases 1-3 (105; 19). Rofecoxib, on the other hand, was found to result in the decreased expression of COX-2, PGE<sub>2</sub>, cyclin D1, matrix metalloprotease 2 and 9, interleukin 10, and  $\beta$ -

catenin; and enhanced expression of interleukin 12; all of which are linked with growth inhibition and prevention of metastasis (160).

As mentioned above, celecoxib has been found to produce its pro-carcinogenic effect at least in part through the induction of apoptosis. This can be done through either the intrinsic pathway, through the release of cytochrome c from the mitochondria, or through the extrinsic pathway, which involves the activation of death receptors (49; 83). The activation of several caspases is required in both pathways in order to cleave certain proteins and activate DNases that ultimately lead to DNA fragmentation (29). The decrease of antiapoptotic proteins, including Bcl-xL, survivin, Bcl-2, and Mcl-1; increase in expression of proapoptotic proteins such as Bad; release of cytochrome c and the subsequent activation of Apaf-1 and caspases 3, 8, and 9 after cells are treated with celecoxib are all evidence that celecoxib activates the intrinsic apoptotic pathway (64; 85; 95; 96; 156; 18; 30; 68). With regards to the extrinsic apoptotic pathway, the effect of celecoxib is much less clear. Some studies have found celecoxib to activate the pathway through increased DR5 expression or activation of the FAS-FADD pathway; however these results varied based on the cell line being examined (71; 87; 109). It is of note that while rofecoxib has been found to induce apoptosis, the mechanisms behind this effect are so far undetermined (74; 108; 135; 146). Furthermore, celecoxib has been found to inhibit PKB, which results in the promotion of apoptosis through the reduction of PKB-related antiapoptotic mechanisms including the inactivation of BAD, phosphorylation of procaspase 9 to prevent its activation (4; 84; 78; 169; 60; 164). On the other hand, rofecoxib does not inhibit PKB to the same extent as celecoxib, and as a result PKB has

not been found to be a part of the mechanism through which rofecoxib induces apoptosis (78; 104; 164).

Another celecoxib-specific effect on apoptosis is via the inhibition of ER  $\text{Ca}^{2+}$  ATPase activity, resulting in high intracellular  $\text{Ca}^{2+}$  concentration due to the prevention of cytosolic  $\text{Ca}^{2+}$  reuptake (65). The  $\text{Ca}^{2+}$  concentration change affects a variety of mechanisms involved in apoptosis including caspases, proteases, and endonucleases that are sensitive to  $\text{Ca}^{2+}$ , as well as the opening of mitochondrial permeability transition pores responsible for the release of cytochrome c (65). Celecoxib has additionally been found to modify NF- $\kappa$ B binding activity and activation, resulting in apoptosis and the reduction of NF- $\kappa$ B-regulated gene expression, respectively (96; 71; 123; 98). While rofecoxib has also been found to inhibit NF- $\kappa$ B binding activity, it is not yet known whether this contributes to its anticarcinogenic effect (97).

Celecoxib and valdecoxib have also been found to inhibit both cytosolic (I, II) and membrane bound (IV, IX) carbonic anhydrases (152). These enzymes catalyze carbon dioxide hydration, and their increased expression levels are thought to be involved in acidification of hypoxic tumours, cell-cell adhesion, tumour growth and development, and cell proliferation (42; 162; 62; 80). Tumours with increased carbonic anhydrase levels have been found to be more aggressive and result in poorer patient prognosis compared to those without enhanced expression (42). Rofecoxib, however, does not inhibit carbonic anhydrase activity as it contains a methyl sulfone group rather than a sulphonamide group, as found in celecoxib, preventing it from binding to the catalytic zinc of the enzyme (152).

This knowledge of the ability of celecoxib to inhibit carbonic anhydrase activity is important when examining the results of the blocking study of [ $^{18}\text{F}$ ]pyricoxib. As carbonic anhydrase is responsible for glycoprotein efflux, its inhibition results in the inability of the tracer to leave the cell. This could then produce a false-positive result of tracer uptake, providing an explanation as to why the uptake of the [ $^{18}\text{F}$ ]pyricoxib could not be reduced to zero. While celecoxib was the only compound to produce a significant blocking effect, there is the possibility of unknown off-target effects of the other compounds that could be responsible for the lack of a significant blocking effect.

### 4.3 *SIPS AND p53*

When cells are exposed to radiation, there are a wide variety of responses they can exhibit, including the commonly known death pathways apoptosis, autophagy, and necrosis; as well as endopolyploidy and stress-induced premature senescence (SIPS). It is becoming increasingly clear that while the majority of these responses may result in a seemingly positive growth delay, not all of these responses are ideal in order to produce the best possible therapeutic outcome. For example, SIPS is detrimental as it not only allows cells to survive, but to negatively affect surrounding cells through the secretion of tumour- and growth-promoting factors (116; 28). p53 has an important role in the response mediated by radiation-damaged cells, as it affects the route the critical cell takes to cope with the damage including apoptosis and SIPS, and regulates DNA repair and cell cycle checkpoints (57). While WT p53 normally resides in cells in low levels to limit the effect it has, cells that are exposed to radiation have been found to alter p53, resulting in its activation and accumulation (57). The p53 protein elicits its many effects through both transcription-dependent and –independent targets (57).

One such protein targeted by p53 is p21, which is able to affect cell cycle progression, apoptosis, and SIPS. Of particular importance to this study is the ability of p21 to stimulate the SIPS program and its effect on apoptosis. p21 regulates genes implicated in senescence and growth arrest (21). It is believed that p21 induces SIPS by activating the G1/S checkpoint, which can be attributed to the ability of the protein to inhibit cyclin/CDK complexes and proliferating cell nuclear antigen (PCNA), and degrade retinoblastoma protein (pRB) (158; 117; 13).

p21 is able to inhibit the release of cytochrome c from the mitochondria, inhibit pro-apoptotic proteins including caspases (caspase 3, 8, 9, and 10), and can negatively regulate pro-apoptotic genes and positively regulate genes responsible for anti-apoptotic secreted factors, all of which result in the avoidance of apoptosis (166-168; 133).

It has been found that in cancer cells expressing wild-type p53, treatment with chemotherapeutic agents that induce DNA damage results in cell cycle arrest, while in mutant or non-expressing p53 cells, the same treatment resulted in apoptosis (136). Furthermore, in a study examining isogenic cell line pairs differing in expression of p53 or p21, activation of senescence in the parental cells was found to correspond with increased expression of p53 and p21, while cells lacking the proteins were unable to induce senescence (137). This suggests that both proteins have a pivotal role in inducing senescence (137). In this same study, HCA-7 cells, which express a dominant mutant form of p53 in addition to WT p53, were found to mainly undergo apoptosis when exposed to DNA-damaging chemotherapeutics; however, over time an increasing number of senescent cells were observed (137). HCT-116 cells, on the other hand, which express only WT p53, showed no significant levels of apoptosis but very high levels of senescence indicated by  $\beta$ -galactosidase staining (137). The reasoning behind the tendency of HCA-7 cells to initially undergo apoptosis and switch to senescence, while HCT-116 cells only showed a tendency to undergo senescence is unclear. Perhaps it is somehow related to the COX-2 pathway and a switch in cell crisis strategies when DNA damage is induced, as our study hints at.

As our study did not find HCA-7 cells to exhibit a significant amount of apoptosis after exposure to a combined treatment of coxibs and radiation, but to in fact demonstrate

a radioprotective effect, an effect which was not evident in COX-2-negative cells, we surmised this could be due to the coxibs, possibly through the inhibition of COX-2, affecting p53 and/or p21, and causing the cells to switch from the apoptosis pathway to senescence or autophagy. As mentioned in the previous section, some of the off-target effects of celecoxib are to activate p53, and activate and increase expression of p21. It has been found that the ability of celecoxib to activate p53 leads to senescence and autophagy rather than apoptosis (66). However, celecoxib also results in activation of caspase 3, which cleaves p21 (163). While intact p21 leads to growth arrest of cancer cells, cleavage of p21 allows cells to undergo apoptosis (163). The ability of celecoxib to inadvertently result in the cleavage of p21, leading to apoptosis, is the opposite effect found in the study by Kang *et al*, and does not agree with our study in the component involving coxib co-application with radiation. Perhaps in the presence of DNA damage caused by radiation, the ability of celecoxib to indirectly cleave p21 is limited, and instead its effect on p53 leading to senescence and autophagy moves to the forefront. Perhaps, like celecoxib, pyrcoxib is able to activate p53 and stimulate senescence and autophagy, which would explain the seemingly radioprotective effect observed in the flow cytometry experiments and no more than additive effects in the senescence study.

The form of p21 expressed in HCA-7 cells could be a possible alternative explanation to this lack of radiosensitization. Both cell lines have been found to express p21, but it is unknown whether HCA-7 cells express a mutant form of p21. If the form is mutant, it may be resistant to cleavage by caspase-3. If not, this may be a matter of cleaved versus intact p21 in relation to the COX-2 pathway and its interaction with pathways induced by DNA damage caused by radiation. As celecoxib has many off-target

effects related to this interplay between DNA damage, senescence, and apoptosis, it is likely that pyrroxicam has some similar effects. Future studies should examine this complex issue, perhaps by starting with the effect of chemoradiation with coxibs on the levels and functionality of p53 and p21 in cells in order to determine the reason and possible mechanism behind the lack of radiosensitizing response.

## 5. SUMMARY AND CONCLUSIONS

In summary, our research found the novel compound pyricoxib to act at least in part through the inhibition of COX-2, and to have a higher potency than celecoxib. Further, pyricoxib was able to induce apoptosis through the inhibition of COX-2 in the absence of radiation. We also found HCA-7 and HCT-116 cells to be highly radioresistant. Our study revealed some important results that should be carefully considered for future work regarding COX-2 inhibitors as radiosensitizing agents for cancer therapy. Neither compound appeared to produce a significant radiosensitization response based on apoptotic events at the conditions studied, but rather appeared to produce a radioprotective effect in HCA-7 cells. Furthermore, both drugs produced more large cells with less tumour-like populations when combined with irradiation compared to either treatment alone in COX-2 positive cells. Finally, chemoradiation with coxibs did not result in an increased number of senescent cells compared to either therapy alone, which is in agreement with the MTT assay. Only pyricoxib in the COX-2 positive cells produced an enhanced level of senescence, but it was not greater than an additive effect.

Based on these results, we propose there to be a possible interaction between the COX-2 pathway and the DNA repair pathway when chemoradiation with coxibs is given to cells, leading to the switch from apoptosis to senescence or autophagy.

## 6. FUTURE DIRECTIONS

Future studies should take into consideration the biological model can have on results, and proceed with a suitable model.. One possible future study that would be interesting would be to use isogenic cell lines that differ in COX-2 and p53 expression. For example, through siRNAs or CRISPR technology, isogenic HCA-7 cells could be produced with COX-2 silenced in one line and p53 in another. This could then also be applied to the HCT-116 cell line, to silence p53 in a line that does not express COX-2. These isogenic lines could then be subject to the flow cytometry and  $\beta$ -galactosidase staining experiments and compared back to the results from the original cell lines to examine any possible interplay between COX-2, p53 status, and cell fate after irradiation. Furthermore, future work should examine the possible radioprotective effect observed in this study and possible mechanisms behind it, including p53 and p21 expression levels and mutations, in order to shed more light on this complex phenomenon

## BIBLIOGRAPHY

1. Altorki, N. K., Keresztes, R. S., Port, J. L., Libby, D. M., Korst, R. J., Flieder, D. B. et al. (2003). Celecoxib, a selective cyclooxygenase-2 inhibitor, enhances the response to preoperative paclitaxel/carboplatin in early-stage non-small cell lung cancer. *J. Clin. Oncol.*, *21*, 2645-2650.
2. Antonarakis, E. S., Heath, E. I., Walczak, J. R., Nelson, W. G., Fedor, H., De Marzo, A. M. et al. (2009). Phase II, randomized, placebo-controlled trial of neoadjuvant celecoxib in men with clinically localized prostate cancer: evaluation of drug-specific biomarkers. *J. Clin. Oncol.*, *27*(30), 4986-4993.
3. Arber, N., Eagle, C. J., Spicak, J., Racz, I., Dite, P., Hajer, J. et al. (2006). Celecoxib for the prevention of colorectal adenomatous polyps. *N. Engl. J. Med.*, *355*, 885-895.
4. Arico, S., Pattingre, S., Bauvy, C., Gane, P., Barbat, A., Codogno, P. et al. (2002). Celecoxib induces apoptosis by inhibiting 3-phosphoinositide-dependent protein kinase-1 activity in the human colon cancer HT-29 cell line. *J Biol Chem*, *277*, 27613-27621.
5. Bamatraf, M. M. M., O'Neill, P., & Rao, B. S. M. (1998). Redox dependence of the rate of interaction of hydroxyl radical adducts of DNA nucleobases with oxidants: consequences for DNA strand breakage. *J. Am. Chem.*, *120*, 11852-11857.
6. Baron, J. A., Sandler, R. S., Bresalier, R. S., Lanas, A., Morton, D. G., Riddell, R. et al. (2008). Cardiovascular events associated with rofecoxib: final analysis of the APPROVe trial. *Lancet.*, *372*, 1756-1764.
7. Baron, J. A., Sandler, R. S., Bresalier, R. S., Quan, H., Riddell, R., Lanas, A. et al. (2006). A randomized trial of rofecoxib for the chemoprevention of colorectal adenomas. *Gastroenterology*, *131*, 1674-1682.
8. Bertagnolli, M. M., Eagle, C. J., Zauber, A. G., Redston, M., Solomon, S. D., Kim, K. M. et al. (2006). Celecoxib for the prevention of sporadic colorectal adenomas. *N. Engl. J. Med.*, *355*, 873-874.
9. Bi, N., Yang, M., Zhang, L., Chen, X., Ji, W., Ou, G. et al. (2010). Cyclooxygenase-2 genetic variants are associated with survival in unresectable locally advanced non-small cell lung cancer. *Clin. Cancer Res.*, *16*, 2383-2390.
10. Bienz, M., & Clevers, H. (2005). Linking colorectal cancer to Wnt signalling. *Cell*, *103*, 311-320.
11. Boucher, M. J., Morisset, J., Vachon, P. H., Reed, J. C., Laine, J., & Rivard, N. (2000). MEK/ERK signaling pathway regulates the expression of Bcl2, Bcl-XL, and Mcl-1 and promotes survival of human pancreatic cancer cells. *J. Cell. Biochem.*, *79*, 355-369.
12. Breyer, R. M., Bagdassarian, C. K., Myers, S. A., & Breyer, M. D. (2001). Prostanoid receptors: subtypes and signalling. *Annual Rev. of Pharm. and Toxic.*, *41*, 661-690.
13. Broude, E. V., Swift, M. E., Vivo, C., Chang, B. D., Davis, B. M., Kalurupalle, S. et al. (2007). p21waf1/cip1/sdi1 mediates retinoblastoma protein degradation. *Oncogene*, *26*, 6954-6958.
14. Buchanan, F. G., Gorden, D. L., Matta, P., Shi, Q., Matrisian, L. M., & DuBois, R. N. (2006). Role of beta-arrestin 1 in the metastatic progression of colorectal cancer.

- Proc. Natl. Acad. Sci. U.S.A.*, 103, 1492-1497.
15. Buchanan, F. G., Wang, D., Bargiacchi, F., & DuBois, R. N. (2003). Prostaglandin E2 regulates cell migration via the intracellular activation of the epidermal growth factor receptor. *J. Biol. Chem.*, 278, 35451-35457.
  16. Cannon, C. P., & Cannon, P. J. (2012). COX-2 inhibitors and cardiovascular risk. *Science*, 336, 1386-1387.
  17. Castelano, J. E., Yuan, J. M., Gago-Dominguez, M., Yu, M. C., & Ross, R. K. (2000). Non-steroidal anti-inflammatory drugs and bladder cancer prevention. *Br. J. Cancer*, 82(7), 1364-1369.
  18. Catalano, A., Graciotti, L., Rinaldi, L., Raffaelli, G., Rodilossi, S., Betta, P. et al. (2004). Preclinical evaluation of the nonsteroidal anti-inflammatory agent celecoxib on malignant mesothelioma chemoprevention. *Int J Cancer*, 109, 322-328.
  19. Cha, H. S., Ahn, K. S., Jeon, C. H., Kim, J., & Koh, E. M. (2004). Inhibitory effect of cyclo-oxygenase-2 inhibitor on the production of matrix metalloproteinases in rheumatoid fibroblast-like synoviocytes. *Rheumatol Int*, 24, 207-211.
  20. Chandrasekharan, N. V., Dai, H., Roos, K. L., Evanson, N. K., Tomsik, J., Elton, T. S. et al. (2002). COX-3, a cyclooxygenase-1 variant inhibited by acetaminophen and other analgesic/antipyretic drugs; cloning, structure, and expression. *Proc. Natl. Acad. Sci. U.S.A.*, 99, 13926-13931.
  21. Chang, B. D., Watanabe, K., Broude, E. V., Fang, J., Poole, J. C., Kalinichenko, T. V. et al. (2000). Effects of p21waf1/cip1/sdi1 on cellular gene expression: implications for carcinogenesis, senescence, and age-related diseases. *Proc. Natl. Acad. Sci. U.S.A.*, 97, 4291-4296.
  22. Chen, C. C., Sun, Y. T., Chen, J. J., & Chang, Y. J. (2001). Tumor necrosis factor- $\alpha$ -induced cyclooxygenase-2 expression via sequential activation of ceramide-dependent mitogen-activated protein kinases, and I-kappaB kinase  $\frac{1}{2}$  in human alveolar epithelial cells. *Mol. Pharmacol.*, 59(3), 493-500.
  23. Chen, C. Y., & Shyu, A. B. (1995). AU-rich elements: characterization and importance in mRNA degradation. *Trends Biochem. Sci.*, 20, 465-470.
  24. Chen, G., Wilson, R., McKillop, J. H., & Walker, J. J. (1994). The role of cytokines in the production of prostacyclin and thromboxane in human mononuclear cells. *Immunol. Invest.*, 23(4-5), 269-279.
  25. Cianchi, F., Cortesini, C., Bechi, P., Fantappie, O., Messerini, L., Vannacci, A. et al. (2001). Up-regulation of cyclooxygenase-2 gene expression correlates with tumor angiogenesis in human colorectal cancer. *Gastroenterology*, 121(6), 1339-1347.
  26. Cobben, D. C., Elsinga, P. H., Suurmeijer, A. J., Vaalburg, W., Maas, B., Jager, P. L. et al. (2004). Detection and grading of soft tissue sarcomas of the extremities with 18-F-3-Fluoro-3-deoxy-L-Thymidine. *Clin Canc Res*, 10, 1685-1690.
  27. Cok, S. J., & Morrison, A. R. (2001). The 3'-untranslated region of murine cyclooxygenase-2 contains multiple regulatory elements that alter message stability and translational efficiency. *J. Biol. Chem.*, 276(25), 23179-23185.
  28. Coppe, J. P., Patil, C. K., Rodier, F., Sun, Y. T., Munoz, D. P., Goldstein, J. et al. (2008). Senescence-associated secretory phenotypes reveal cell-nonautonomous functions of oncogenic RAS and the p53 tumor suppressor. *PLoS Biol*, 6, 2853-2868.

29. Cryns, V., & Yuan, J. (1998). Proteases to die for. *Genes Dev.*, *12*, 1551-1570.
30. Dandekar, D. S., Lopez, M., Carey, R. I., & Lokeshwar, B. L. (2005). Cyclooxygenase-2 inhibitor celecoxib augments chemotherapeutic drug-induced apoptosis by enhancing activation of caspase-3 and -9 in prostate cancer cells. *Int J Cancer*, *115*, 484-492.
31. Dannenberg, A. J., Lippman, S. M., Mann, J. E., Subbaramaiah, K., & DuBois, R. N. (2005). Cyclooxygenase-2 and epidermal growth factor receptor: pharmacologic targets for chemoprevention. *J. Clin. Oncol.*, *23*(2), 254-266.
32. Davis, T. W., Hunter, N., Trifan, O. C., Milas, L., & Masferrer, J. L. (2003). COX-2 inhibitors as radiosensitizing agents for cancer therapy. *Am. J. Clin. Oncol. (CCT)*, *26*, S58-S61.
33. Davis, T. W., O'Neal, J. M., Pagel, M. D., Zweifel, B. S., Mehta, P. P., Heuvelman, D. M. et al. (2004). Synergy between celecoxib and radiotherapy results from inhibition of cyclooxygenase-2-derived prostaglandin E<sub>2</sub>, a survival factor for tumor and associated vasculature. *Cancer Res.*, *64*, 279-285.
34. Debucquoy, A., Devos, E., Vermaelen, P., Landuyt, W., De Weer, S., Van Den Heuvel, F. et al. (2009). 18F-FLT and 18F-FDG PET to measure response to radiotherapy combined with celecoxib in two colorectal xenograft models. *Int. J. Radiat. Bio.*, *85*(9), 763-771.
35. Debucquoy, A., & Hausermans, K. (2009). Targeted treatments for rectal cancer: molecular effects and predicted response. *Belgian J. Med. Onc.*, *3*(4), 168-171.
36. Delbeke, D., Martin, W. H., Patton, J. A., & Sandler, M. P. (2002). *Practical FDG imaging: a teaching File*. New York, NY: Springer.
37. Dicker, A. P., Williams, T. L., & Grant, D. S. (2001). Targeting angiogenic processes by combination rofecoxib and ionizing radiation. *Am. J. Clin. Oncol.*, *24*, 438-442.
38. Dittman, H., Dohmen, B. M., Paulsen, F., Eichhorn, K., Eschmann, S. M., Horger, M. et al. (2003). 18-FLT PET for diagnosis and staging of thoracic tumors. *Eur J Nucl Med Mol Iman*, *30*, 1407-1412.
39. Dittman, K. H., Mayer, C., Ohneseit, P. A., Raju, U., Andratschke, N. H., Milas, L. et al. (2008). Celecoxib induced tumor cell radiosensitization by inhibiting radiation induced nuclear EGFR transport and DNA-repair: a COX-2 independent mechanism. *Int. J. Radiat. Oncol. Biol. Phys.*, *70*, 203-212.
40. Dixon, D. A., Tolley, N. D., King, P. H., Nabors, L. B., McIntyre, T. M., Zimmerman, G. A. et al. (2001). Altered expression of the mRNA stability factor HuR promotes cyclooxygenase-2 expression in colon cancer cells. *J. Clin. Invest.*, *108*(11), 1657-1665.
41. Douple, E. B., Richmond, R. C., O'Hara, J. A., & Coughlin, C. T. (1985). Carboplatin as a potentiator of radiation therapy. *Cancer Treat. Rev.*, *12*(Suppl. A), 111-124.
42. Driessen, A., Landuyt, W., Pastorekova, S., Moons, J., Goethals, L., Haustermans, K. et al. (2006). Expression of carbonic anhydrase ix (ca ix), a hypoxia-related protein, rather than vascular-endothelial growth factor (vegf), a pro-angiogenic factor, correlates with an extremely poor prognosis in esophageal and gastric adenocarcinomas. *Ann Surg*, *243*, 334-340.
43. Eberhart, C. E., Coffey, R. J., Radhika, A., Giardiello, F. M., Ferrenbach, S., &

- DuBois, R. N. (1994). Up-regulation of cyclooxygenase 2 gene expression in human colorectal adenomas and adenocarcinomas. *Gastroenterology*, *107*, 1183-1188.
44. Eisinger, A. L., Nadauld, L. D., Shelton, D. N., Peterson, P. W., Phelps, R. A., Chidester, S. et al. (2006). The APC tumor suppressor gene regulates expression of cyclooxygenase-2 by a mechanism that involves retinoic acid. *J. Biol. Chem.*, *281*(29), 20474-20482.
  45. Erdi, Y. E., Macapinlac, H., Rosenweig, K. E., Humm, J. L., Larson, S. M., Erdi, A. K. et al. (2000). Use of PET to monitor the response of lung cancer to radiation treatment. *Eur J Nucl Med*, *27*, 861-866.
  46. Forman, B. M., Chen, J. J., & Evans, R. M. (1996). The peroxisome proliferator-activated receptors: ligands and activators. *Ann. NY Acad. Sci.*, *804*, 266-275.
  47. Francis, D. L., Visviskis, D., Costa, D. C., Arulampalam, T. H., Townsend, C., Luthra, S. K. et al. (2003). Potential impact of 18-F-3-Fluoro-3-deoxy-thymidine versus 18-F-Fluoro-2-deoxy-D-glucose in positron emission tomography for colorectal cancer. *Eur J Med Mol Imag*, *30*, 988-994.
  48. Fujisaki, Y., Kawamura, K., Wang, W. J., Ishiwata, K., Yamamoto, F., Kuwano, T. et al. (2005). Radiosynthesis and in vivo evaluation of <sup>11</sup>C\_labeled 1,5-diarylpyrazole derivatives for mapping cyclooxygenases. *Ann. Nucl. Med.*, *19*, 617-625.
  49. Green, D. R., & Evan, G. I. (2002). A matter of life and death. *Cancer Cell*, *1*, 19-30.
  50. Gregorieff, A., & Clevers, H. (2005). Wnt signalling in the intestinal epithelium: from endoderm to cancer. *Genes Dev.*, *19*, 877-890.
  51. Grosch, S., Maier, T. J., Schiffmann, S., & Geisslinger, G. (2006). Cyclooxygenase-2 (COX-2)-independent anticarcinogenic effects of selective COX-2 inhibitors. *J. Nat. Cancer Inst.*, *98*, 736-747.
  52. Grosch, S., Tegeder, I., Niederberger, E., Brautigam, L., & Geisslinger, G. (2001). COX-2 independent induction of cell cycle arrest and apoptosis in colon cancer cells by the selective COX-2 inhibitor celecoxib. *FASEB J*, *15*, 2742-2744.
  53. Grosser, T., Fries, S., & Fitzgerald, G. A. (2006). Biological bases for the cardiovascular consequences of COX-2 inhibition: therapeutic challenges and opportunities. *J. Clin. Invest.*, *116*, 4-15.
  54. Gualde, N., & Harizi, H. (2004). Prostanoids and their receptors that modulate dendritic cell-mediated immunity. *Immunol. and Cell Biol.*, *82*, 353-360.
  55. Gupta, R. A., & DuBois, R. N. (2001). Colorectal cancer prevention and treatment by inhibition of cyclooxygenase-2. *Nat. Rev. Cancer*, *1*, 11-21.
  56. Han, C., Leng, J., Demetris, A. J., & Wu, T. (2004). Cyclooxygenase-2 promotes human cholangiocarcinoma growth: evidence for cyclooxygenase-2-independent mechanism in celecoxib-mediated induction of p21waf1/cip1 and p27kip1 and cell cycle arrest. *Cancer Res.*, *64*, 1369-1376.
  57. Hasty, P., & Christy, B. A. (2013). p53 as an intervention target for cancer and aging. *Pathobiol. Aging Age. Relat. Dis.*, *3*, 22702.
  58. Hia, T., Ristimaki, A., Appleby, S., & Barriocanal, J. G. (1993). Cyclooxygenase gene expression in inflammation and angiogenesis. *Ann. N.Y. Acad. Sci.*, *696*, 197-204.

59. Hsi, L. C., Baek, S. J., & Eling, T. E. (2000). Lack of cyclooxygenase-2 activity in HT-29 human colorectal carcinoma cells. *Exp. Cell Res.*, 256(2), 563-570.
60. Hsu, A. L., Ching, T. T., Wang, D. S., Song, X., Rangnekar, V. M., & Chen, C. S. (2000). The cyclooxygenase-2 inhibitor celecoxib induces apoptosis by blocking Akt activation in human prostate cancer cells independently of Bcl-2. *J Biol Chem*, 275, 11397-11403.
61. Hwang, J.-T., Ha, J., & Park, O. J. (2005). Combination of 5-fluorouracil and genistein induces apoptosis synergistically in chemo-resistant cancer cells through the modulation of AMPK and COX-2 signaling pathways. *Biochem. and Biophys. Research Communications*, 332(2), 433-440.
62. Ivanov, S., Liao, S. Y., Ivanova, A., Danilkovitch-Miagkova, A., Tarasova, N, Weirich, G., Merrill, M. J. et al. (2001). Expression of hypoxia-inducible cell-surface transmembrane carbonic anhydrases in human cancer. *Am J Pathol*, 158, 905-919.
63. Izuishi, K., Yamamoto, Y., Mori, H., Kameyama, R., Fujihara, S., Masaki, T. et al. (2014). Molecular mechanisms of [18F]fluorodeoxyglucose accumulation in liver cancer. *Oncology Reports*, 31(2), 701-706.
64. Jendrossek, V., Handrick, R., & Belka, C. (2003). Celecoxib activates a novel mitochondrial apoptosis signaling pathway. *Faseb J*, 17, 1547-1549.
65. Johnson, A. J., Hsu, A. L., Lin, H. P., Song, X., & Chen, C. S. (2002). The cyclooxygenase-2 inhibitor celecoxib perturbs intracellular calcium by inhibiting endoplasmic reticulum Ca<sup>2+</sup>-ATPases: a plausible link with its anti-tumour effect and cardiovascular risks. *Biochem J*, 366(Pt3), 831-837.
66. Kang, K. M., Zhu, C., Yong, S. K., Gao, Q., & Wong, M. C. (2009). Enhanced sensitivity of celecoxib in human glioblastoma cells: induction of DNA damage leading to p53-dependent G1 cell cycle arrest and autophagy. *Mol Cancer*, 8.
67. Kardosh, A., Blumenthal, M., Wang, W. J., Chen, T. C., & Schonthal, A. H. (2004). Differential effects of selective COX-2 inhibitors on cell cycle regulation and proliferation of glioblastoma cell lines. *Cancer Biol. Ther.*, 3, 55-62.
68. Kern, M. A., Schubert, D., Sahi, D., Schoneweiss, M. M., Moll, I., Haugg, A. M. et al. (2002). Proapoptotic and antiproliferative potential of selective cyclooxygenase-2 inhibitors in human liver tumor cells. *Hepatology*, 36, 885-894.
69. Khachigian, L. M. (2004). Early growth response-1: blocking angiogenesis by shooting the messenger. *Cell Cycle*, 3, 10-11.
70. Kim, S. F., Huri, D. A., & Snyder, S. H. (2005). Inducible nitric oxide synthase binds, S-nitrosylates, and activates cyclooxygenase-2. *Science*, 310, 1966-1970.
71. Kim, S. H., Song, S. H., Kim, S. G., Chun, K. S., Lim, S. Y., Na, H. K. et al. (2004). Celecoxib induces apoptosis in cervical cancer cells independent of cyclooxygenase using NF-kappaB as a possible target. *J Cancer Res Clin Oncol*, 130, 551-560.
72. Koki, A. T., Leahy, K. M., & Masferrer, J. L. (1999). Potential utility of COX-2 inhibitors in chemoprevention and chemotherapy. *Expert Opin. Investig. Drugs*, 8(10), 1623-1638.
73. Komatsu, K., Buchanan, F. G., Katkuri, S., Morrow, J. D., Inoue, H., Otaka, M. et al. (2005). Oncogenic potential of MEK1 in rat intestinal epithelial cells is mediated via cyclooxygenase-2. *Gastroenterology*, 129, 577-590.

74. Konturek, P. C., Konturek, S. J., Bielanski, W., Kania, J., Zuchowicz, M., Hartwich, A. et al. (2003). Influence of COX-2 inhibition by rofecoxib on serum and tumor progastrin and gastrin levels and expression of PPARgamma and apoptosis-related proteins in gastric cancer patients. *Dig Dis Sci*, 48, 2005-2017.
75. Kraemer, S. A., Meade, E. A., & DeWitt, D. L. (1992). Prostaglandin endoperoxide synthase gene structure: identification of the transcriptional start site and 5'-flanking regulatory sequences. *Arch. Biochem. Biophys.*, 293, 391-400.
76. Kuipers, G. K., Slotman, B. J., Wedekind, L. E., Stoter, T. R., Van den Berg, J., Sminia, P. et al. (2007). Radiosensitization of human glioma cells by cyclooxygenase-2 (COX-2) inhibition: Independent on COX-2 expression and dependent on the COX-2 inhibitor and sequence of administration. *Int. J. Radiat. Oncol. Bio.*, 83(10), 677-685.
77. Kujubu, D. A., & Herschman, H. R. (1992). Dexamethasone inhibits mitogen induction of the TIS10 prostaglandin synthase/cyclooxygenase gene. *J. Biol. Chem.*, 267, 7991-7994.
78. Kulp, S. K., Yang, Y. T., Hung, C. C., Chen, K. F., Lai, J. P., Tseng, P. H. et al. (2004). 3-phosphoinositide-dependent protein kinase-1/Akt signaling represents a major cyclooxygenase-2-independent target for celecoxib in prostate cancer cells. *Cancer Res.*, 64, 1444-1451.
79. Kundu, N., Smyth, M. J., Samsel, L., & Fulton, A. M. (2002). Cyclooxygenase inhibitors block cell growth, increase ceramide and inhibit cell cycle. *Breast Cancer Res Treat*, 76, 57-64.
80. Lankat-Buttgereit, B., Gregel, C., Knolle, A., Hasilik, A., Arnold, R., & Goke, R. (2004). Pcd4 inhibits growth of tumor cells by suppression of carbonic anhydrase type II. *Mol Cell Endocrinol*, 214, 149-153.
81. (Eds.). (2008). *Principles of Radiation Oncology*. (8 ed.). Philadelphia: Lippincott Williams and Wilkins.
82. Liao, Z., Komaki, R., Milas, L., Yuan, C., Kies, M., Chang, J. Y. et al. (2005). A phase I clinical trial of thoracic radiotherapy and concurrent celecoxib for patients with unfavorable performance status inoperable/unresectable non-small cell lung cancer. *Clin Canc Res*, 11, 3342-3348.
83. Lim, M. L., Lum, M. G., Hansen, <sup>TM</sup>, Roucou, X., & Nagley, O. (2002). On the release of cytochrome c from mitochondria during cell death signaling. *J. Biomed. Sci.*, 9, 488-506.
84. Lin, H. P., Kulp, S. K., Tseng, P. H., Yang, Y. T., Yang, C. C., & Chen, C. S. (2004). Growth inhibitory effects of celecoxib in human umbilical vein endothelial cells are mediated through G1 arrest via multiple signaling mechanisms. *Mol Cancer Ther*, 3, 1671-1680.
85. Lin, M. T., Lee, R. C., Yang, P. C., Ho, F. M., & Kuo, M. L. (2001). Cyclooxygenase-2 inducing Mcl-1-dependent survival mechanism in human lung adenocarcinoma CL1.0 cells. Involvement of phosphatidylinositol 3-kinase/Akt pathway. *J Biol Chem*, 276, 48997-489002.
86. Liu, S. F., Ye, X., & Malik, A. B. (1999). Inhibition of NF-kappaB activation by pyrrolidinedithiocarbamate prevents in vivo expression of proinflammatory genes. *Circulation*, 100, 1330-1337.
87. Liu, X., Yue, P., Zhou, Z., Khuri, F. R., & Sun, S. Y. (2004). Death receptor

- regulation and celecoxib-induced apoptosis in human lung cancer cells. *J Natl Cancer Inst*, 96, 1769-1780.
88. Maier, T. J., Schilling, K., Schmidt, R., Geisslinger, G., & Grosch, S. (2004). Cyclooxygenase-2 (COX-2)-dependent and -independent anticarcinogenic effects of celecoxib in human colon carcinoma cells. *Biochem Pharmacol*, 67, 1469-1478.
  89. Marnett, L. J. (1995). Aspirin and related nonsteroidal anti-inflammatory drugs as chemopreventive agents against colon cancer. *Prev. Med.*, 24(2), 103-106.
  90. Masterrer, J. L., Leahy, K. M., Koki, A. T., Zweifel, B. S., Settle, S. L., Woerner, B. M. et al. (2000). Antiangiogenic and antitumor activities of cyclooxygenase-2 inhibitors. *Cancer Res.*, 60, 1306-1311.
  91. McKinley, E. T., Ayers, G. D., Smith, R. A., Saleh, S. A., Zhao, P., Washington, M. K. et al. (2013). Limits of [18F]-FLT PET as a biomarker of proliferation in oncology. *Plos One*, 8.
  92. Meric, J. P., Rottey, S., Olausson, K., Soria, J.-C., Khayat, D., Rixe, O. et al. (2006). Cyclooxygenase-2 as a target for anticancer drug development. *Crit. Rev. in Oncol/Hemat.*, 59(1), 51-64.
  93. Milas, L., Kishi, K., Hunter, N., Mason, K., Masferrer, J. L., & Tofilon, P. J. (1999). Enhancement of tumor response to gamma radiation by an inhibitor of cyclooxygenase-2 enzyme. *J Natl Cancer Inst*, 91, 1501-1504.
  94. Nakata, E., Mason, K. A., Hunter, N., Husain, A., Raju, U., Liao, Z. et al. (2004). Potentiation of tumor response to radiation or chemoradiation to selective cyclooxygenase-2 enzyme inhibitors. *Int. J. Radiat. Oncol. Bio. Phys.*, 58, 369-375.
  95. Nam, D. H., Park, K., Park, C., Im, Y. H., Kim, M. H., Lee, S. et al. (2004). Intracranial inhibition of glioma cell growth by cyclooxygenase-2 inhibitor celecoxib. *Oncol Rep*, 11, 263-268.
  96. Narayanan, B. A., Condon, M. S., Bosland, M. C., Narayanan, N. K., & Reddy, B. S. (2003). Suppression of N-methyl-N-nitrosourea/testosterone-induced rat prostate cancer growth by celecoxib: effects on cyclooxygenase-2 cell cycle regulation, and apoptosis mechanism(s). *Clin Canc Res*, 9, 3503-3513.
  97. Niederberger, E., Tegeder, I., Schafer, C., Seegel, M., Grosch, S., & Geisslinger, G. (2003). Opposite effects of rofecoxib on nuclear factor-kappaB and activating protein-1 activation. *J Pharmacol Exp Ther*, 304, 1153-1160.
  98. Niederberger, E., Tegeder, I., Vetter, G., Schmidtko, A., Schmidt, H., Euchenhofer, C. et al. (2001). Celecoxib loses its anti-inflammatory efficacy at high doses through activation of NF-kappaB. *FASEB J*, 15, 1622-1624.
  99. Niino, H., Otsuka, T., & Izuhara, K. (1997). Regulation by interleukin-10 and interleukin-4 of cyclooxygenase-2 expression in human neutrophils. *Blood*, 89, 1621-1628.
  100. Ohneseit, P. A., Krebiehl, G., Dittman, K., Kehlbach, R., & Rodemann, H. P. (2007). Inhibition of cyclooxygenase-2 activity by celecoxib does not lead to radiosensitization of human prostate cancer cells *in vitro*. *Radiotherapy and Oncology*, 82, 229-238.
  101. Ostrowski, J., Wocial, T., Skurzak, H., & Bartnik, W. (2004). Do altering in ornithine decarboxylase activity and gene expression contribute to antiproliferative properties of COX inhibitors? *Br J Cancer*, 88, 1143-1151.
  102. Otto, J. C., DeWitt, D. L., & Smith, W. L. (1993). N-glycosylation of prostaglandin

- endoperoxide synthases-1 and -2 and their orientations in the endoplasmic reticulum. *J. Biol. Chem.*, 268, 18234-18242.
103. Pai, R., Sorgehan, B., Szabo, I. L., Pavelka, M., Baatar, D., & Tarnawski, A. S. (2002). Prostaglandin E2 transactivates EGF receptor: a novel mechanism for promoting colon cancer growth and gastrointestinal hypertrophy. *Nat. Med.*, 8(3), 289-293.
  104. Patti, R., Gumired, K., Reddanna, P., Sutton, L. N., Phillips, P. C., & Reddy, C. D. (2002). Overexpression of cyclooxygenase-2 (COX-2) in human primitive neuroectodermal tumors: effect of celecoxib and rofecoxib. *Cancer Lett*, 180, 13-21.
  105. Peluffo, G. D., Stillitani, I., Rodriguez, V. A., Diament, M. J., & Klein, S. M. (2004). Reduction of tumor progression and paraneoplastic syndrome development in murine lung adenocarcinoma by nonsteroidal antiinflammatory drugs. *Int J Cancer*, 110, 825-830.
  106. Peters, K. B., & Brown, J. M. (2002). Tirapazamine: a hypoxia-activated topoisomerase II poison. *Cancer Res.*, 62, 5248-5253.
  107. Petersen, C., Petersen, S., Milas, L., Lang, F. F., & Tofilon, P. J. (2000). Enhancement of intrinsic tumor cell radiosensitivity induced by a selective cyclooxygenase-2 inhibitor. *Clin Cancer Res*, 6, 2513-2520.
  108. Qadri, S. S., Wang, J. H., Redmond, K. C., OD, A. F., Aherne, T., & Redmond, H. P. (2002). The role of COX-2 inhibitors in lung cancer. *Ann Thorac Surg*, 74, 1648-1652.
  109. Qiu, W., Zhou, B., Zou, H., Liu, X., Chu, P. G., Lopez, R. et al. (2004). Hypermethylation of growth arrest DNA damage-inducible gene 45 beta promoter in human hepatocellular carcinoma. *Am J Pathol*, 165, 1689-1699.
  110. Raju, U., Ariga, H., Dittman, K., Nakata, E., Ang, K. K., & Milas, J. (2005). Inhibition of DNA repair as a mechanism of enhanced radioresponse of head and neck carcinoma cells by a selective cyclooxygenase-2 inhibitor, celecoxib. *Int. J. Radiat. Oncol. Biol. Phys.*, 63, 520-528.
  111. Raju, U., Nakata, E., Yang, P., Newman, R. A., Ang, K. K., & Milas, L. (2002). In vitro enhancement of tumor cell radiosensitivity by a selective inhibitor of cyclooxygenase-2 enzyme: mechanistic considerations. *Int. J. Radiat. Oncol. Biol. Phys.*, 54, 886-894.
  112. Ramsay, R. G., Friend, A., Vizantios, Y., Freeman, R., Sicurella, C., Hammett, F. et al. (2000). Cyclooxygenase-2, a colorectal cancer nonsteroidal anti-inflammatory drug target, is regulated by c-MYB. *Cancer Res.*, 60(7), 1805-1809.
  113. Rasey, J. S., Grierson, J. R., Wiens, L. W., Kolb, P. D., & Schwartz, J. L. (2002). Validation of FLT uptake as a measure of thymidine-kinase-1 activity in A549 carcinoma cells. *J Nucl Med*, 43, 1210-1217.
  114. Ristimaki, A., Garfinkel, S., Wessendorf, J., Maciag, T., & Hla, T. (1994). Induction of cyclooxygenase-2 by interleukin-1 alpha. Evidence for post-transcriptional regulation. *J. Biol. Chem.*, 269, 11769-11775.
  115. Roman, C. D., Morrow, J., Whitehead, R., & Beauchamp, R. D. (2002). Induction of cyclooxygenase-2 and invasiveness by transforming growth factor-beta (1) in immortalized mouse colonocytes expressing oncogenic Ras. *Gastrointest. Surg.*, 6, 304-309.

116. Roninson, I. B. (2003). Tumor cell senescence in cancer treatment. *Cancer Res.*, *63*, 2705-2715.
117. Rousseau, D., Cannella, D., Boulaire, J., Fitzgerald, P., Fotedar, A., & Fotedar, R. (1999). Growth inhibition by CDK-cyclin and PCNA binding domains of p21 occurs by distinct mechanisms and is regulated by ubiquitin-proteasome pathway. *Oncogene*, *18*, 4313-4325.
118. Salcedo, R., Zhang, X., HA, Y., Michael, N., Wasserman, K., Ma, W. H. et al. (2003). Angiogenic effects of prostaglandin E2 are mediated by up-regulation of CXCR4 on human microvascular endothelial cells. *Blood*, *102*, 1966-1977.
119. Sevigny, M. B., Li, C. F., Alas, M., & Hughes-Fulford, M. (2006). Glycosylation regulates turnover of cyclooxygenase-2. *FEBS Lett*, *580*, 6533-6536.
120. Shah, T., Ryu, S., Lee, H. J., Brown, S., & Kim, J. H. (2002). Pronounced radiosensitization of cultured human cancer cells by COX inhibitor under acidic microenvironment. *Int. J. Radiat. Oncol. Bio. Phys.*, *53*(5), 1314-1318.
121. Shao, J., Jung, C., Liu, C., & Sheng, H. (2005). Prostaglandin E2 stimulates the beta-catenin/T cell factor-dependent transcription in colon cancer. *J. Biol. Chem.*, *280*, 26565-26572.
122. Shao, J., Lee, S. B., Guo, H., Evers, B., & Sheng, H. (2003). Prostaglandin E2 stimulates the growth of colon cancer cells via induction of amphiregulin. *Cancer Res.*, *63*(17), 5218-5223.
123. Shishodia, S., & Aggarwal, B. B. (2004). Cyclooxygenase (COX)-2 inhibitor celecoxib abrogates activation of cigarette smoke-induced nuclear factor (NK)-kappaB by suppressing activation of IkappaBalpha kinase in human non-small cell lung carcinoma: correlation with suppression of cyclin D1, COX-2, and matrix metalloproteinase-9. *Cancer Res.*, *64*, 5004-5012.
124. Sminia, P., Kuipers, G., Geldof, A., Lafleur, V., & Slotman, B. (2005). COX-2 inhibitors act as radiosensitizer in tumor treatment. *Biomedicine & Pharmacotherapy*, *59*, S272-S275.
125. Smith, T. A. (2001). The rate-limiting step for tumor [18F]fluoro-2-deoxy-Dglucose (FDG) incorporation. *Nucl Med Biol*, *28*(1), 1-4.
126. Smith, W. L. (1989). The eicosanoids and their biochemical mechanisms of action. *Biochem. J.*, *259*, 315-324.
127. Smith, W. L., Garavito, R. M., & DeWitt, D. L. (1996). Prostaglandin endoperoxide H synthase (Cyclooxygenases)-1 and -2. *J. Biol. Chem.*, *271*, 33157-33160.
128. Sonoshita, M., Takaku, K., Oshima, M., Sugihara, K., & Taketo, M. M. (2002). Cyclooxygenase-2 expression in fibroblasts and endothelial cells of intestinal polyps. *Cancer Res.*, *62*, 6846-6849.
129. Subbaramaiah, K., Altorki, N., Chung, W. J., Mestre, J. R., Sampat, A., & Dannenberg, A. J. (1999). Inhibition of cyclooxygenase-2 gene expression by p53. *J. Biol. Chem.*, *274*, 10911-10915.
130. Subbaramaiah, K., Chung, W. J., & Dannenberg, A. J. (1998). Ceramide regulates the transcription of cyclooxygenase-2. Evidence for involvement of extracellular signal-regulated kinase/c-Jun N-terminal kinase and p38 mitogen-activated protein kinase pathways. *J. Biol. Chem.*, *273*(49), 32943-32949.
131. Subbaramaiah, K., & Dannenberg, A. J. (2003). Cyclooxygenase 2: a molecular target for cancer prevention and treatment. *Trends Pharmacol. Sci.*, *24*, 296-302.

132. Sugimoto, Y., & Narumiya, S. (2007). Prostaglandin E receptors. *J. Biol. Chem.*, *282*, 11613-11617.
133. Suzuki, A., Tsutomi, Y., Yamamoto, N., Shibutani, T., & Akahane, K. (1999). Mitochondrial regulation of cell death: mitochondria are essential for procaspase 3-p21 complex formation to resist Fas-mediated cell death. *Molecular and Cellular Biology*, *19*, 3842-3847.
134. Takashima-Hirano, M., Takashima, T., Katayama, Y., Wada, Y., Sugiyama, Y., Watanabe, Y. et al. (2001). Efficient sequential synthesis of PET probes of the COX-2 inhibitor [11C]celecoxib and its major metabolite [11C]SC-62807 and in vivo PET evaluation. *Bioorg. Med. Chem.*, *19*, 2997-3004.
135. Tang, C., Liu, C., Zhou, X., & Wang, C. (2004). Enhanced inhibitive effects of combination of rofecoxib and octreotide on the growth of human gastric cancer. *Int J Cancer*, *112*, 470-474.
136. te Poele, R. H., & Joel, S. P. (1999). Schedule dependent cytotoxicity of SN-38 in p53 wild-type and mutant colon adenocarcinoma cell lines. *Br. J. Cancer*, *81*, 1285-1293.
137. te Poele, R. H., Okorokov, A. L., Jardine, L., Cummings, J., & Joel, S. P. (2002). DNA damage is able to induce senescence in tumor cells in vitro and in vivo. *Cancer Res.*, *62*, 1876-1883.
138. Thiel, G., & Cibelli, G. (2002). Regulation of life and death by the zinc finger transcription factor Egr-1. *J Cell Physiol*, *193*, 287-292.
139. Tietz, O., Marshall, A., Wuest, M., Wang, M., & Wuest, F. (2013). Radiotracers for molecular imaging of cyclooxygenase-2 (COX-2) enzyme. *Curr. Med. Chem.*, *20*, 4350-4369.
140. Tietz, O., Sharma, S. K., Kaur, J., Way, J., Marshall, A., Wuest, M. et al. (2013). Synthesis of three 18F-labelled cyclooxygenase-2 (COX-2) inhibitors based on a pyrimidine scaffold. *Org. Biomol. Chem.*, *11*(46), 8052-8064.
141. Tsuji, M., Kawano, S., & DuBois, R. N. (1997). Cyclooxygenase-2 expression in human colon cancer cells increases metastatic potential. *Proc. Natl. Acad. Sci. U.S.A.*, *94*(7), 3336-2240.
142. Tsujii, M., & DuBois, R. N. (1995). Alterations in cellular adhesion and apoptosis in epithelial cells overexpressing prostaglandin endoperoxide synthase 2. *Cell*, *83*(3), 493-501.
143. Tuorkey, M. J. (2012). Bioelectrical Impedance as a Diagnostic Factor in the Clinical Practice and Prognostic Factor for Survival in Cancer Patients: Prediction, Accuracy and Reliability. *J. Biosens Bioelectron*, *3*, 121.
144. Uddin, M., Crews, B., Ghebreselasie, K., Huda, I., Kingsley, P., Ansari, M. et al. (2011). Fluorinated COX-2 inhibitors as agents in PET imaging of inflammation and cancer. *Can. Prev. Res.*, *4*, 1536-1545.
145. von Sonntag, C. (1987). *The chemical basis of radiation biology*. Taylor and Francis.
146. Vona-Davis, L., Riggs, D. R., Jackson, B. J., & McFadden, D. W. (1999). Antiproliferative and apoptotic effects of rofecoxib on esophageal cancer in vitro(1). *J Surn Res*, *119*, 143-148.
147. Waddell, W. R., Ganser, G. F., Cerise, E. J., & Loughry, R. W. (1989). Sulindac for polyposis of the colon. *Am. J. Surg.*, *157*, 175-179.

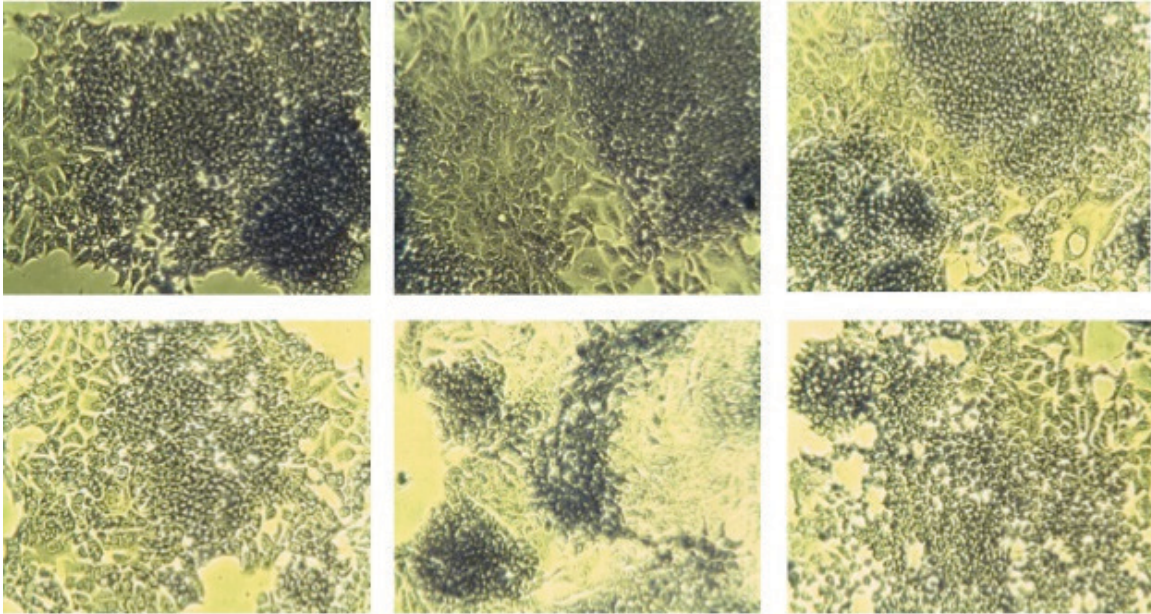
148. Wang, D., & DuBois, R. N. (2007). Inflammatory mediators and nuclear receptor signalling in colorectal cancer. *Cell Cycle*, 6, 682-685.
149. Wang, D., Wang, H., Brown, J. M., Saikoku, T., Ning, W., Shi, Q. et al. (2006). CXCL1 induced by prostaglandin E2 promotes angiogenesis in colorectal cancer. *J. Exp. Med.*, 203, 941-951.
150. Wang, D., Wang, H., Shi, Q., Katkuri, S., Walhi, W., Desvergne, B. et al. (2004). Prostaglandin E2 promotes colorectal adenoma growth via transactivation of the nuclear peroxisome proliferator-activated receptor delta. *Cancer Cell*, 6, 285-295.
151. Wang, Z., Hu, L., Zhu, X., & Song, Y. (2007). Radiosensitivity enhancement by NS-398, a cyclooxygenase(COX)-2 selective inhibitor, via enhancing sensitivity to X-ray irradiation-induced apoptosis on the human colorectal cancer cell line HT-29. *J. Shandong Univ. (Health Sciences)*, 2.
152. Weber, A., Casini, A., Heine, A., Kuhn, D., Supuran, C. T., Scozzafava, A. et al. (2004). Unexpected nanomolar inhibition of carbonic anhydrase by COX-2-selective celecoxib: new pharmacological opportunities due to related binding site recognition. *J Med Chem*, 47, 550-557.
153. Wiese, F. W., Thompson, P. A., & Kadlubar, F. F. (2001). Carcinogen substrate specificity of human COX-1 and COX-2. *Carcinogenesis*, 22(1), 5-10.
154. Williams, C. S., Tsujii, M., Reese, J., Dey, S. K., & DuBois, R. N. (2000). Host cyclooxygenase-2 modulates carcinoma growth. *J. Clin. Invest.*, 105(11), 1589-1594.
155. Williams, K. J., Telfer, B. A., Brave, S., Kendrew, J., Whittaker, L., Stratford, I. J. et al. (2004). ZD6474, a potent inhibitor of vascular endothelial growth factor signalling, combined with radiotherapy: schedule-dependent enhancement of antitumor activity. *Clin. Cancer Res.*, 10, 8587-8593.
156. Wun, T., McKnight, H., & Tuscano, J. M. (2004). Increased cyclooxygenase-2 (COX-2): a potential role in the pathogenesis of lymphoma. *Leuk Res*, 28, 179-190.
157. Xie, W., & Herschman, H. R. (1996). Transcriptional regulation of prostaglandin synthase 2 gene expression by platelet-derived growth factor and serum. *J. Biol. Chem.*, 271(49), 31742-31748.
158. Xiong, Y., Hannon, G. J., Zhang, H., Casso, D., Kobayashi, R., & Beach, D. (1993). p21 is a universal inhibitor of cyclin kinases. *Nature*, 366, 701-704.
159. Yamamoto, K., Arakawa, T., Ueda, N., & Yamamoto, S. (1995). Transcriptional roles of nuclear factor kappa B and nuclear factor-interleukin-6 in the tumor necrosis factor alpha-dependent induction of cyclooxygenase-2 in MC3T3-E1 cells. *J. Biol. Chem.*, 270, 31315-31320.
160. Yao, M., Kargman, S., Lam, E. C., Kelly, C. R., Zheng, Y., & Luk, P. (2003). Inhibition of cyclooxygenase-2 by rofecoxib attenuates the growth and metastatic potential of colorectal carcinoma in mice. *Cancer Res.*, 63, 586-592.
161. Yiu, G. K., & Toker, A. (2006). NFAT induces breast cancer cell invasion by promoting the induction of cyclooxygenase-2. *J. Biol. Chem.*, 281(18), 12210-12217.
162. Zavada, J., Zavadova, Z., Pastorek, J., Biesova, Z., Jezek, J., & Velek, J. (2000). Human tumour-associated cell adhesion protein MN/CA IX: identification of M75 epitope and of the region mediating cell adhesion. *Br J Cancer*, 82, 1808-1813.
163. Zhang, Y., Fujita, N., & Tsuruo, T. (1999). Caspase-mediated cleavage of

- p21waf1/cip1 converts cancer cells from growth arrest to undergoing apoptosis. *Nature*, *18*, 1131-1138.
164. Zhang, Z., Lai, G. H., & Sirica, A. E. (2004). Celecoxib-induced apoptosis in rat cholangiocarcinoma cells mediated by Akt inactivation and Bax translocation. *Hepatology*, *39*, 1028-1037.
  165. Zheng, L., Wang, L., Qing, S., Han, M., Xu, X., & Zhou, J. (2011). Study on enhancement of radiosensitivity in colon cancer carcinoma cell line HT-29 by celecoxib in vitro and in vivo. *J. of Soochow Univ. (Med. Sci. Edition)*, *04*.
  166. Zhou, B. P., & Hung, M. C. (2002). Novel targets of Akt, p21cip1/waf1, and MDM2. *Seminars in Oncology*, *29*, 62-70.
  167. Zhou, B. P., & Hung, M. C. (2003). Dysregulation of cellular signaling by HER2/neu in breast cancer. *Seminars in Oncology*, *30*, 38-48.
  168. Zhou, B. P., Liao, Y., Xia, W., Spohn, B., Lee, M. H., & Hung, M. C. (2001). Cytoplasmic localization of p21cip1/waf1 by Akt-induced phosphorylation in HER-2/neu-overexpressing cells. *Nature Cell Biology*, *3*, 245-252.
  169. Zhu, J., Huang, J. W., Tseng, P. H., Yang, Y. T., Fowble, J., Shiau, C. W. et al. (2004). From the cyclooxygenase-2 inhibitor celecoxib to a novel class of 3-phosphoinositide-dependent protein kinase-1/Akt signaling represents a major cyclooxygenase-2 independent target for celecoxib in prostate cancer cells. *Cancer Res.*, *64*, 4309-4318.

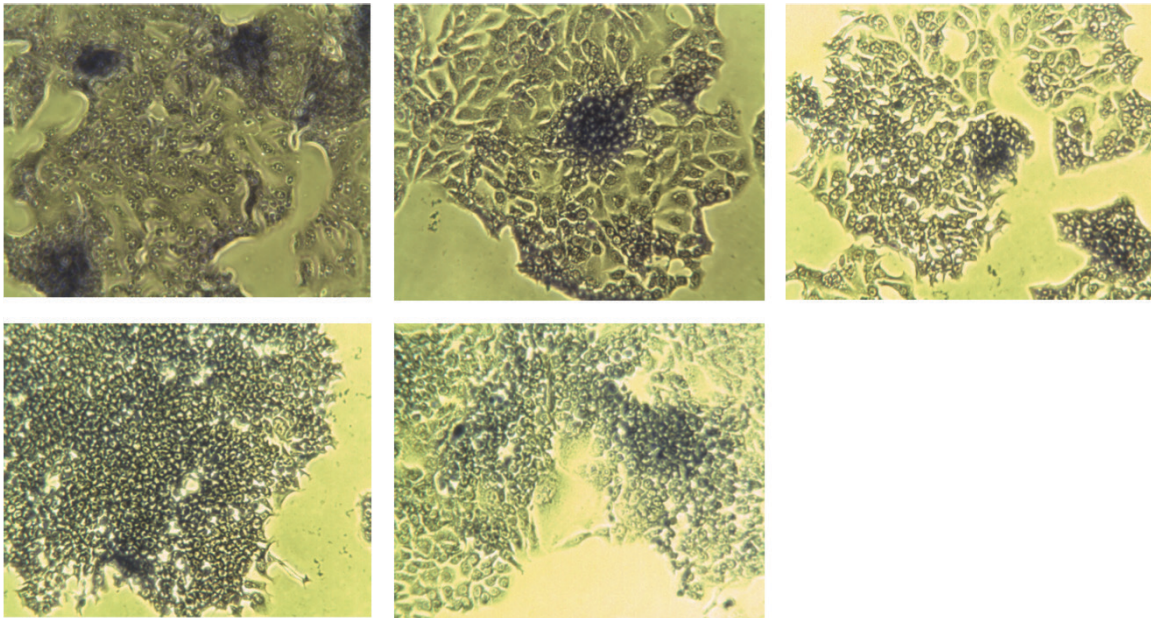
## APPENDICES

### I. GIEMSA stained images

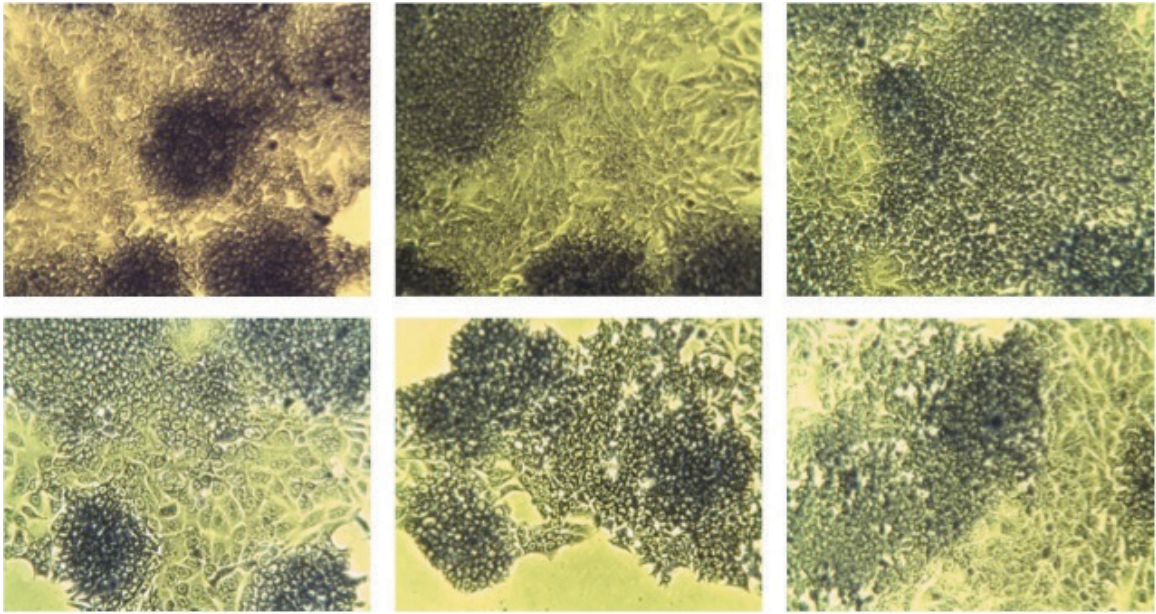
#### a. HCA-7 cells



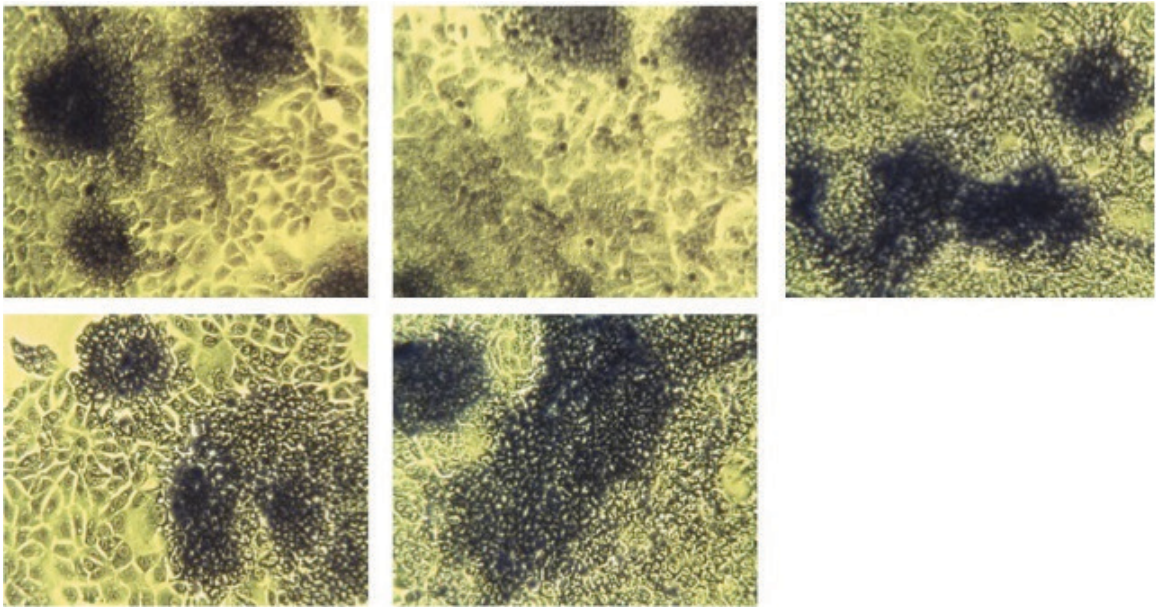
GIEMSA stained HCA-7 cells treated with 30  $\mu$ M celecoxib and 0 Gy.



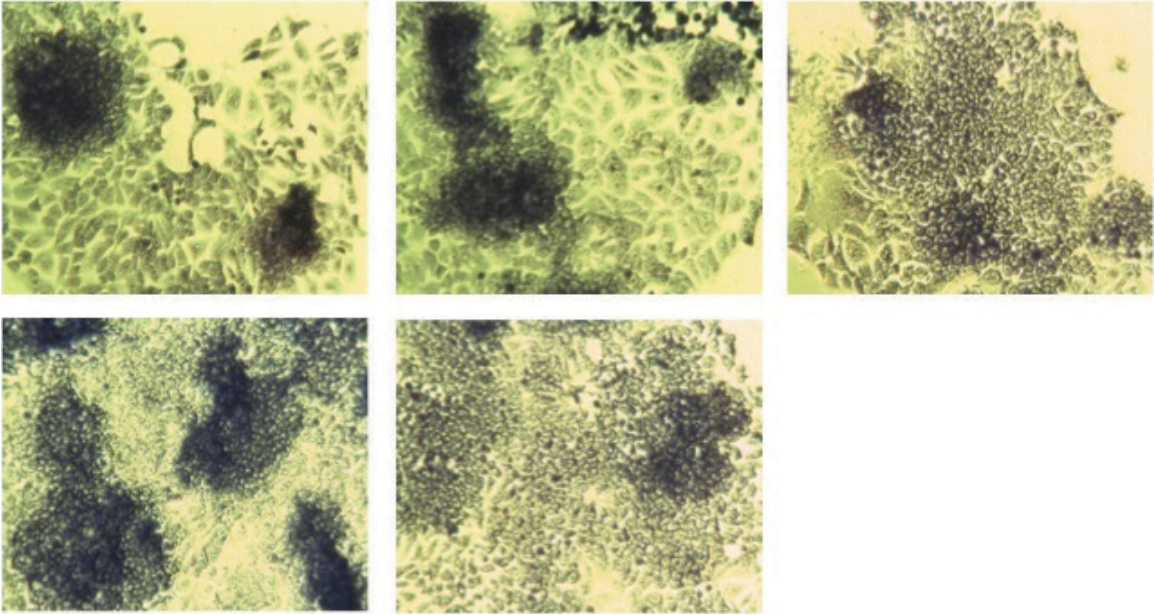
GIEMSA stained HCA-7 cells treated with 75  $\mu$ M celecoxib and 0 Gy.



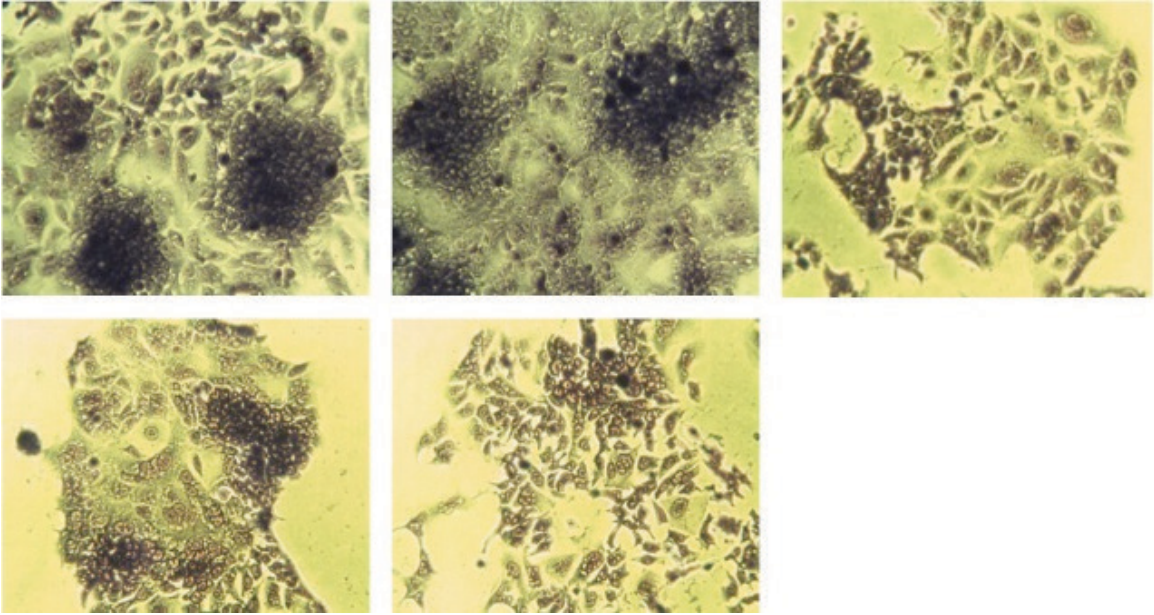
GIEMSA stained HCA-7 cells treated with DMSO and 0 Gy.



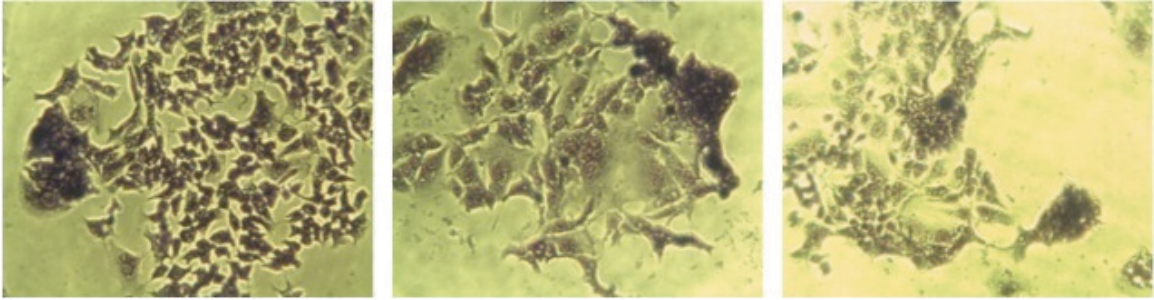
GIEMSA stained HCA-7 cells treated with 30  $\mu$ M pyrcoxib and 0 Gy.



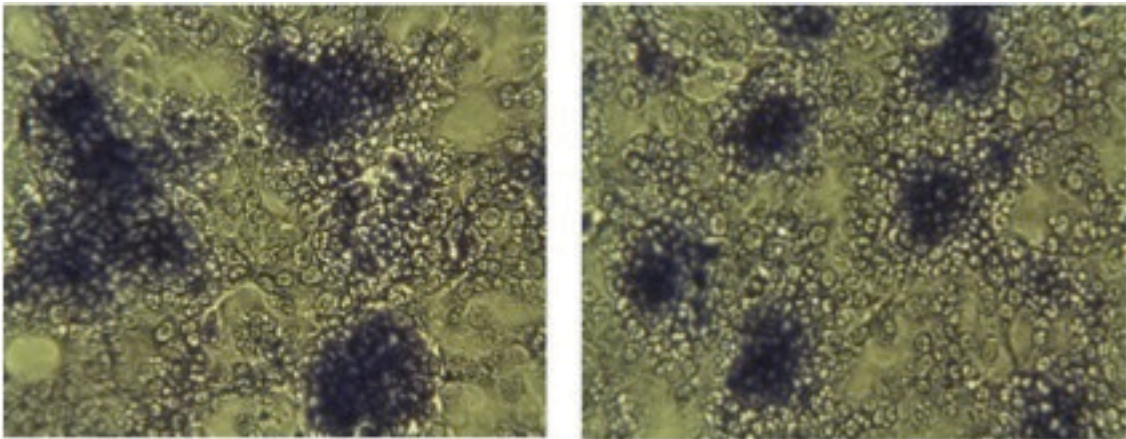
GIEMSA stained HCA-7 cells treated with 75  $\mu$ M pyrcoxib and 0 Gy.



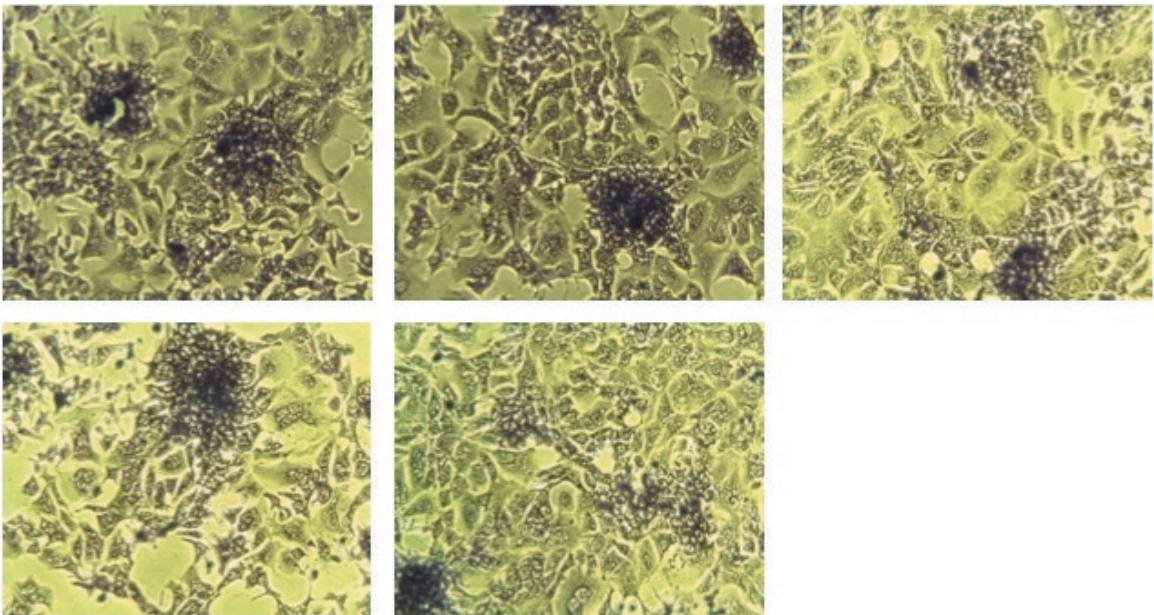
GIEMSA stained HCA-7 cells treated with 30  $\mu$ M celecoxib and 5 Gy.



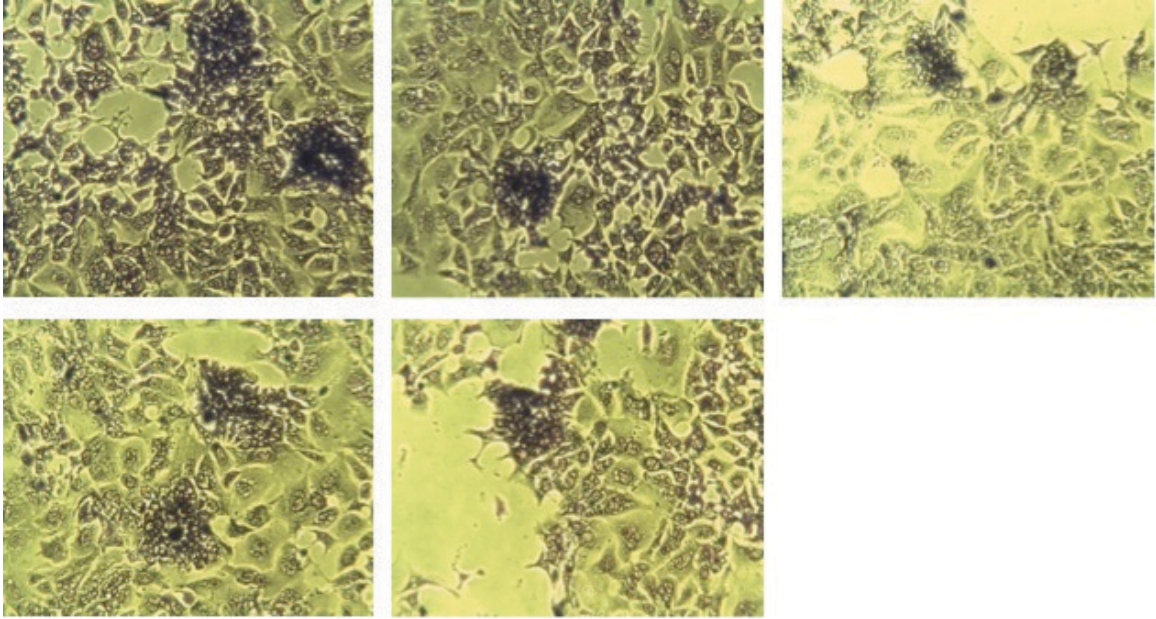
GIEMSA stained HCA-7 cells treated with 75  $\mu$ M celecoxib and 5 Gy.



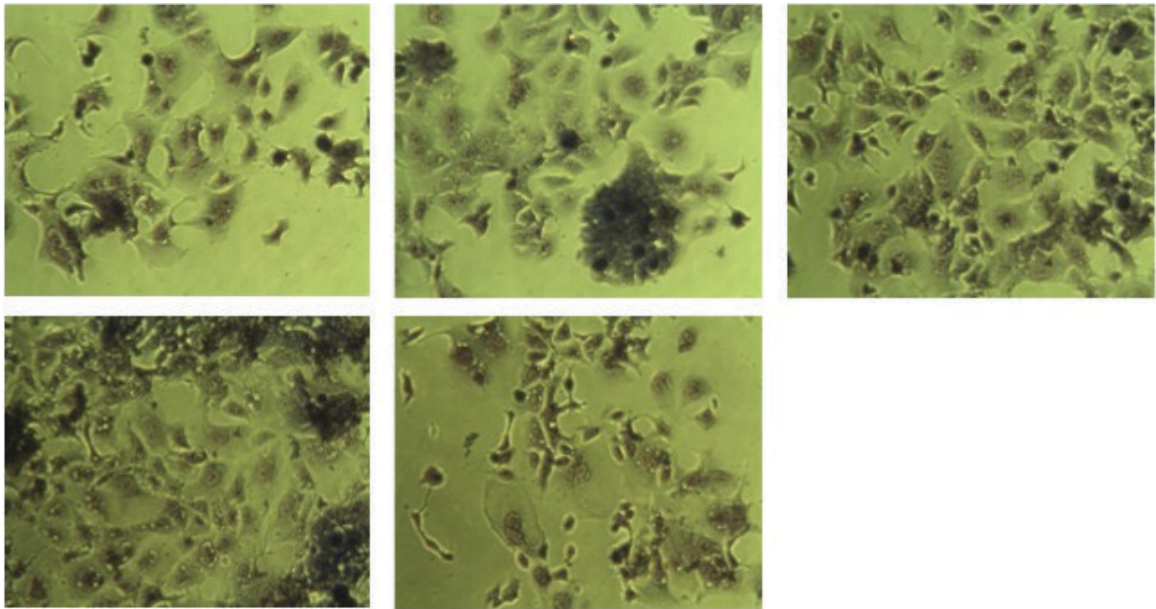
GIEMSA stained HCA-7 cells treated with DMSO and 5 Gy.



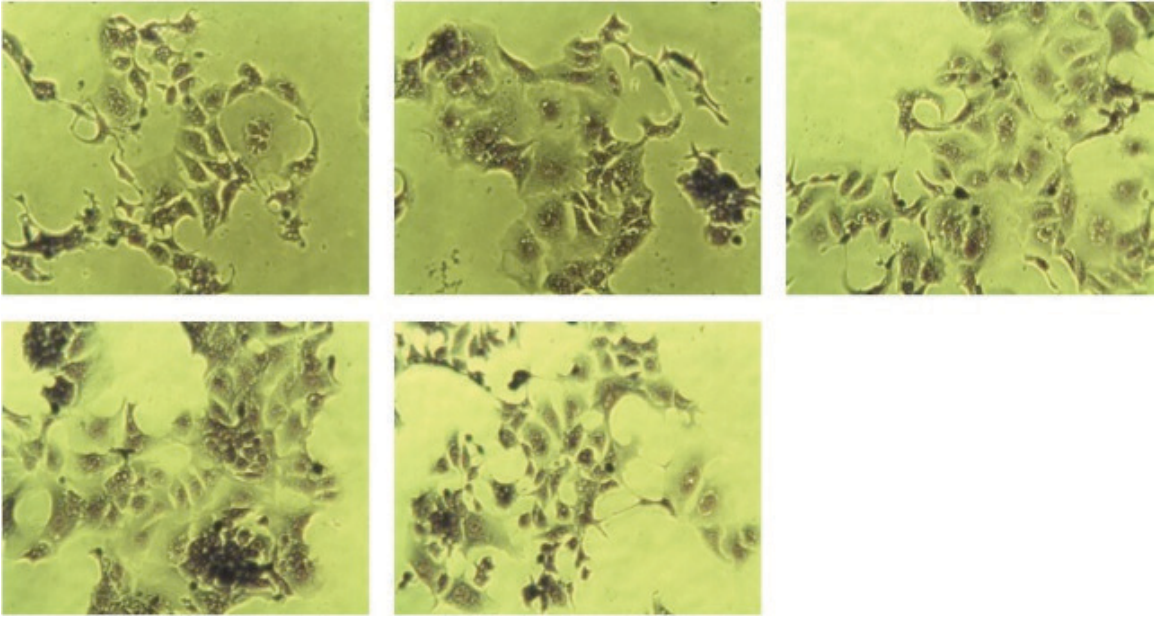
GIEMSA stained HCA-7 cells treated with 30  $\mu$ M pyrcoxib and 5 Gy.



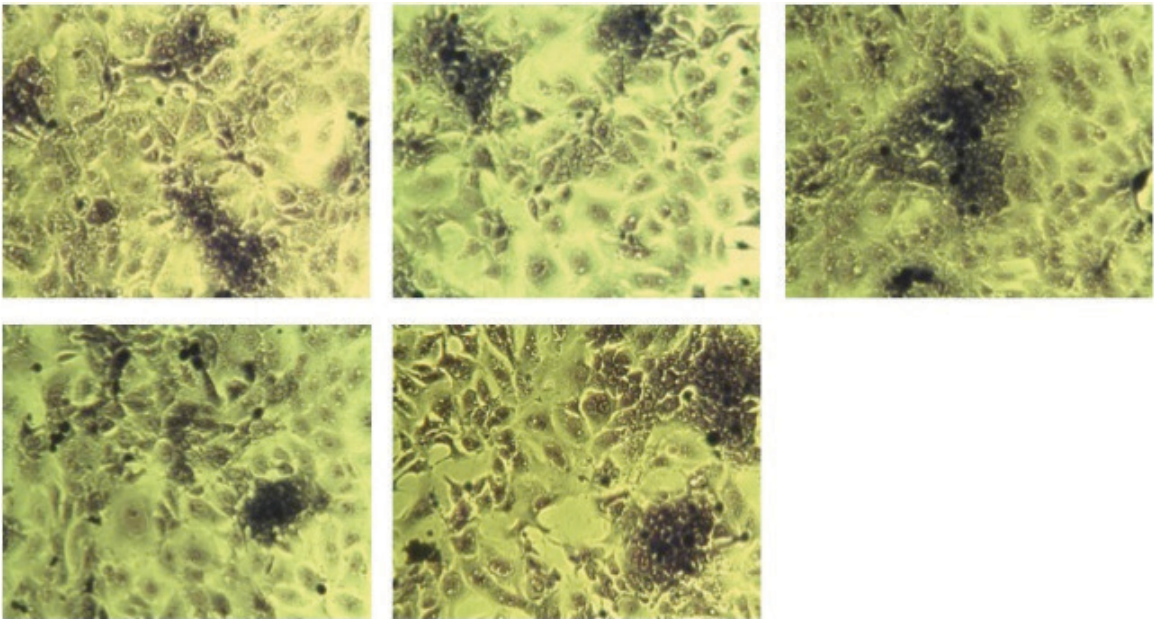
GIEMSA stained HCA-7 cells treated with 75  $\mu$ M pyrcoxib and 5 Gy.



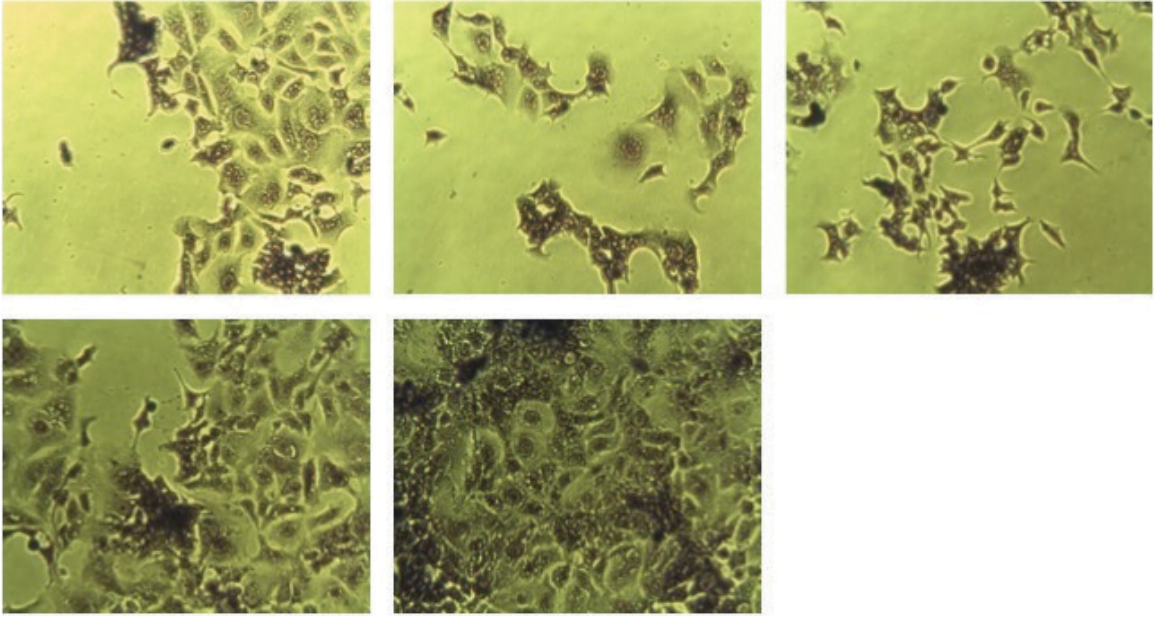
GIEMSA stained HCA-7 cells treated with 30  $\mu$ M celecoxib and 10 Gy.



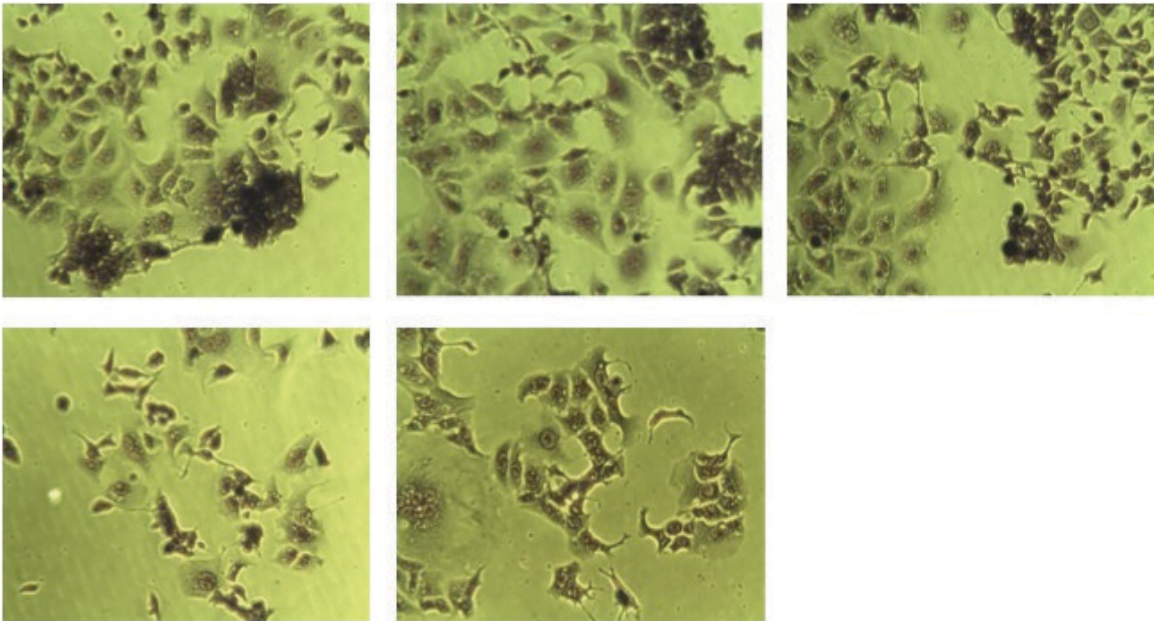
GIEMSA stained HCA-7 cells treated with 75  $\mu$ M celecoxib and 10 Gy.



GIEMSA stained HCA-7 cells treated with DMSO and 10 Gy.

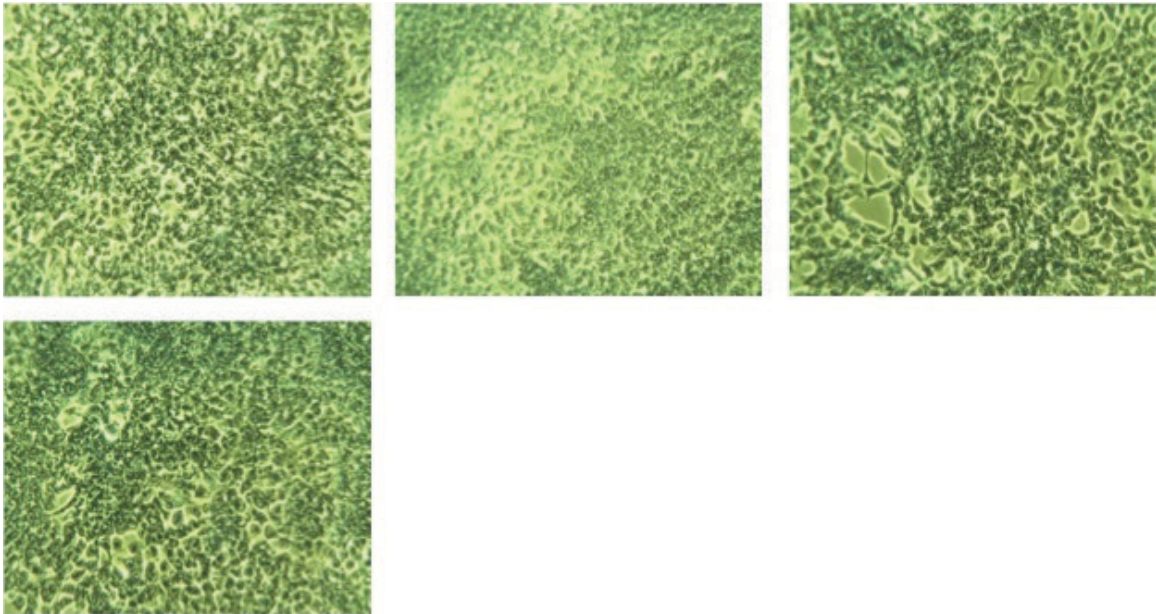


GIEMSA stained HCA-7 cells treated with 30  $\mu\text{M}$  pyricoxib and 10 Gy.

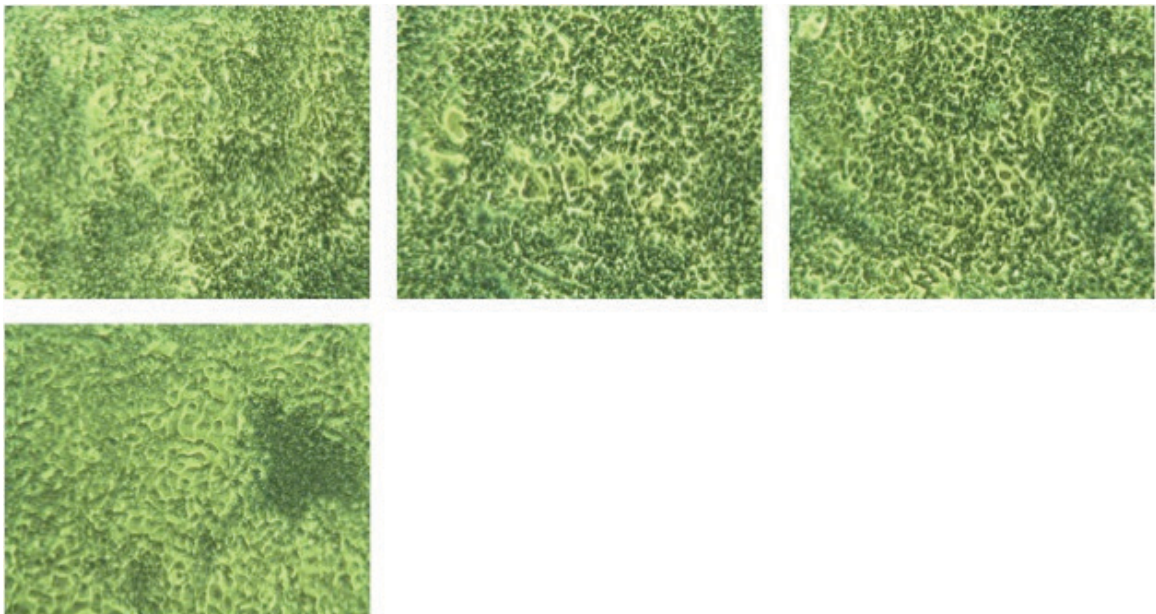


GIEMSA stained HCA-7 cells treated with 75  $\mu\text{M}$  pyricoxib and 10 Gy.

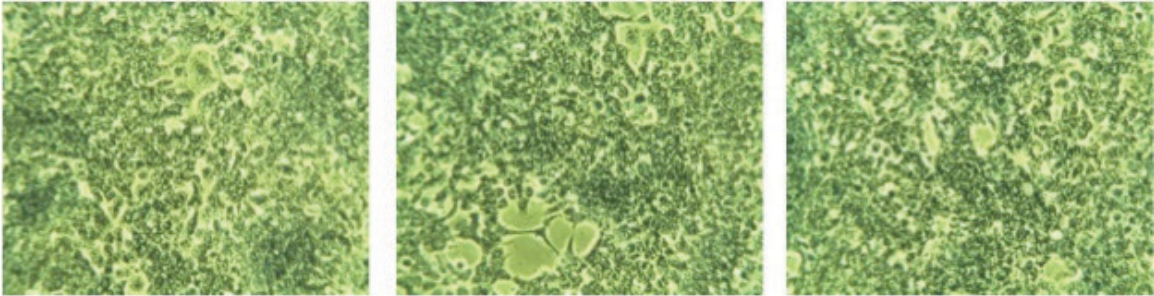
b. HCT-116 cells



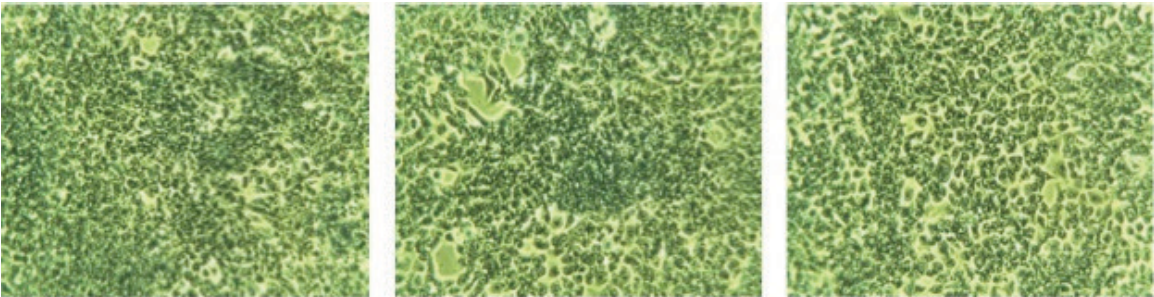
GIEMSA stained HCT-116 cells treated with 30  $\mu$ M celecoxib and 0 Gy.



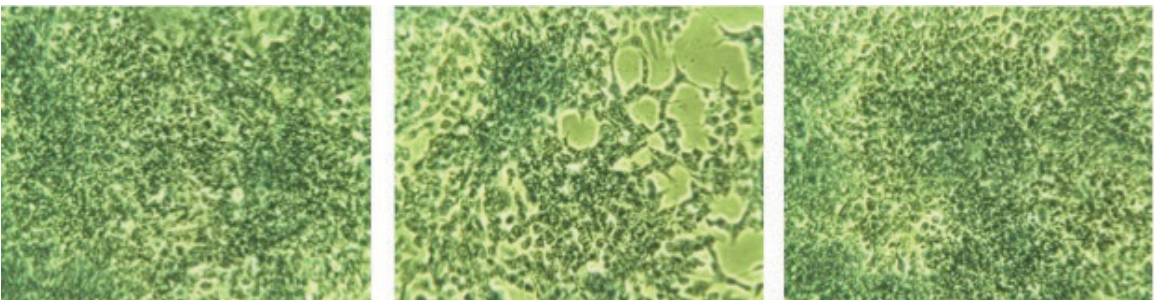
GIEMSA stained HCT-116 cells treated with 75  $\mu$ M celecoxib and 0 Gy.



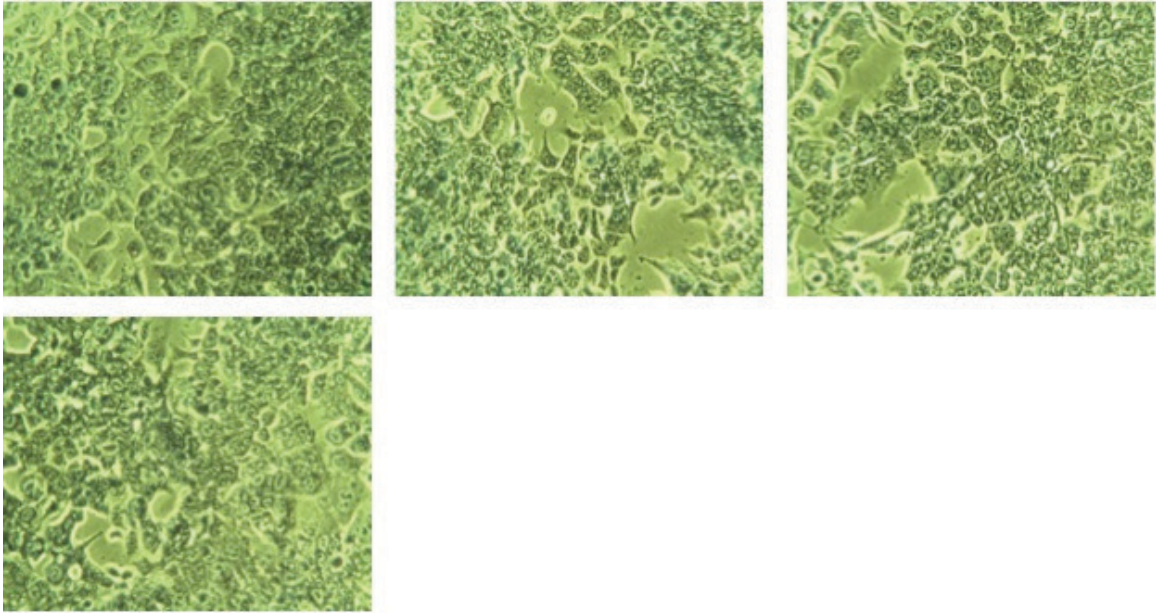
GIEMSA stained HCT-116 cells treated with DMSO and 0 Gy.



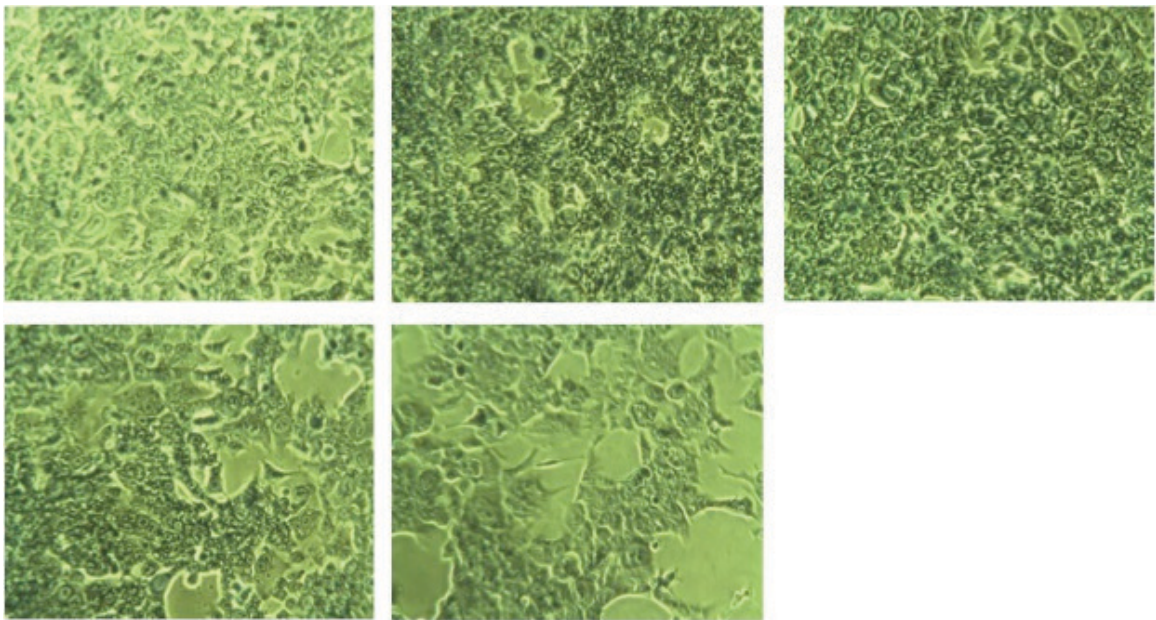
GIEMSA stained HCT-116 cells treated with 30  $\mu\text{M}$  pyradoxib and 0 Gy.



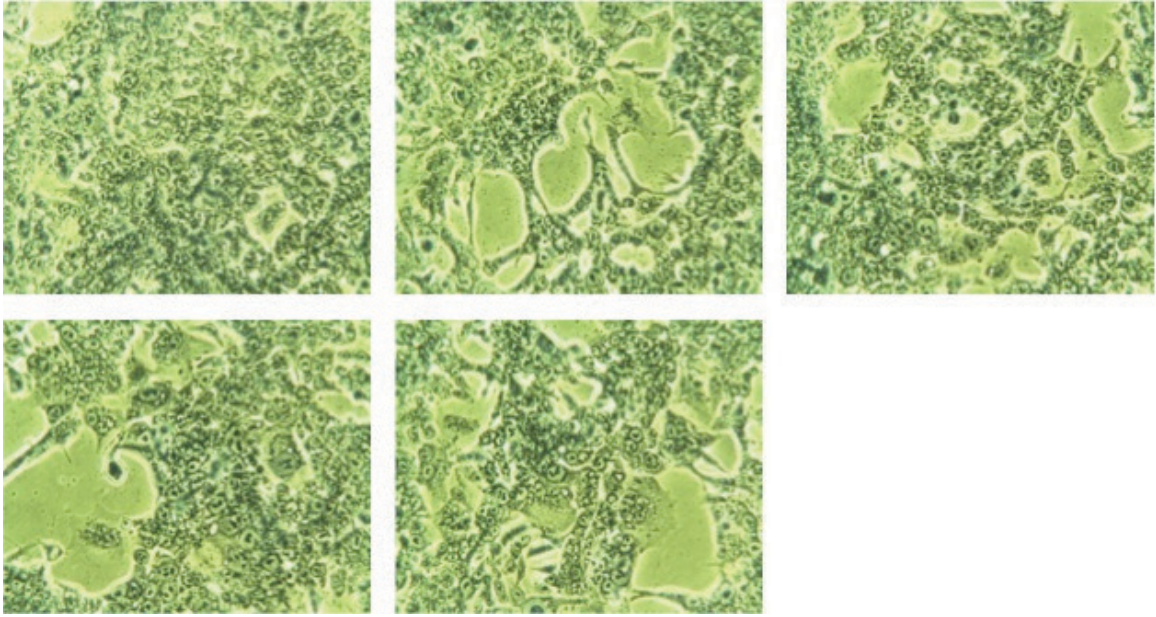
GIEMSA stained HCT-116 cells treated with 75  $\mu\text{M}$  pyradoxib and 0 Gy.



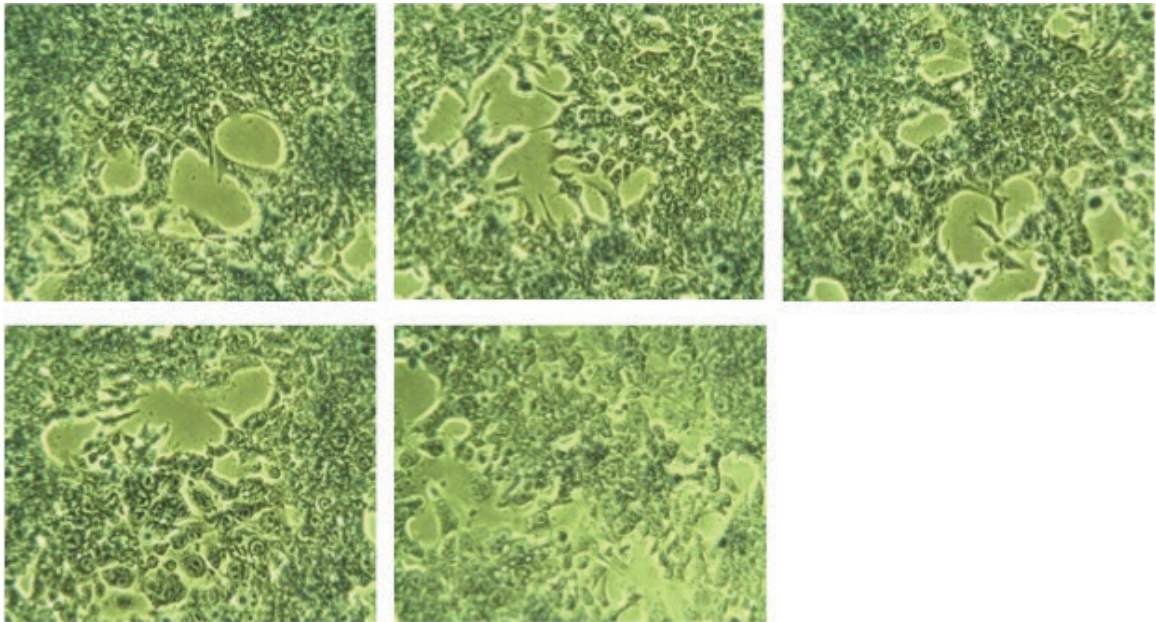
GIEMSA stained HCT-116 cells treated with 30  $\mu$ M celecoxib and 5 Gy.



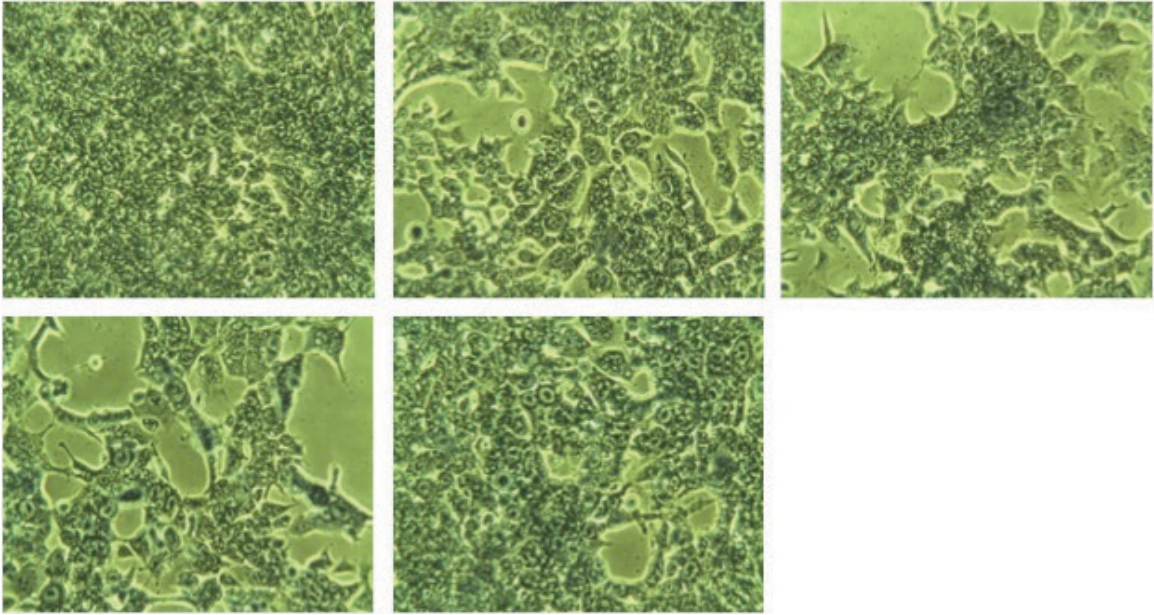
GIEMSA stained HCT-116 cells treated with 75  $\mu$ M celecoxib and 5 Gy.



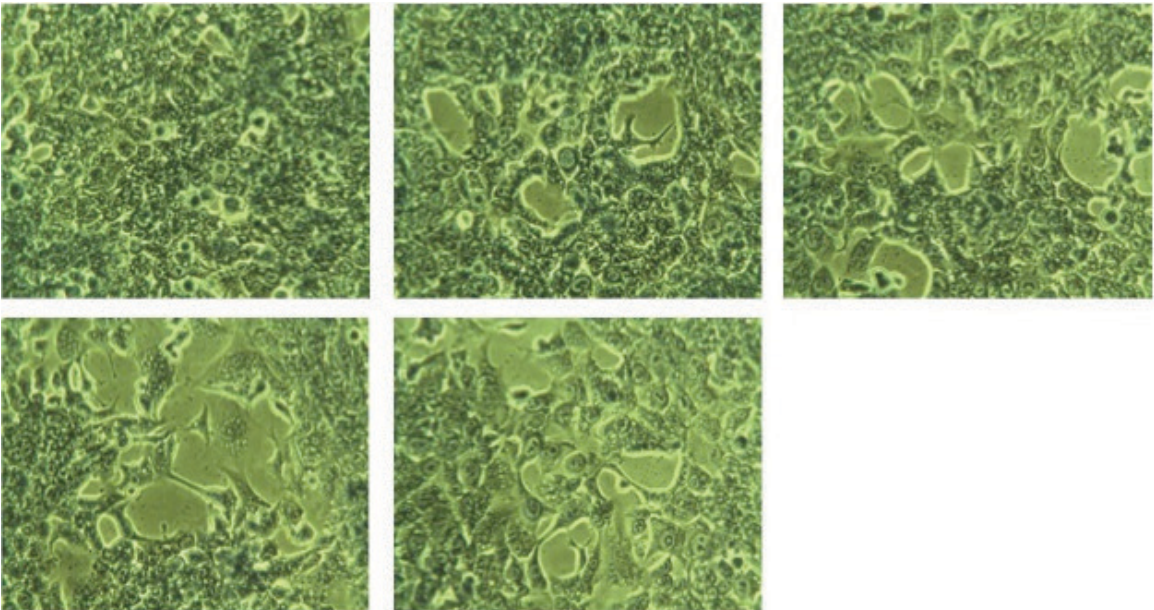
GIEMSA stained HCT-116 cells treated with DMSO and 5 Gy.



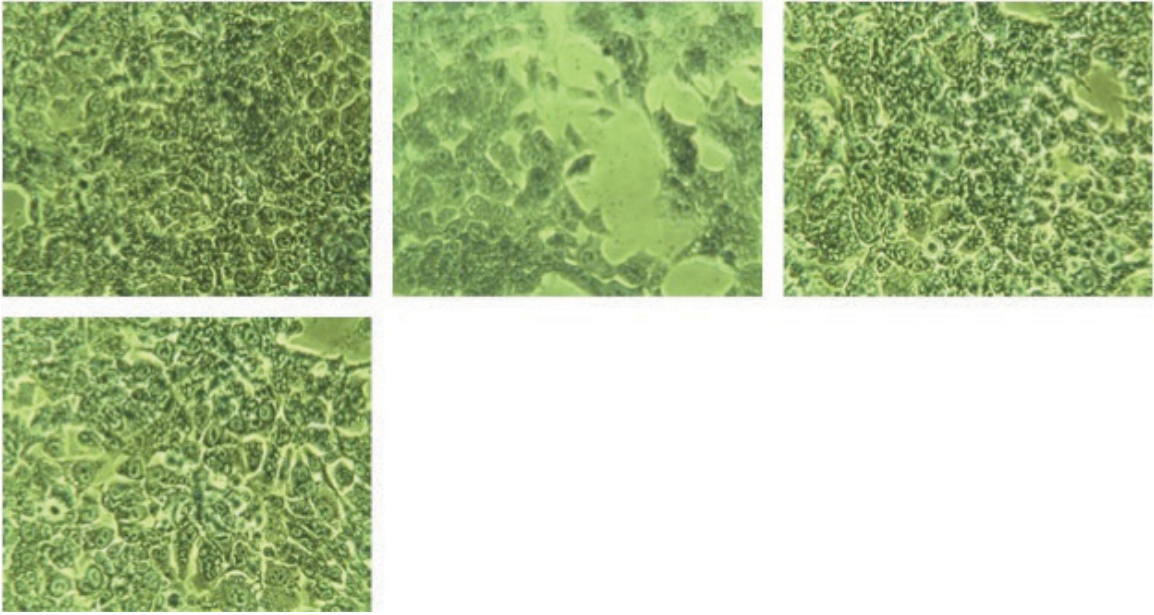
GIEMSA stained HCT-116 cells treated with 30  $\mu$ M pyricoxib and 5 Gy.



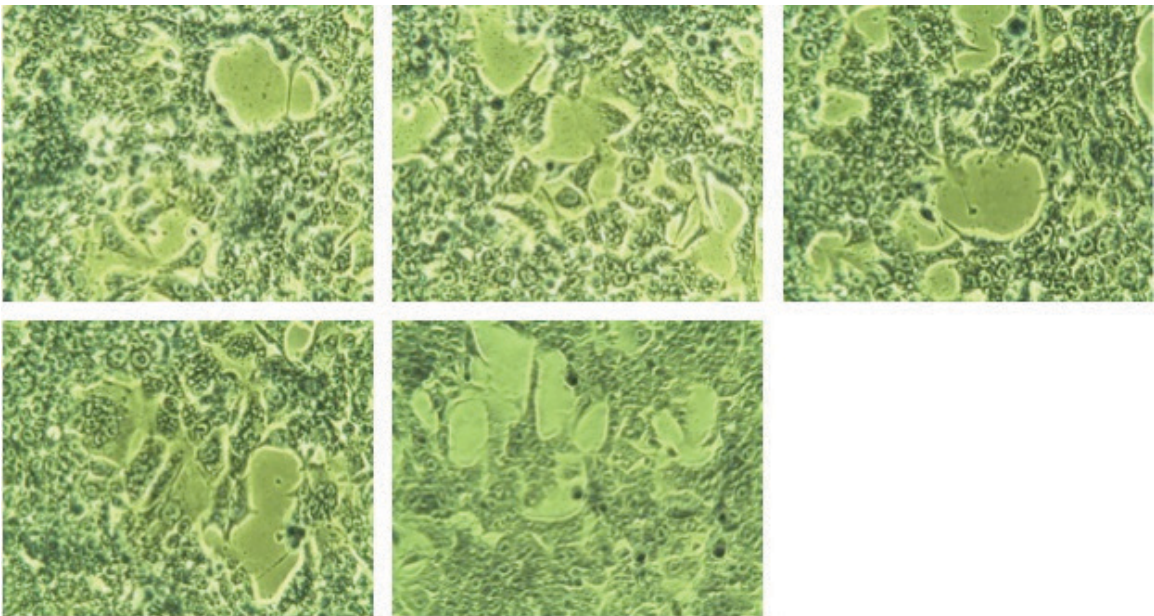
GIEMSA stained HCT-116 cells treated with 75  $\mu$ M pyrcoxib and 5 Gy.



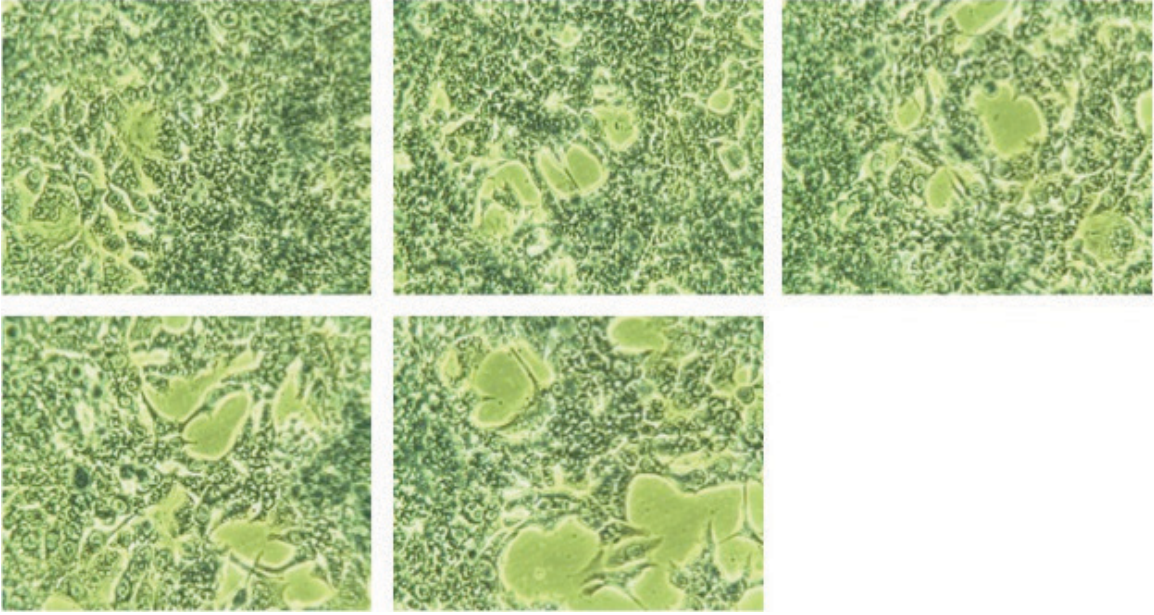
GIEMSA stained HCT-116 cells treated with 30  $\mu$ M celecoxib and 10 Gy.



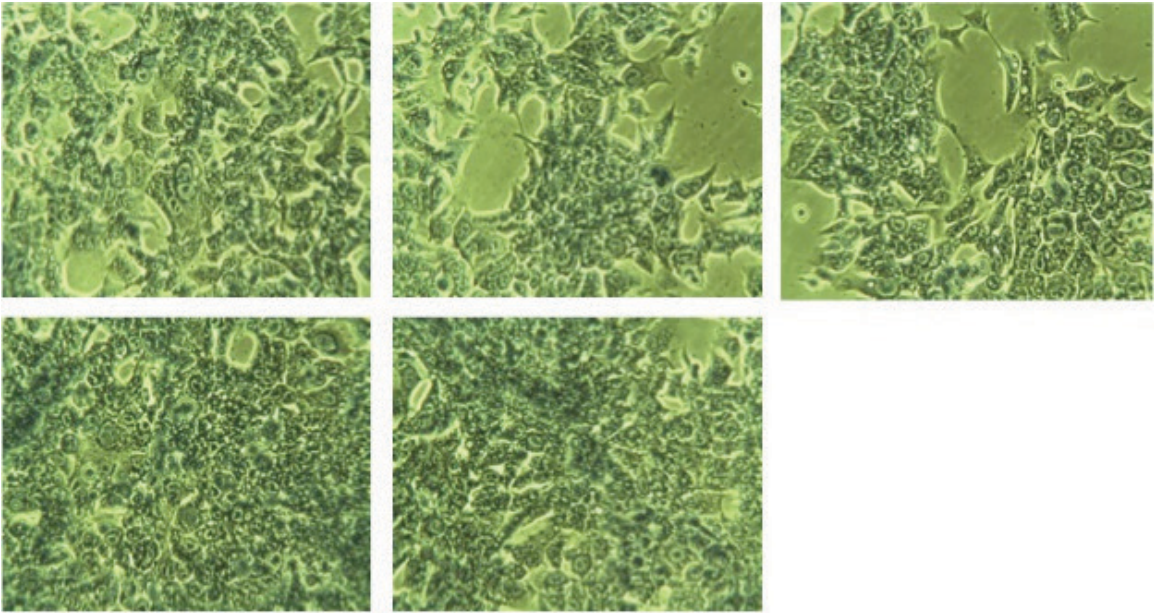
GIEMSA stained HCT-116 cells treated with 75  $\mu$ M celecoxib and 10 Gy.



GIEMSA stained HCT-116 cells treated with DMSO and 10 Gy.



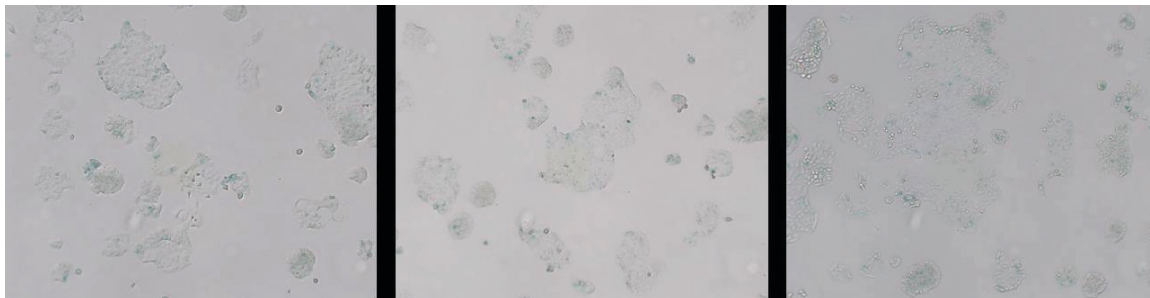
GIEMSA stained HCT-116 cells treated with 30  $\mu$ M pyricoxib and 10 Gy.



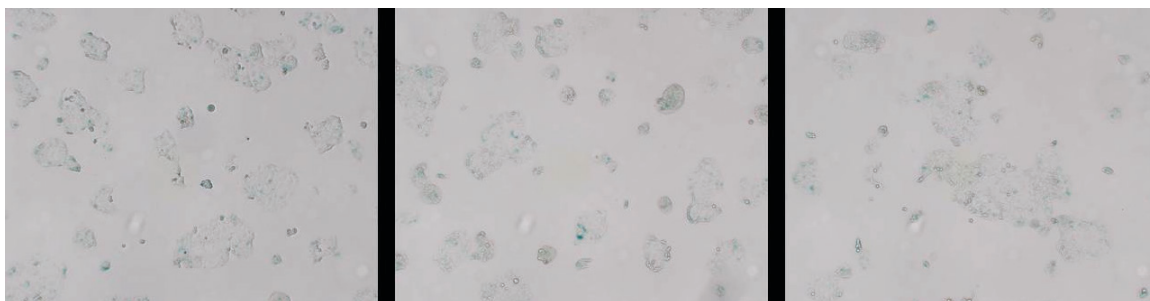
GIEMSA stained HCT-116 cells treated with 75  $\mu$ M pyricoxib and 10 Gy.

## II. $\beta$ -glucosidase stained images

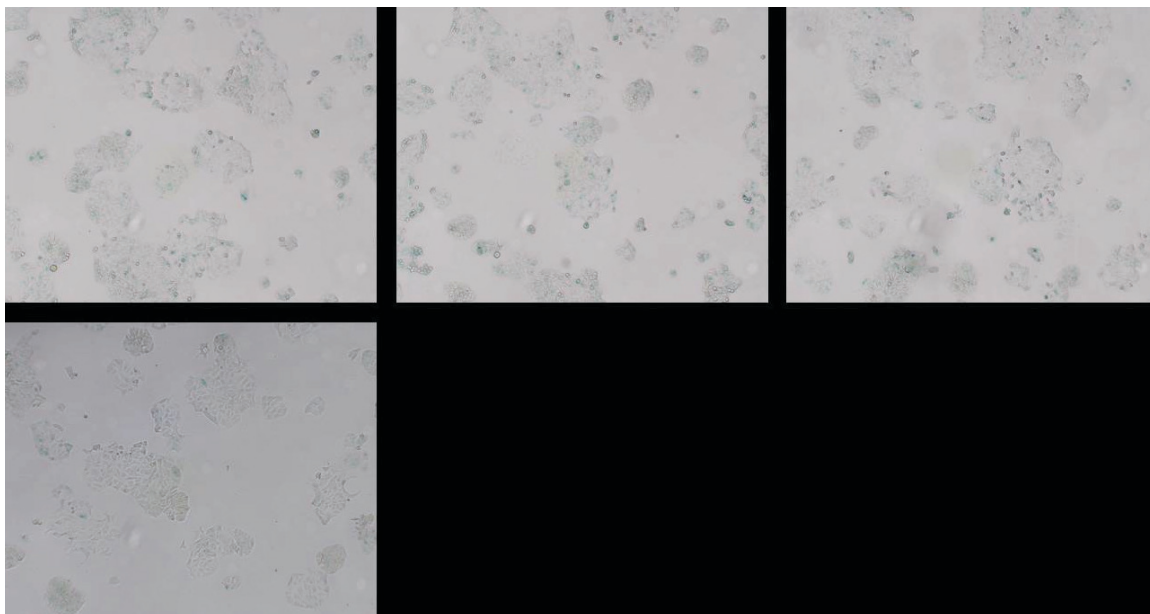
### a. HCA-7 cells



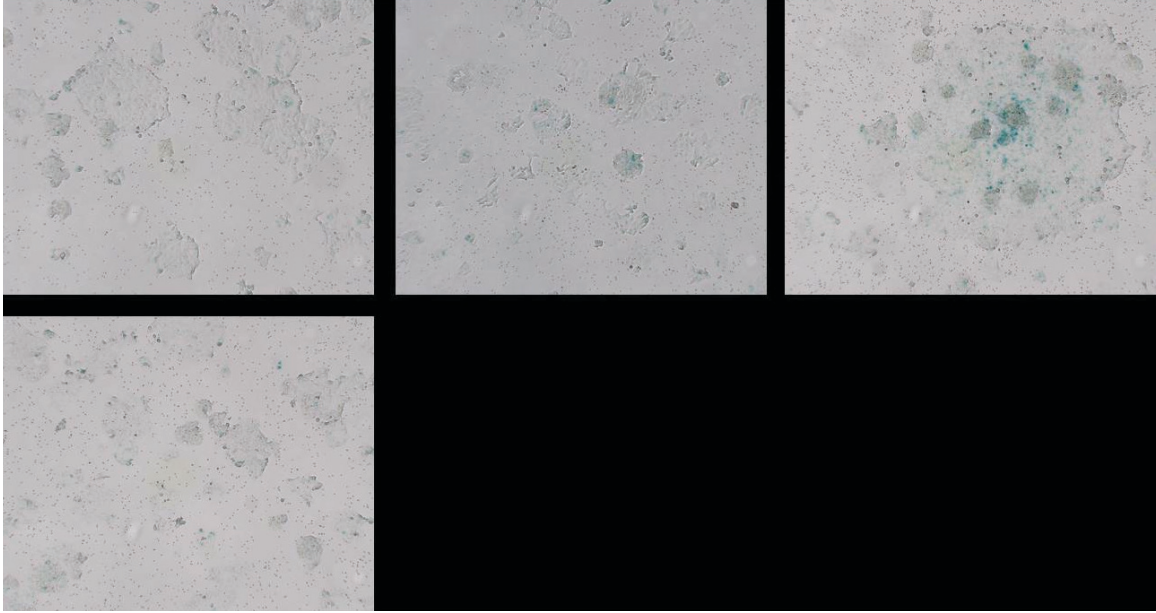
$\beta$ -glucosidase stained HCA-7 cells treated with 30  $\mu$ M celecoxib and 0 Gy.



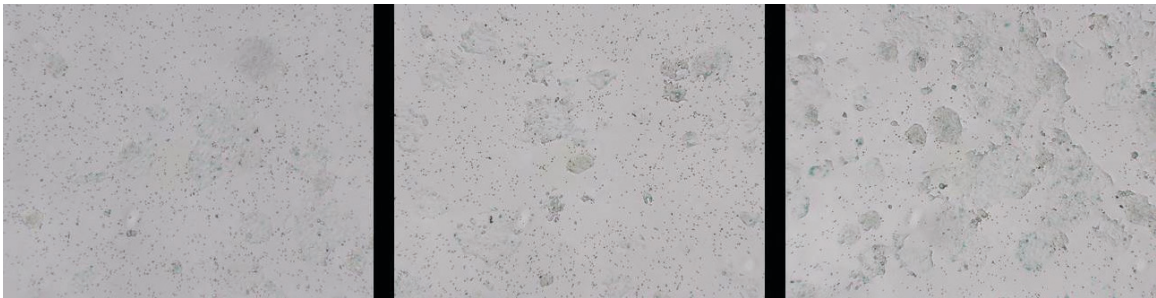
$\beta$ -glucosidase stained HCA-7 cells treated with 75  $\mu$ M celecoxib and 0 Gy.



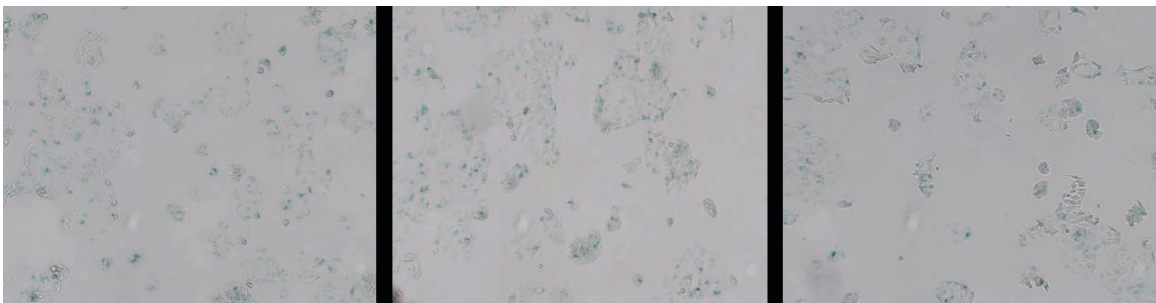
$\beta$ -glucosidase stained HCA-7 cells treated with DMSO and 0 Gy.



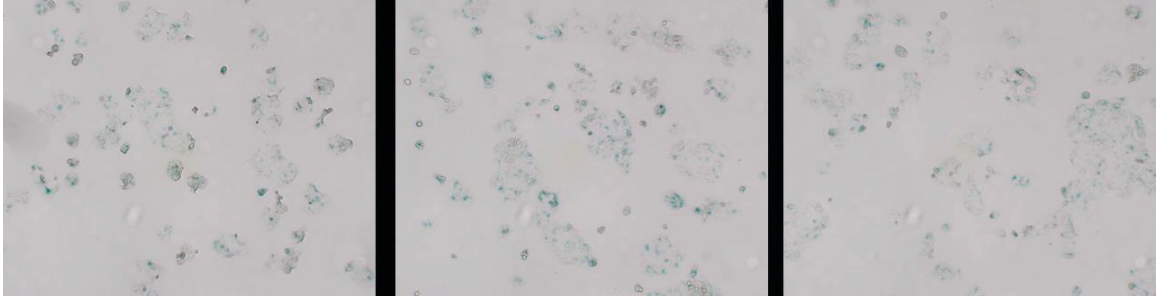
$\beta$ -glucosidase stained HCA-7 cells treated with 30  $\mu$ M pyrcoxib and 0 Gy.



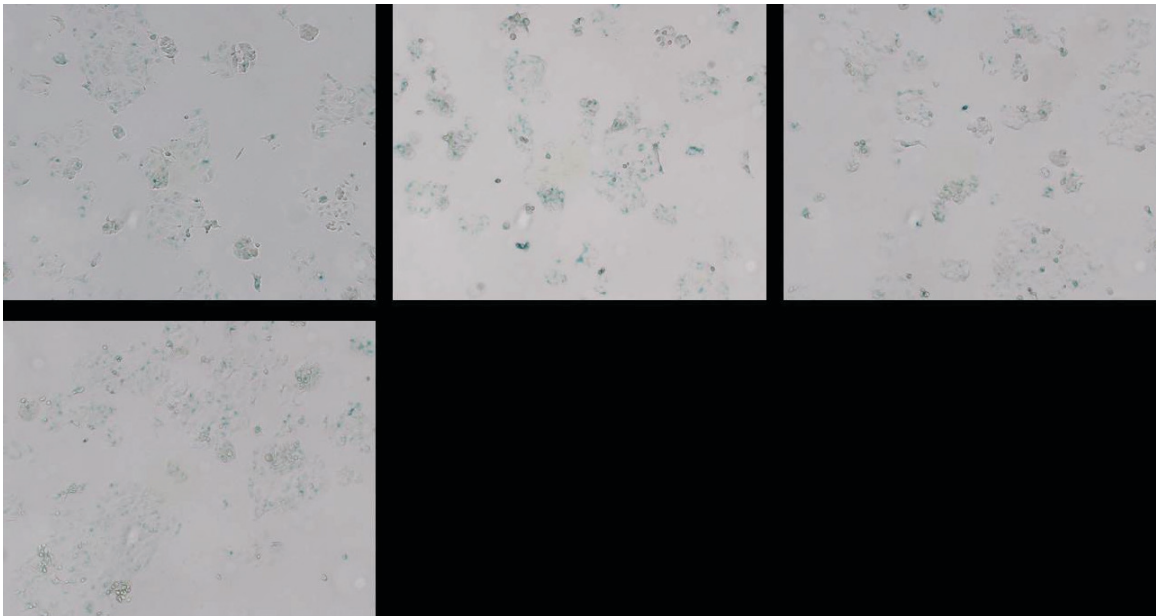
$\beta$ -glucosidase stained HCA-7 cells treated with 75  $\mu$ M pyrcoxib and 0 Gy.



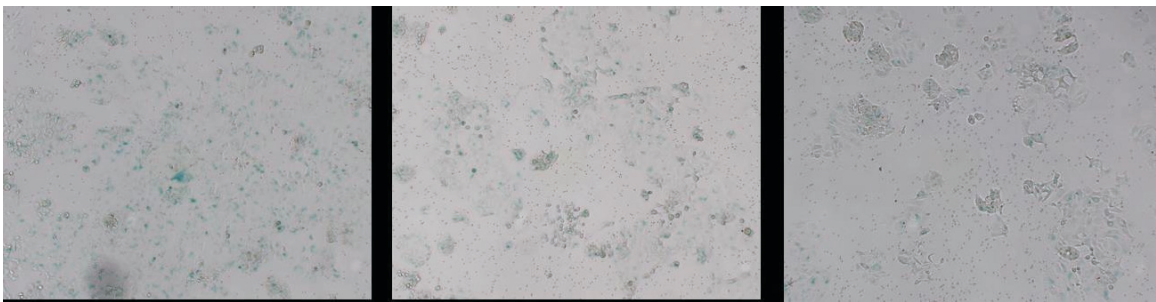
$\beta$ -glucosidase stained HCA-7 cells treated with 30  $\mu$ M celecoxib and 5 Gy.



$\beta$ -glucosidase stained HCA-7 cells treated with 75  $\mu$ M celecoxib and 5 Gy.



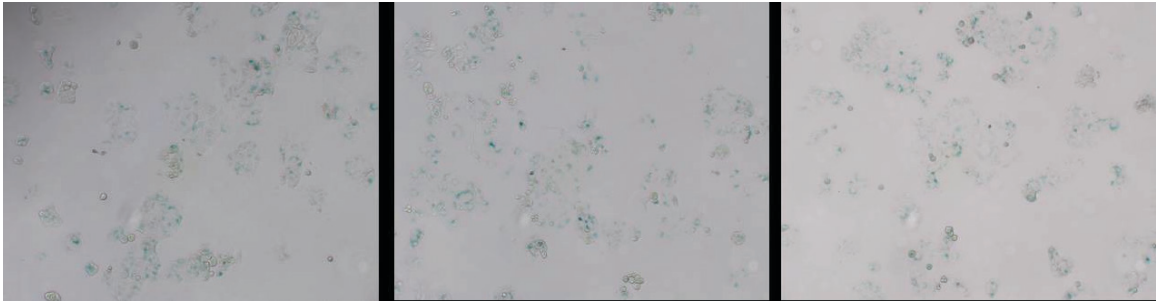
$\beta$ -glucosidase stained HCA-7 cells treated with DMSO and 5 Gy.



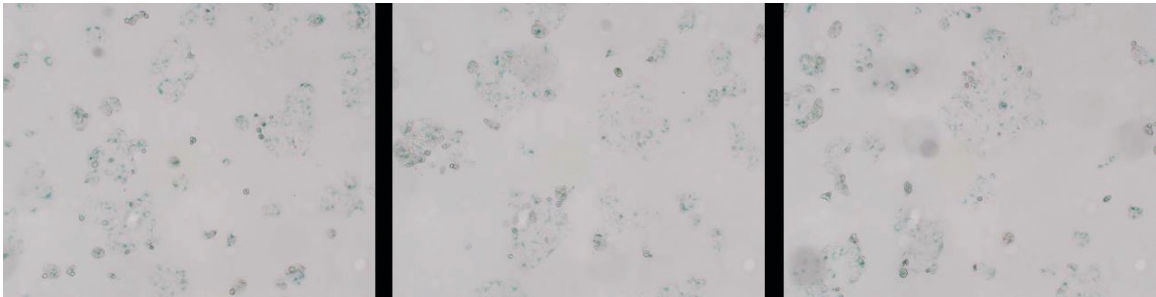
$\beta$ -glucosidase stained HCA-7 cells treated with 30  $\mu$ M pyrcoxib and 5 Gy.



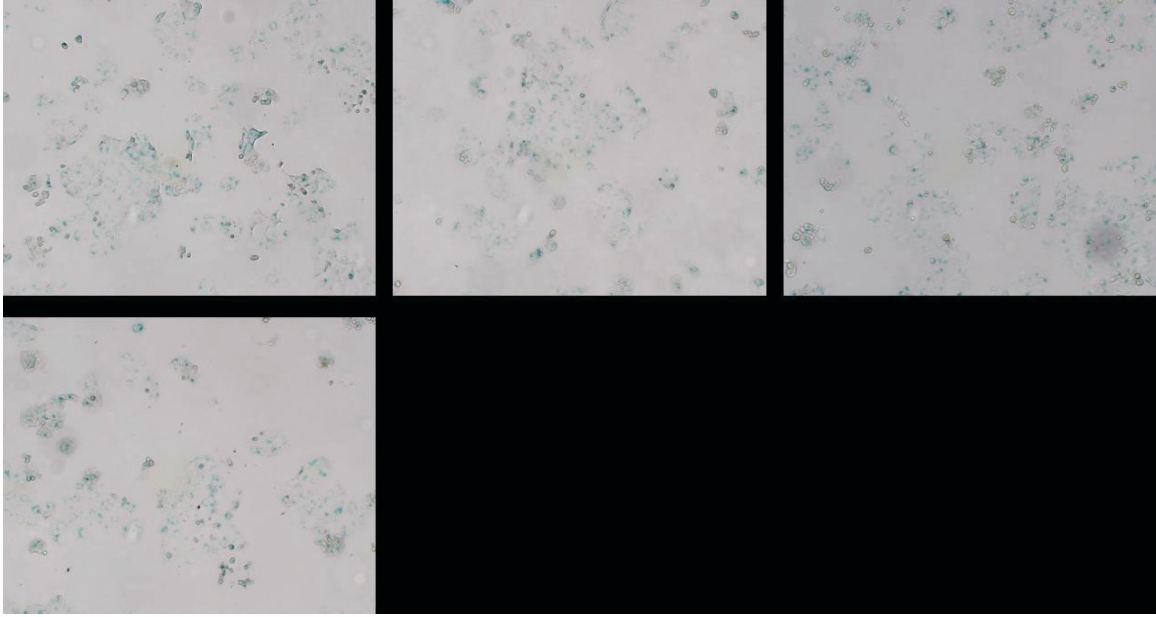
$\beta$ -glucuronidase stained HCA-7 cells treated with 75  $\mu$ M pyrcoxib and 5 Gy.



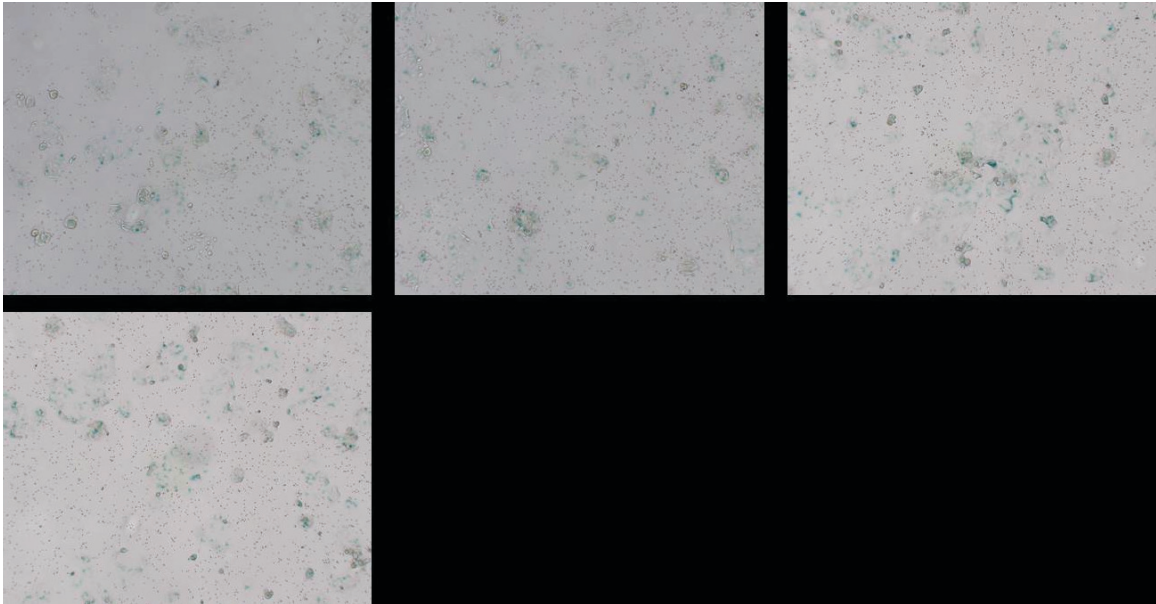
$\beta$ -glucuronidase stained HCA-7 cells treated with 30  $\mu$ M celecoxib and 10 Gy.



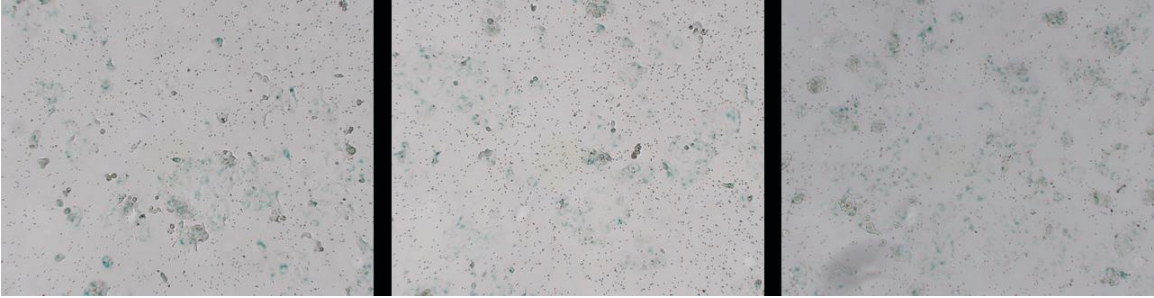
$\beta$ -glucuronidase stained HCA-7 cells treated with 75  $\mu$ M celecoxib and 10 Gy.



$\beta$ -glucosidase stained HCA-7 cells treated with DMSO and 10 Gy.



$\beta$ -glucosidase stained HCA-7 cells treated with 30  $\mu$ M pyricoxib and 10 Gy.



$\beta$ -glucuronidase stained HCA-7 cells treated with 75  $\mu$ M pyrcoxib and 10 Gy.

b. HCT-116 cells



$\beta$ -glucosidase stained HCT-116 cells treated with 30  $\mu$ M celecoxib and 0 Gy.



$\beta$ -glucosidase stained HCT-116 cells treated with 75  $\mu$ M celecoxib and 0 Gy.



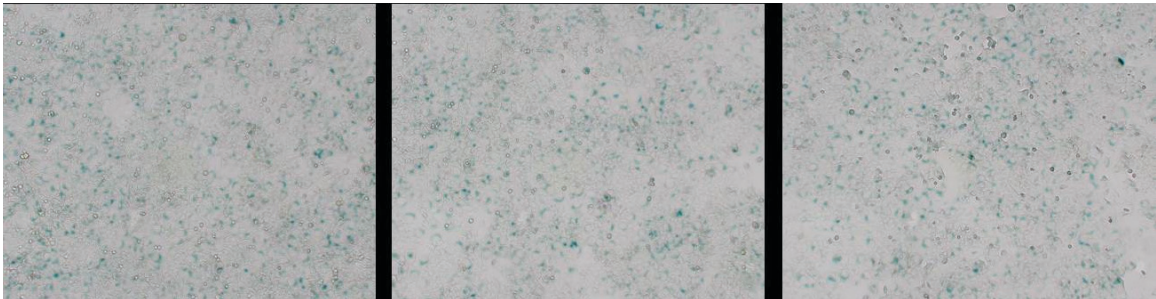
$\beta$ -glucosidase stained HCT-116 cells treated with DMSO and 0 Gy.



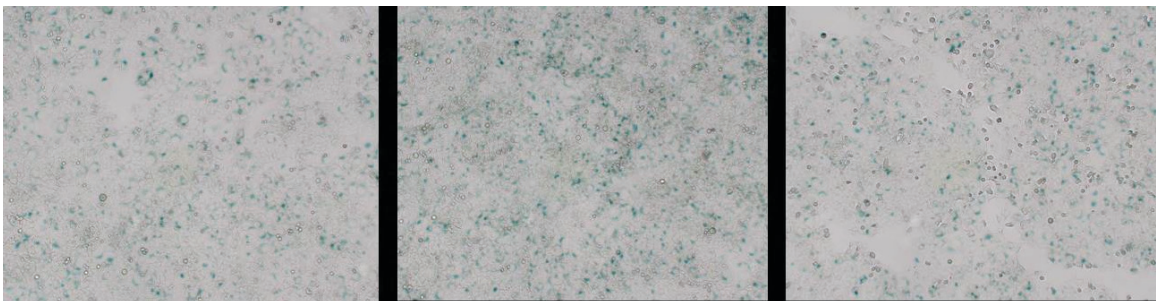
$\beta$ -glucosidase stained HCT-116 cells treated with 30  $\mu$ M pyrcoxib and 0 Gy.



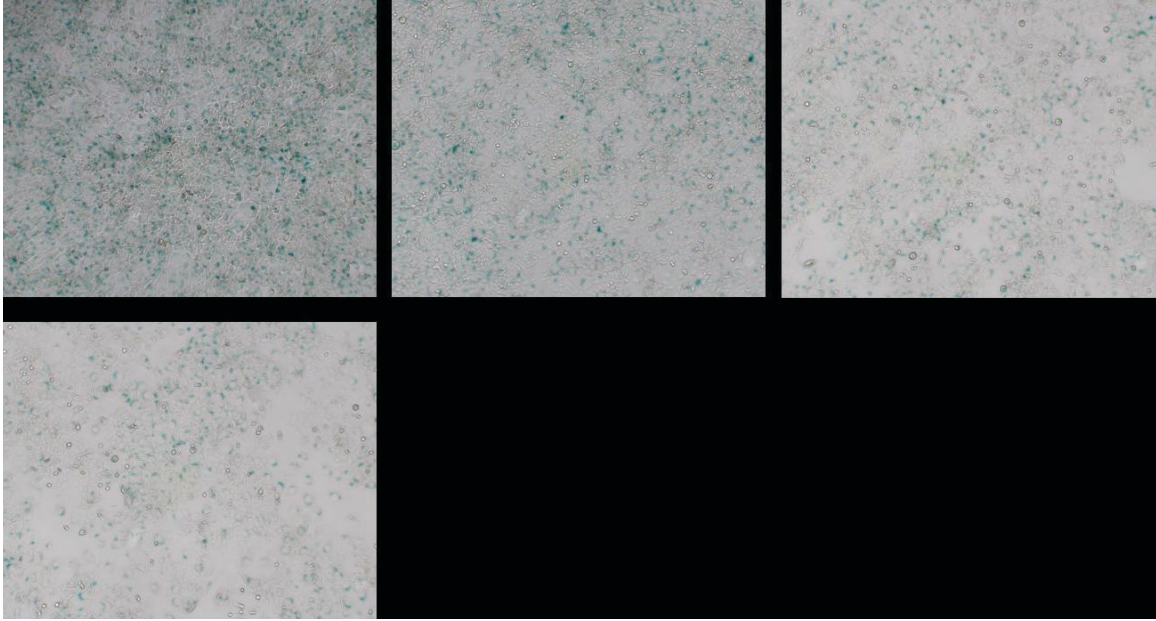
$\beta$ -glucosidase stained HCT-116 cells treated with 75  $\mu$ M pyrcoxib and 0 Gy.



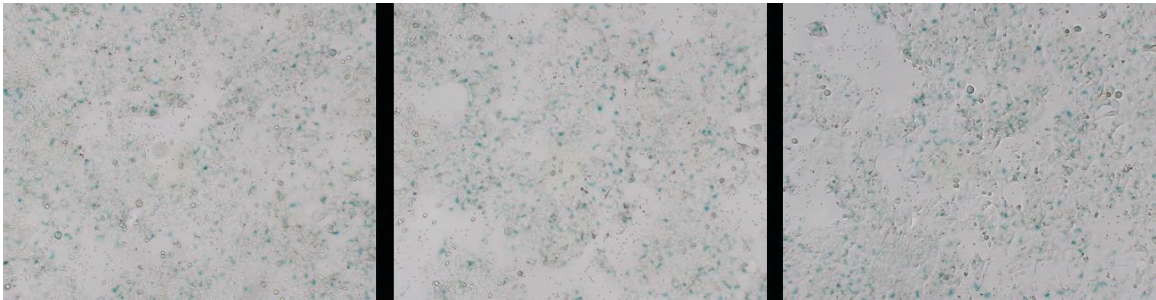
$\beta$ -glucosidase stained HCT-116 cells treated with 30  $\mu$ M celecoxib and 5 Gy.



$\beta$ -glucosidase stained HCT-116 cells treated with 75  $\mu$ M celecoxib and 5 Gy.



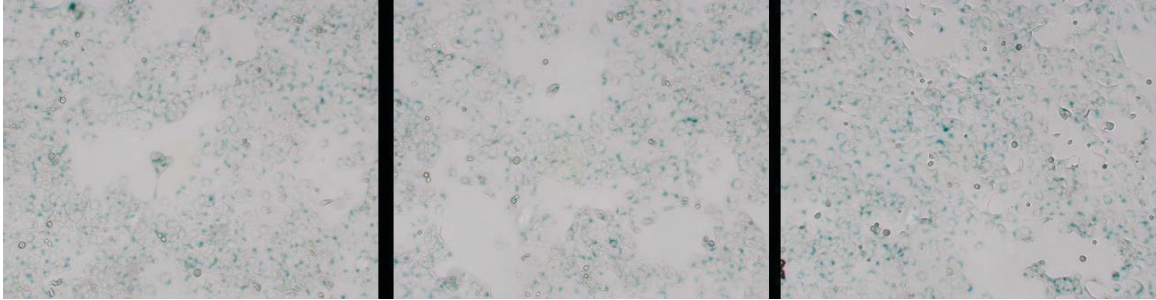
$\beta$ -glucosidase stained HCT-116 cells treated with DMSO and 5 Gy.



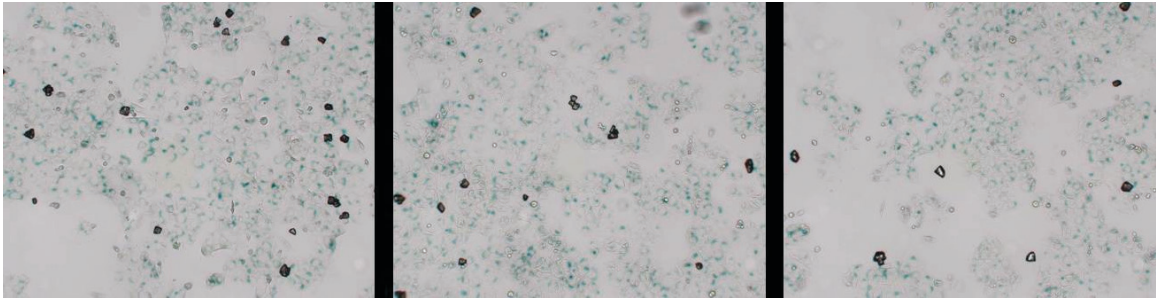
$\beta$ -glucosidase stained HCT-116 cells treated with 30  $\mu$ M pyrcoxib and 5 Gy.



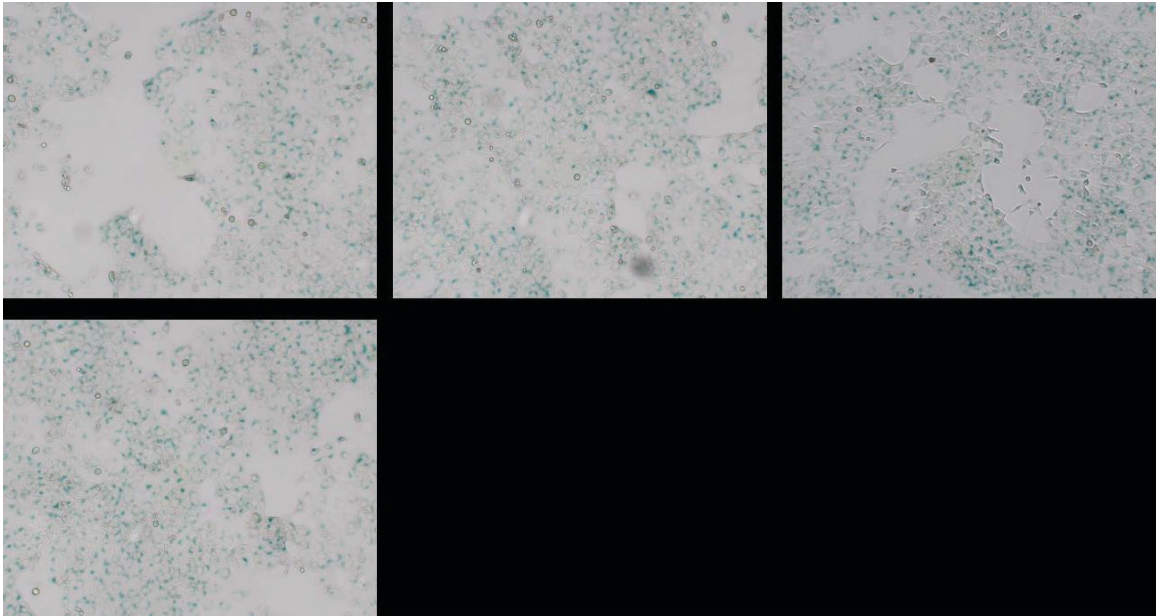
$\beta$ -glucosidase stained HCT-116 cells treated with 75  $\mu$ M pyrcoxib and 5 Gy.



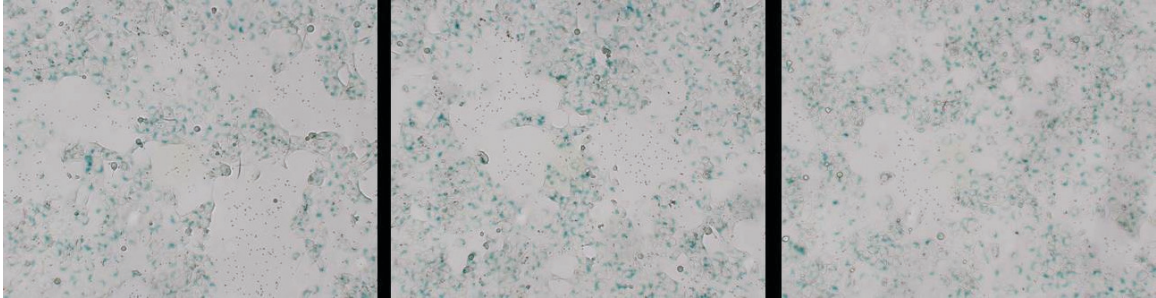
β-glucosidase stained HCT-116 cells treated with 30 μM celecoxib and 10 Gy.



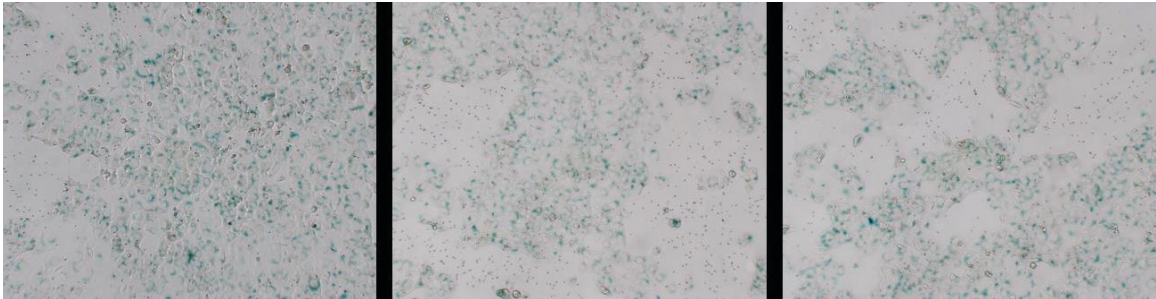
β-glucosidase stained HCT-116 cells treated with 75 μM celecoxib and 10 Gy.



β-glucosidase stained HCT-116 cells treated with DMSO and 10 Gy.



$\beta$ -glucosidase stained HCT-116 cells treated with 30  $\mu$ M pyrcoxib and 10 Gy.



$\beta$ -glucosidase stained HCT-116 cells treated with 75  $\mu$ M pyrcoxib and 10 Gy.